

**POLITECNICO DI TORINO**

**Master of Science in Automotive Engineering**

*Master Thesis*

**Energy management of mild hybrid vehicles  
exploiting ADAS sensor information**



**Supervisors:**

*Prof. Andrea Tonoli*

*Prof. Sanjarbek Ruzimov*

**Author:**

*Simone Parentela*

March 2021

*A mio fratello Mattia*  
*insostituibile punto di riferimento*

# Acknowledgements

This thesis work was carried out during my Erasmus project at the FH Joanneum in Graz. There are many people without whom this work would not be possible.

I would like to thank Professor Andrea Tonoli for giving me the opportunity to live this experience by proposing an innovative thesis during a period of great crisis and uncertainty. I sincerely thank Professor Sanjarbek Ruzimov for his great support and for guiding me in the right direction, not only concerning technical issues, but also for the mental support during the whole project. My acknowledgements to all the professors and teachers at Politecnico di Torino.

Finally, I convey special acknowledgement to my parents, for their loving and continuous support, I am eternally grateful for all his sacrifices that made my education and achievements possible.

Thank you all for your support!

# Abstract

Electric vehicles are viewed as the most effective way of reducing emissions. Recovering kinetic and potential energy is an effective method to extend their driving range. The purpose of this work is to integrate the ADAS sensor information in the energy management system of a 48 V mild hybrid to minimise the fuel consumption. Previous research has focused on developing connected and automated vehicle systems, mostly for safety reason. A case study is undertaken using data from a common hybrid commercial vehicle 2.3 liter diesel. The proposed strategy and numerical analysis have been verified by the NEDC and WLTC driving cycle under the MATLAB/Simulink software environment. The simulator already available in the LIM-Mechatronics Laboratory group of Politecnico di Torino has been modified to achieve the desired results. The work is focused on studying the control system and its optimisation. In this perspective, the knowledge of a short-range horizon such as that coming from the ADAS (Advanced Driver Assistance Systems) sensors (LIDAR, stereo-camera) has contributed to optimising the e-powertrain components' usage to start the regenerative braking in a condition that allows recovering all possible energy. These results provided evidence of more electrical motor power contribution compared to a conventional hybrid vehicle. It can be concluded from the results that a good control strategy supported by ADAS technology aims to handle the energy management problem for a hybrid vehicle. A further extension of this work could incorporate future traffic conditions into the long forecast horizon.

# List of Figures

Figure 1- The spectrum of vehicle hybridization levels (Simona, Lorenzo, & Giorgio, 2016).....	16
Figure 2- Series Hybrid schematic.....	17
Figure 3-Series Hybridization Level.....	18
Figure 4-Engine mode of a S-HEV .....	19
Figure 5-Electric mode of a S-HEV .....	19
Figure 6-Hybrid mode of a S-HEV .....	20
Figure 7-Engine traction and charging mode of a S-HEV .....	20
Figure 8-Regenerative braking mode of a S-HEV.....	20
Figure 9-Charging mode of a S-HEV .....	21
Figure 10-Hybrid battery-charging mode of a S-HEV.....	21
Figure 11-Parallel Hybrid schematic .....	23
Figure 12-Parallel Hybridization Level .....	23
Figure 13-Classification of parallel hybrid according to the EMs position .....	24
Figure 14-Engine mode of a P-HEV .....	25
Figure 15-Electric mode of a P-HEV .....	25
Figure 16-Hybrid mode of a P-HEV .....	26
Figure 17-Engine and battery charging mode of a P-HEV .....	26
Figure 18-Regenerative braking mode of a P-HEV.....	26
Figure 19-Parallel/Series Hybrid schematic .....	28
Figure 20-Engine-heavy series-parallel hybrid operating modes .....	29
Figure 21-Electric-heavy series-parallel hybrid operating modes .....	30
Figure 22-State-of-the-art ADAS and different sensors (V.K., J., S., & T, 2018) .....	31
Figure 23- Information flow in a forward simulator (Simona, Lorenzo, & Giorgio, 2016) .....	38

Figure 24- Information flow in a backward simulator (Simona, Lorenzo, & Giorgio, 2016).....	39
Figure 25- Generic speed profile.....	39
Figure 26- Time axis discretisation.....	40
Figure 27-Discrete and analytical speed profile .....	40
Figure 28- Backward Simulator of HEV P2 .....	42
Figure 29 - New European Driving Cycle.....	43
Figure 30 - NEDC summary parameters (DieselNet, s.d.) .....	43
Figure 31 - Urban Driving Cycle.....	44
Figure 32 - Extra Urban Driving Cycle .....	44
Figure 33 - Worldwide Harmonised Light-duty Vehicles Test Cycles .....	45
Figure 34 - WLTC summary parameters (DieselNet, s.d.).....	45
Figure 35 - WLTC LOW part.....	46
Figure 36 - WLTC MEDIUM part.....	46
Figure 37 - WLTC HIGH part .....	47
Figure 38 - WLTC EXTRA HIGH part.....	47
Figure 39 - Comparison of NEDC and WLTC parameters.....	48
Figure 40 - Comparison of speed profiles between NEDC and WLTC cycles.....	48
Figure 41- Drive Cycle Block.....	48
Figure 42- Gear shift strategy .....	49
Figure 43- Vehicle Dynamics Block .....	49
Figure 44- Vehicle Dynamics block from inside .....	50
Figure 45- Brake split block (Ideal Braking Subsystem) .....	51
Figure 46- Ideal braking curve.....	52
Figure 47- Wheels Block.....	53
Figure 48-Gearbox block.....	53

Figure 49- Gearbox block from inside .....	54
Figure 50- Power Flow Direction Subsystem .....	54
Figure 51- Controller block .....	55
Figure 52-Controller block from inside .....	55
Figure 53-Stateflow chart .....	56
Figure 54- Engine block .....	57
Figure 55- Engine map .....	57
Figure 56- Engine block from inside.....	58
Figure 57- Fuel Consumption and CO <sub>2</sub> emission block .....	58
Figure 58-Fuel Consumption block from inside .....	59
Figure 59- ICE fuel consumed subsystem. ....	59
Figure 60- Electric Motor block.....	60
Figure 61- Electric motor map .....	60
Figure 62- Electric Motor block from inside .....	61
Figure 63 - Battery block .....	61
Figure 64 - Battery block from inside.....	62
Figure 65 - Discharge/Charge power vs SOC .....	63
Figure 66- Capacity vs Discharge Time (Battery and Energy Technologies, 2019) .....	64
Figure 67- The block diagram of the method based on Peukert's law proposed in (Gong, Li, & Liao, 2020) .....	66
Figure 68- The average error varies with Peukert's constant (Gong, Li, & Liao, 2020) .....	66
Figure 69 - vehicle architecture .....	67
Figure 70- Simulator "Power Management" strategy .....	70
Figure 71-Torque-Speed map: Traction .....	71
Figure 72-Torque-Speed map: Braking .....	72

Figure 73-BSFC map .....	74
Figure 74-Optimal Operating Line .....	74
Figure 75- Optimal Operating Line def. ....	75
Figure 76 - Look-ahead scenario .....	75
Figure 77- Information model.....	76
Figure 78- Future information procedure.....	77
Figure 79-Information model (top) vehicle model (bottom).....	78
Figure 80- Speed profile information model and vehicle model.....	78
Figure 81- deltaSOC information .....	79
Figure 82-Simulator “Look-Ahead” strategy .....	80
Figure 83 – Engine & Motor Map (NEDC) .....	81
Figure 84 - Speed profile, SOC & Operating modes (NEDC) .....	82
Figure 85 - Fuel consumption & CO <sub>2</sub> emission (NEDC) .....	83
Figure 86 - ECE15 & EUDC fuel consumptions.....	83
Figure 87 - ECE15 & EUDC CO <sub>2</sub> emissions .....	83
Figure 88 - Engine & Motor Map (WLTC).....	84
Figure 89 - Speed profile, SOC & Operating modes (WLTC) .....	85
Figure 90 - Fuel consumption & CO <sub>2</sub> emission (WLTC) .....	85
Figure 91 - LOW, MEDIUM, HIGH, EXTRA HIGH fuel consumptions.....	86
Figure 92 - LOW, MEDIUM, HIGH, EXTRA HIGH CO <sub>2</sub> emissions.....	86
Figure 93 - SOC profile & operating modes .....	87
Figure 94 - E-motor torques.....	88
Figure 95 - ICE torques.....	88
Figure 96 - Fuel consumption Look-Ahead .....	89



# Index

<i>Acknowledgements</i> .....	3
<i>Abstract</i> .....	4
<i>List of Figures</i> .....	5
<i>1 Introduction</i> .....	12
1.1 Background .....	12
1.2 Solutions .....	12
1.2.1 Technological solutions .....	12
1.2.2 Energy efficient utilization .....	13
<i>2 Literary review and background</i> .....	15
2.1 Hybrid Electric Vehicle .....	15
2.1.1 Degrees of Hybridization .....	15
2.1.2 Series Hybrid configurations .....	17
2.1.2.1 Operating modes .....	19
2.1.2.2 Advantages and Disadvantages .....	21
2.1.3 Parallel Hybrid configurations .....	22
2.1.3.1 Parallel Hybrid architectures .....	24
2.1.3.2 Operating modes .....	25
2.1.3.3 Advantages and Disadvantages .....	27
2.1.4 Parallel-Series Hybrid configurations .....	27
2.1.4.1 Operating modes .....	28
2.2 Advanced Driver Assistance System (ADAS) .....	30
2.3 Connected and automated vehicle .....	34
<i>3 Modelling Approach</i> .....	37
3.1 Forward Approach Model .....	37

3.1.1 Dynamic method .....	38
3.2 Backward Approach Model .....	38
3.2.1 Quasi-Static method .....	39
3.3 Conclusion .....	41
4 Model Overview .....	42
4.1 Drive Cycle .....	42
4.1.1 NEDC .....	42
4.1.2 WLTP .....	44
4.1.3 Drive Cycle block .....	48
4.2 Vehicle Dynamics .....	49
4.2.1 Longitudinal force .....	50
4.2.2 Ideal Braking .....	51
4.3 Wheels .....	53
4.4 Gearbox .....	53
4.5 Controller .....	55
4.6 Engine .....	57
4.7 Fuel Consumption and CO <sub>2</sub> emission evaluation .....	58
4.8 Electric Motor .....	59
4.9 Battery .....	61
4.9.1 Peukert .....	64
4.9.1.1 Experimental .....	65
5 Case studies .....	67
5.1 Test Case .....	67
5.2 Power management strategy .....	68
5.2.1 Rule-Based Control .....	68

5.2.2 Description .....	69
5.2.3 Control Summary .....	71
5.2.4 Optimal Operating Line (OOL) .....	73
5.2.4.1 Procedure .....	73
5.2 Look-ahead - predictive operation strategy .....	75
5.2.1 Future information .....	76
<i>6 Simulations results .....</i>	<i>81</i>
6.1. Control Strategy results: NEDC .....	81
6.2 Control Strategy results: WLTC .....	84
6.3 Look-ahead strategy results .....	86
<i>Conclusions .....</i>	<i>90</i>
<i>Appendix: Matlab code .....</i>	<i>92</i>
<i>Bibliography .....</i>	<i>98</i>

# 1 Introduction

## 1.1 Background

Growing concern about greenhouse effects has led the United Nations Intergovernmental Panel on Climate Change (IPCC) to conclude that a reduction of at least 50% in global CO<sub>2</sub> emissions, compared to the 2000 levels, has to be achieved by 2050, to limit the long-term rise in the global average temperature (L.Rolando, 2012)

The increase in fossil fuel demand and pollutant emissions from Europe's transport sector will be crucial in achieving 7th EAP's longer-term objectives since it is one of the key economic sectors. In order to give more long-term direction, the new general Union Environment Action Programme sets out a vision beyond that, of where it wants to be by 2050:

“In 2050, we live well, within the planet’s ecological limits. Our prosperity and healthy environment stem from an innovative, circular economy where nothing is wasted and where natural resources are managed sustainably, and biodiversity is protected, valued and restored in ways that enhance our society’s resilience. Our low-carbon growth has long been decoupled from resource use, setting the pace for a safe and sustainable global society.”  
(EuropeanCommision, 2020)

## 1.2 Solutions

There are many ways to counter this problem. Today, two options are being considered. On the one hand, a technical solution uses new energy sources to make vehicles more eco-friendly. The second one is an energy-efficient solution. It involves control strategies that make it possible to use existing technologies to cut polluting emissions and, at the same time, guarantee high-performance vehicles, ease of driving, and reasonable cost.

### 1.2.1 Technological solutions

Over the last century, the drive train of the vehicle has remained largely the same. However, advances in technology have made it possible to achieve good results without modifying the drive train itself. The introduction of direct injection, valve timing control, downsizing, turbocharging, and EGR (emission gas recirculation) system have contributed to improved engine efficiency (Group,

2018). The amount of fuel emitted through stop-and-start or cylinder deactivation has been significantly reduced. Also considered are advances in transmission such as the CVT (continuously variable transmission), which allows the engine to work at its most efficient points. In parallel with these improvements, other approaches are investigating the design of alternative transmission architectures. New vehicle architectures are beginning to be massively marketed in recent years, including battery-electric and hybrid electric vehicles. Hybrid Electric Vehicles (HEVs) are generally an effective intermediate solution between traditional internal combustion engine vehicles and fully electric vehicles. To date, HEVs are well established within the global market, but they represent one of the cornerstones to which important improvements can be made, and research studies can be devoted to capturing aspects that may be useful for new architectures and future solutions. The use and coupling of internal combustion engines and electric motors with two different types of energy source make it possible to reduce fuel consumption, local and urban pollutant emissions, while at the same time guaranteeing vehicles with performance, ease of driving and costs that meet market expectations. Combining the internal combustion engine with one or more electric motors, thanks to their reversibility, allows different vehicle operation modes. They can act as generators to recharge the batteries, storing energy used during acceleration or short-range in purely electric mode. The result is a hybrid drive system that allows the internal combustion engine to be used under the most efficient conditions.

### **1.2.2 Energy efficient utilization**

The other direction in which the various countries have decided to move is experimenting with inter-vehicle communications. In previous years, research focused on improving the systems used to reduce the risk of accidents, such as airbags or brake assist systems (ABS). However, the keyword is 'smart', intelligent vehicles capable of communicating with each other, exchanging information. Studies on intelligent vehicle technologies (ITS) propose infrastructure-to-vehicle (I2V) and vehicle-to-vehicle (V2V) communication to improve fuel economy (Fifueiredo, Jesus, Ferreira, & Carvalho, 2001).

For example, a vehicle following close behind will be informed of the speed of the vehicle in front of it, it will be told to increase its safety distance using an acoustic and/or visual message, and it will

be warned of obstacles in the road as well as of road accidents in the vicinity. A representative example of ITS is the “Travolution project” carried out by Audi in Ingolstadt (Munich & Audi, 2018). Audi optimised the traffic light phases in Ingolstadt, but also some traffic lights were equipped with communication modules. These modules transmit the time of the next green phase to the Audi test vehicle. The driver can then be informed of the appropriate vehicle speed to avoid having to stop. V2V communication can be used to transmit information about traffic jams or accidents. Notified drivers can choose an alternative route, and traffic jams can be reduced (Affairs, 2011). This system will also enable proper traffic management, thus avoiding congestion on major roads and diverting vehicle flows onto secondary roads, thus saving drivers time and significantly reducing air pollution.

# 2 Literary review and background

## 2.1 Hybrid Electric Vehicle

A Hybrid Vehicle is a vehicle equipped with two propulsion systems: the ICE (Internal Combustion Engine) and an EM (Electric Machine). Therefore, this type of car can be thought of as a combination of a conventional car equipped with an engine and an electric vehicle. Vehicles equipped with an internal combustion engine provide good performance and a long-range by exploiting the fuel's high energy density. Battery electric vehicles (BEVs) have the advantage of high energy efficiency and zero environmental pollution. The disadvantages of conventional ICE vehicles are poor fuel economy and environmental pollution (Simona, Lorenzo, & Giorgio, 2016). The engine's operating points do not correspond entirely to maximum efficiency points, and the braking system's kinetic energy during braking is entirely converted into heat through the conventional braking system and therefore lost. On the other hand, electric vehicles are less efficient from a long-distance perspective due to the batteries' low energy content. Hybrid vehicles are designed to combine the advantages of electric and conventional systems. The energy needed for propulsion is made available by two or more energy sources of different nature which cooperate according to the rules imposed by an appropriate control system in order to guarantee, as far as possible, an overall reduction in fuel consumption and emissions compared to a conventional vehicle while ensuring similar performance.

### 2.1.1 Degrees of Hybridization

To assess the power distribution ratio between the powertrain components of an HEV, the concept of the degree of hybridisation (DoH) was introduced in (Xue, Zhang, Teng, Zhang, & Feng, 2020). The DoH refers to the percentage of the electrical system's power to the total power of the power source.

$$DoH = \frac{P_{elec}}{P_{total}} \times 100 \quad Eq. 1$$

where  $P_{elec}$  is rated power of motor and  $P_{total}$  is the sum of the rated power of motor and engine. The definition of the DoH is slightly different for different configurations of powertrains. According to different DoHs, HEVs can be divided into the following categories: micro HEV, mild HEV, and full HEV.

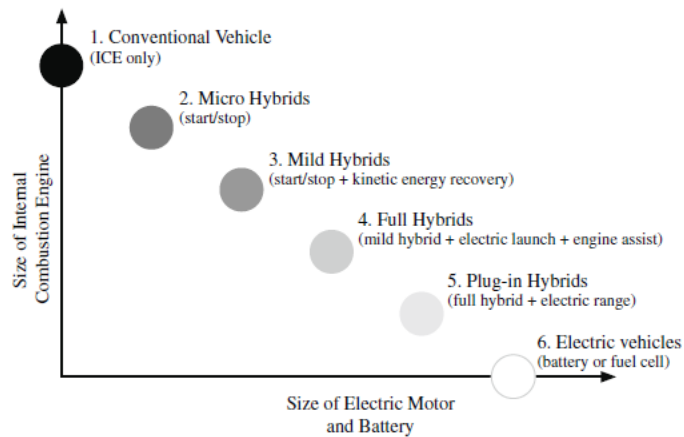


Figure 1- The spectrum of vehicle hybridization levels (Simona, Lorenzo, & Giorgio, 2016)

- **Micro hybrid:** the electric motor works in applications such as stop/start and regenerative braking. The electric motor does not provide additional torque to the engine. Fuel economy can be improved by 5-10% during city driving condition.
- **Mild hybrid** electric vehicles typically have the ICE couples with an electric machine; the electric motor helps the internal combustion engine during aggressive acceleration phases and enables them to recover most of the regenerative energy during deceleration phases. Mild hybrid electric vehicles do not have an exclusive electric-only propulsion mode. The fuel economy improvement is mainly achieved through shutting down the engine when the car stops, using electrical power to initially start the vehicle, optimizing engine operational points, and minimizing engine transients. Typical fuel savings in vehicles using mild hybrid drive systems range from 15 to 20%.
- **Full hybrid:** this type of vehicle is the only one that can cover entire distances, albeit limited to a few tens of kilometres, in purely electric mode, thanks to more powerful electric motors and batteries. Compared with traditional internal combustion engine vehicles, the overall fuel economy of a full hybrid electric vehicle in city driving could improve by up to 40%.



- **Plug-in hybrid:** these cars can be recharged either from the household power socket or from special electric charging stations. There is no need to wait for the batteries to be recharged by the internal combustion engine.
- **Electric vehicles** are propelled only by their onboard electric motor(s), which are powered by a battery (recharged from the power grid) or a hydrogen fuel cell.

### 2.1.2 Series Hybrid configurations

The series hybrid propulsion system has only one powertrain with an electric machine as a torque actuator. The hybridisation is realised at the energy source level with an electric link (realised or directly or through a power converter) connecting one electric source (typically, but not necessarily, a battery pack) to an electric generation system based on an ICE mechanically coupled to an e-machine mainly or solely used as a generator.

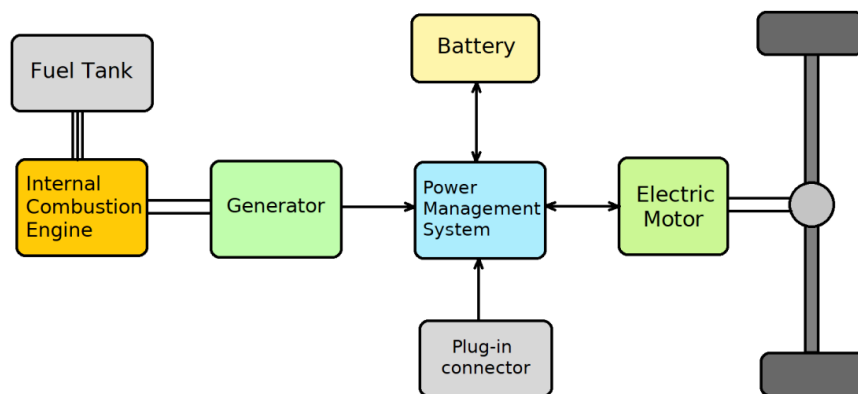


*Figure 2- Series Hybrid schematic*

The electric motor has to be sized for the vehicle's maximum power; therefore, it has to be of considerable size, weight, and cost. An advantage of this architecture is the possibility of decoupling the internal combustion engine from the wheels.

When a large amount of power is required, electrical energy is drawn from both the generator/ICE engine and the battery. Thanks to the decoupling with the wheels, in a series hybrid the conditions can be created to optimise the engine's operation because it only has to produce electricity as efficiently as possible. The electric motor then varies its operating speed to suit the needs of the driver. Thanks to the electric motor's excellent starting and low-speed performance, it is possible to avoid oversizing the internal combustion engine, as is traditionally required for good acceleration and pick-up performance. Downsizing is therefore

implemented, and the engine tends to run at a fixed point or follow the OOL (Optimal Operating Line), a torque characteristic depending on the rpm where there is the lowest specific fuel consumption. However, the engine's mechanical energy is converted twice (from mechanical to electrical in the generator and from electrical to mechanical in the electric traction motor); the losses in these processes add up, reducing the efficiency of the system.

Depending on the hybridisation ratio used in the sizing of the two electric power-energy sources, different series hybrid configurations can be defined to be applied to different vehicle topologies and applications. Considering the power output that can be delivered by the internal combustion engine and by the electric power source, Rh (Hybridization Ratio) is defined as (S & A, 2004):

$$R_{h \text{ Series}} = \frac{P_{el \text{ gen}}}{P_{em}} \quad Eq. 2$$

Where  $P_{el \text{ gen}}$  is the power of electric generator and  $P_{em}$  is the power of the electric machine. The series hybridisation ratio ranges from 0 (pure Battery Electric Vehicle) to 1 (Electric Transmission) as shown in Figure 3:

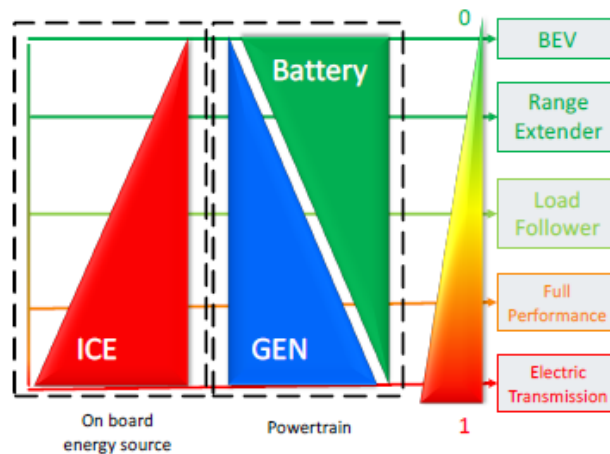


Figure 3-Series Hybridization Level

Hybridisation ratio equal to zero means the vehicle is pure electric, no additional energy source. As the size of the generator increases, the size of the battery decreases. The range-extender is characterised by a small ICE that only works in high power demand cases and when the battery is fully discharged to allow the vehicle to travel the necessary distance before

recharging. The power pack does not work at a fixed point in the load follower, but following the cycle requests up to its maximum power (load follower mode). For higher power levels, the system sums the power pack and the battery pack powers. When ( $Rh Series=1$ ) electric transmission is realised, with no battery, and the ICE provides all the power

### 2.1.2.1 Operating modes

As the energy exchanges within the vehicle can vary according to requirements, such an architecture allows it to operate in the following different ways (Khajepou, Fallah, & Goodarzi, 2014):

- **Pure engine mode:** the vehicle is in motion, the needed power is supplied entirely by the internal combustion engine. The mechanical power is converted into electrical power via the generator and transferred to the electric motor, which converts it into mechanical power for transmission. The batteries do not exchange any power with the rest of the system.

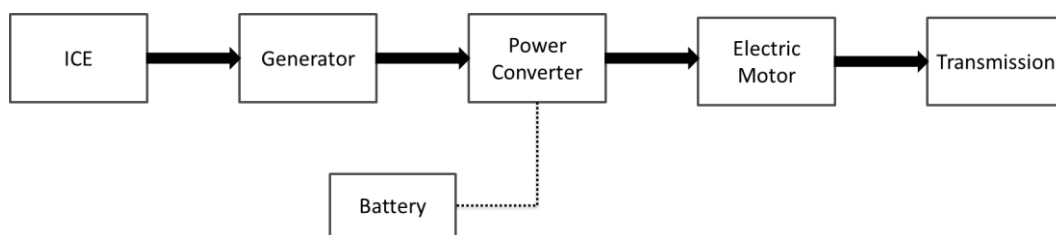


*Figure 4-Engine mode of a S-HEV*

- **Pure electric mode:** the engine is switched off while the electric motor is powered solely by the batteries, the vehicle behaves like an electric vehicle and its range is strictly dependent on the storage system's capacity.

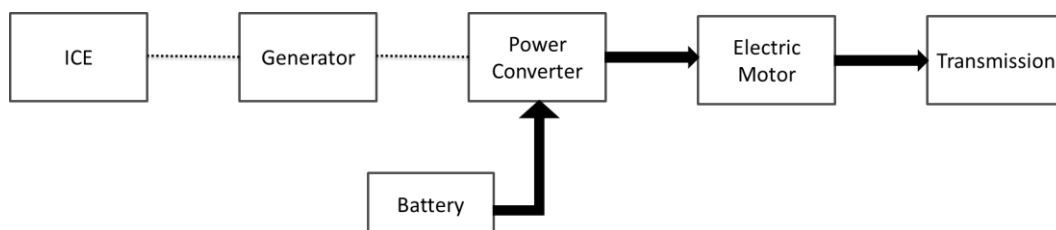


*Figure 5-Electric mode of a S-HEV*

- **Hybrid mode:** energy is supplied simultaneously by the engine and the batteries

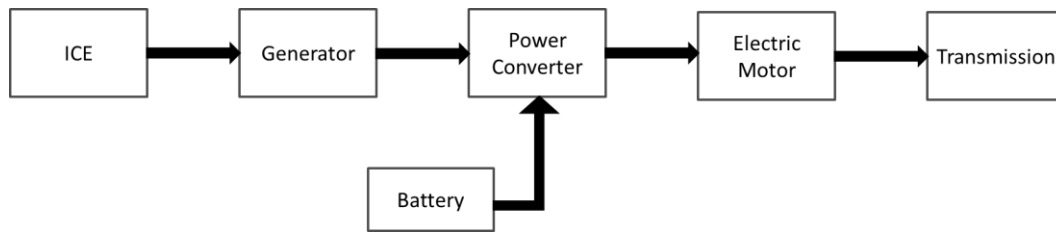


*Figure 6-Hybrid mode of a S-HEV*

- **Engine traction and battery charging mode:** When the state of charge is below the minimum value, the motor simultaneously supplies energy to the electric motor for propulsion and to the power converter for charging the batteries.

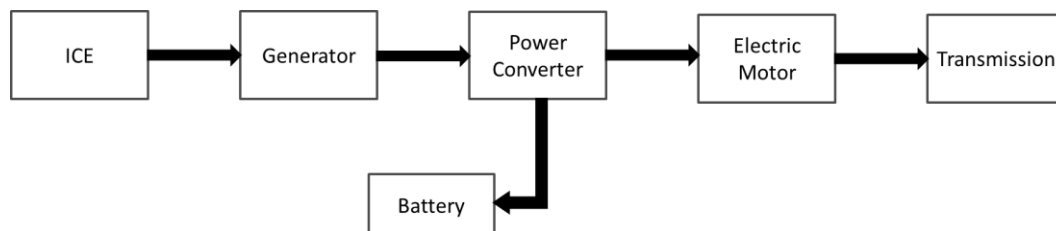


*Figure 7-Engine traction and charging mode of a S-HEV*

- **Regeneration mode:** when the vehicle is braking, and the braking torque is within limits set by the electric motor, the latter acts as a generator. The dissipated kinetic energy is used to charge the batteries while the engine remains switched off.

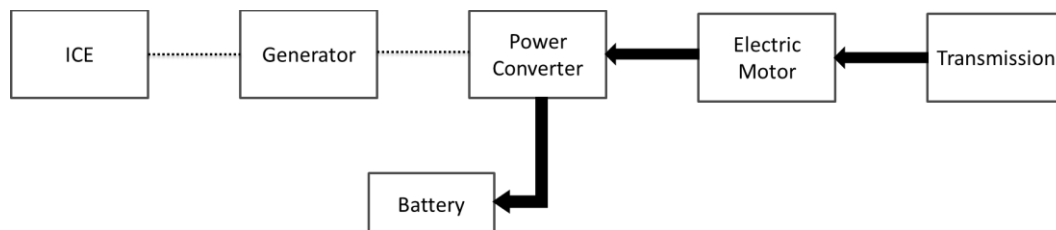


*Figure 8-Regenerative braking mode of a S-HEV*

- **Battery charging mode:** the vehicle is at rest, the electric motor receives no energy, while the engine's energy is used to charge the batteries.

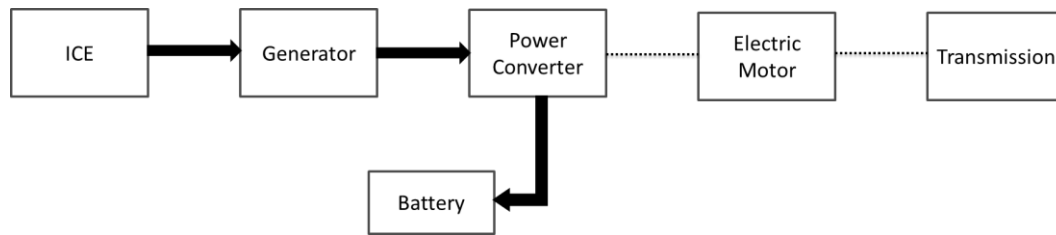


*Figure 9-Charging mode of a S-HEV*

- **Hybrid battery-charging mode:** the vehicle is slowing down, the engine's energy and some of the recovered kinetic energy is used to charge the batteries.

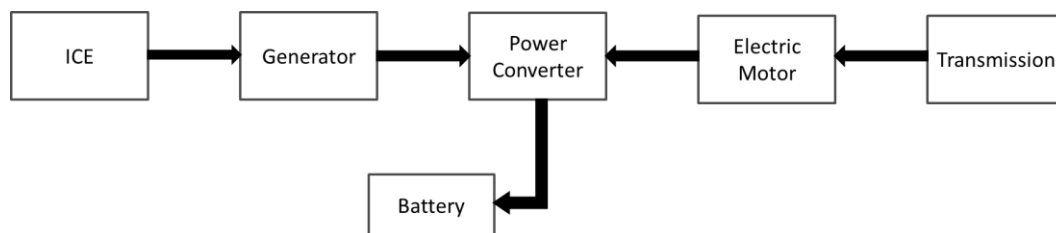


*Figure 10-Hybrid battery-charging mode of a S-HEV*

### 2.1.2.2 Advantages and Disadvantages

To summarise the pros and cons of a series configuration:

Advantages:

- The engine is mechanically detached from the wheels, which allows it to be optimally positioned within the vehicle.
- The internal combustion engine does not follow the driver's requirements and can work at high efficiency.
- The internal combustion engine can be undersized as its main purpose is to maintain the battery charge.

Defects:

- The energy coming from the internal combustion engine is converted twice (from mechanical to electrical and from electrical to mechanical), so considering the efficiency of a single component leads to significant losses.

- The generator increases the weight and cost of the vehicle compared to conventional ones.
- The electric motor must be sized to provide the maximum power required, which increases weight and cost.

Considering the advantages and disadvantages of a series hybrid, it can be concluded that this type of architecture may be unsuitable to replace conventional vehicles due to the need for a significantly higher structure. For this reason, the series solution is generally applied to public transport vehicles and vehicles where the already considerable dimensions do not pose particular limitations.

### **2.1.3 Parallel Hybrid configurations**

The simple parallel hybrid is a traction system made of two elementary traction systems (one based on an ICE and one on an e-machine) with, as the main energy source, the ICE fuel stored in the on-board tank and, as a possible secondary energy source, the electric energy of an electric storage system (typically a battery pack).

The operation of a parallel hybrid vehicle is based on the ability of the two motors to provide energy for propulsion independently and in combination: the chemical energy contained in the fuel is transformed, as in conventional vehicles, into mechanical energy by the internal combustion engine, while the electric motor exchanges energy with the storage system to which it is connected. From a mechanical point of view, the motors cooperate using a device that returns to the transmission shaft a power equal to the sum of the two motors' powers, which, consequently, can operate in parallel or separately.

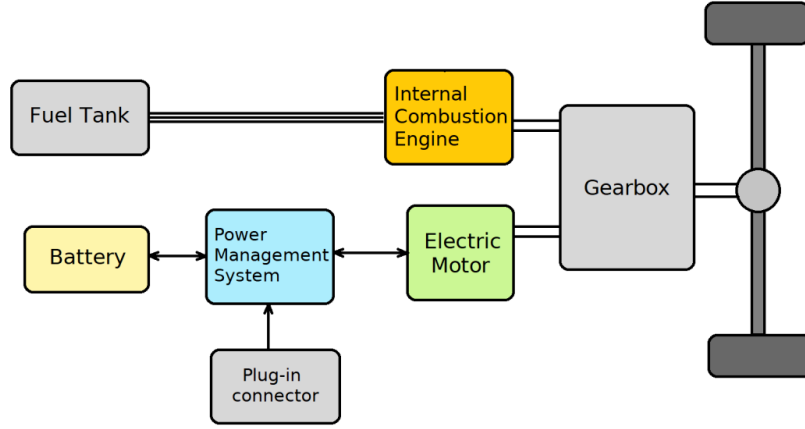


Figure 11-Parallel Hybrid schematic

The hybridization is realized at powertrain level with a mechanical direct (through clutches, joint, gears) or an indirect link (with two powertrains one for each axle and coupled through the road). As for series architecture, it is possible to define the Parallel Hybridization Ratio:

$$R_{h \text{ Parallel}} = \frac{P_{em}}{P_{em} + P_{ICE}} \quad Eq. 3$$

Where  $P_{ICE}$  is the power of the engine, and  $P_{em}$  is the power of the electric machine. As illustrated in Figure 12, a lower value of  $R_{h \text{ Parallel}}$  means that the ICE completely delivers the power. Simultaneously, a higher value of hybridization ratio means simply a behaviour similar to a battery-electric vehicle.

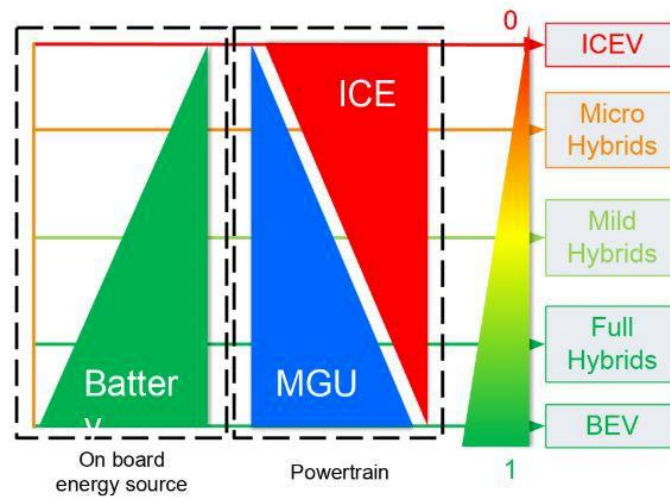
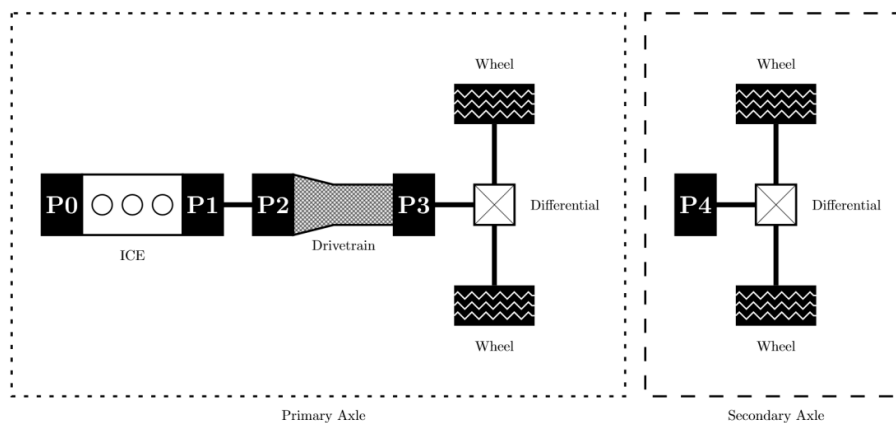


Figure 12-Parallel Hybridization Level

On the other hand, full hybrids are vehicles that can operate in both purely electric and purely thermal modes. Mild hybrids are vehicles equipped with an oversized starter motor so that the ICE can be switched off when the car is braking or while it is in an ideal condition. Finally, micro hybrids use the internal combustion engine as the primary engine for propulsion while the electric motor is used as a boost for torque. They cannot operate in purely electric mode, so they benefit from a smaller battery pack.

### 2.1.3.1 Parallel Hybrid architectures

Depending on the electric motor's position, it is possible to distinguish four different types of a parallel hybrid.



*Figure 13-Classification of parallel hybrid according to the EMs position*

- **P1:** the electrical machine is always connected to the engine. Depending on whether it is connected at the front or the rear in a longitudinal configuration, we distinguish P1f and P1r. The electric machine and the internal combustion engine have the same angular speed. The engine can function as a starter and generator. This solution allows the engine to be switched off when the vehicle is stationary, thus reducing consumption.
- **P2:** the electric machine is located between the engine and the transmission on the transmission's side. In this configuration, there is the possibility of decoupling the electric motor from the wheels through a clutch. The electric motor assists the engine during high power demands or acts as the only actuator to move the vehicle in e-mode.



- **P3:** e-machine between transmission and differential unit (sometimes, mainly in transversal engine layout, with a devoted ratio from e-machine shaft and transmission secondary shaft).
- **P4:** e-machine on a secondary axle (engine on the primary axle) is typically linked to the differential through a devoted transmission.

### 2.1.3.2 Operating modes

In a parallel hybrid architecture, it is possible to classify different operating modes (Guzzella & Sciarretta, 2013):

- **Engine alone traction mode:** the energy required for propulsion is supplied entirely by the internal combustion engine while the electric motor is off. This mode is activated when the engine is operating close to the optimum operating point.

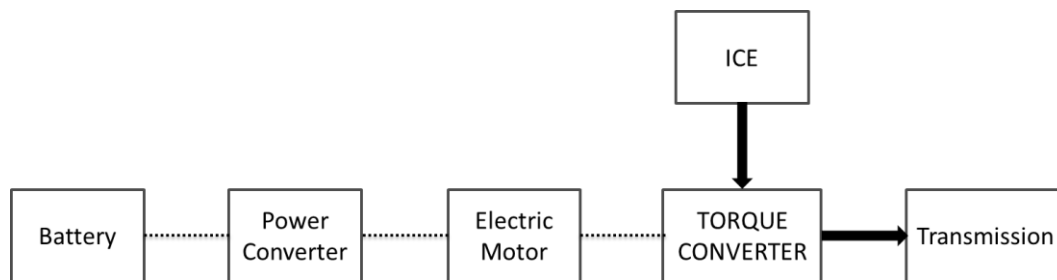


*Figure 14-Engine mode of a P-HEV*

- **Electric alone traction mode:** the energy required for propulsion is supplied entirely by the electric motor, subject to the battery's state of charge. This mode is activated when the motor is expected to work in areas of low efficiency.

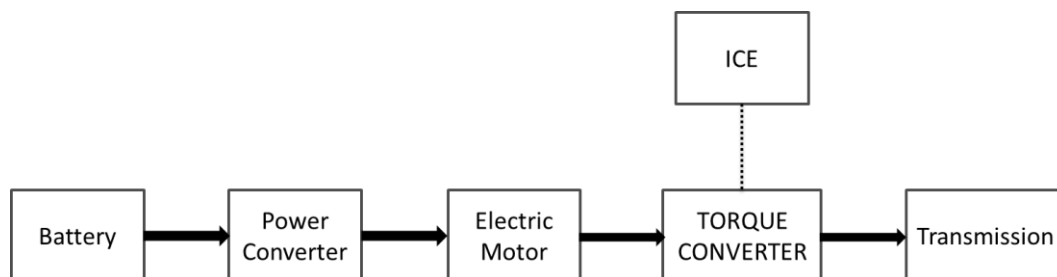


*Figure 15-Electric mode of a P-HEV*

- **Hybrid mode:** the energy required for propulsion is supplied simultaneously by the electric motor and the internal combustion engine. The internal combustion engine

will provide almost constant torque, while the electric machine is responsible for managing the transitory phases, and forces the engine to work close to its optimal operating point, using the batteries as an energy buffer.

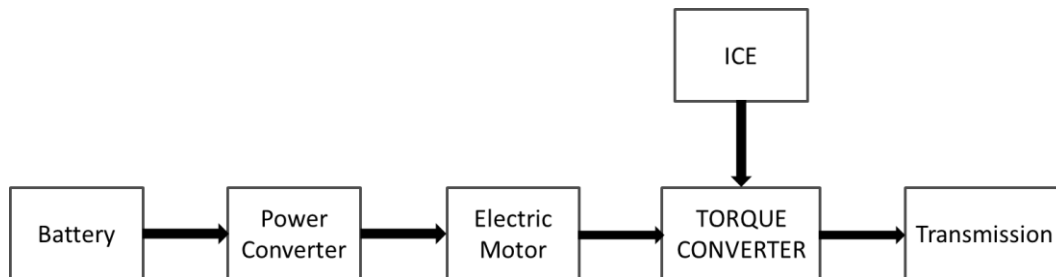


*Figure 16-Hybrid mode of a P-HEV*

- **Engine traction and battery charging mode:** this mode is involved when the batteries' state of charge is low, and the engine produces more than the power required for vehicle motion. The additional power recharges the battery by switching the electric motor to operate as a generator.

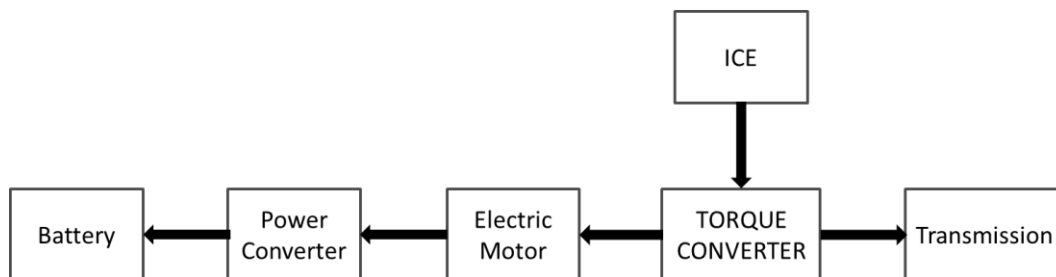


*Figure 17-Engine and battery charging mode of a P-HEV*

- **Regeneration mode:** it is usually referred to as regenerative braking, and this mode is activated when the vehicle is braking or during downhill motion. It allows recuperating the kinetic energy that would be wasted with regular braking mode.

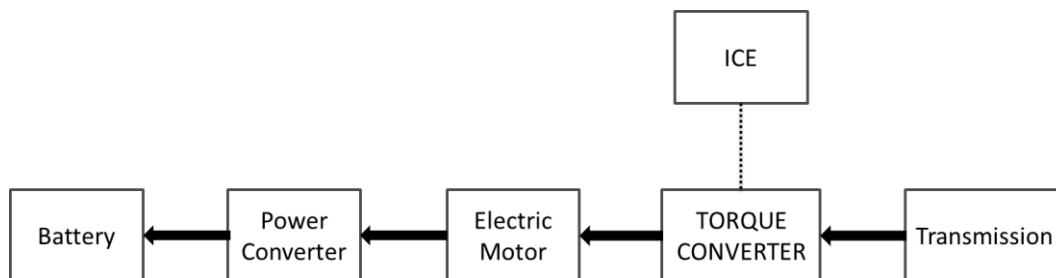


*Figure 18-Regenerative braking mode of a P-HEV*

### **2.1.3.3 Advantages and Disadvantages**

To summarise the pros and cons of a parallel configuration:

Advantages:

- for the same performance as a conventional vehicle, it allows the installation of a smaller and more efficient internal combustion engine.
- the vehicle can provide high performance because the internal combustion engine and electric motor cooperate to generate the overall power.
- a large part of the energy supplied by the internal combustion engine is directly supplied to the wheels, avoiding two conversions as in the series configuration.

Disadvantage:

- increased system complexity
- the internal combustion engine operates at variable speed, which leads to a deterioration in efficiency.

Ultimately, the parallel architecture lends itself to effective implementation in traditional cars, where the small size of the vehicle does not allow the adoption of a series architecture.

### **2.1.4 Parallel-Series Hybrid configurations**

The parallel-series configuration is generally similar to the parallel architecture, but also it has an electric motor which functions primarily as a generator. This configuration combines the advantages of the series-parallel hybrid. The engine can drive the wheels directly (as in the parallel drivetrain), and be effectively disconnected, with only the electric motor providing power (as in the series drivetrain). With gas-only and electric-only options, the engine operates at near optimum efficiency more often. It operates more like a series vehicle at lower speeds, while at high speeds, where the series drivetrain is less efficient, the engine takes over and energy loss is minimized (Rind, 2017). This architecture can guarantee a regenerative braking system, reducing the amount of energy dissipated through friction.

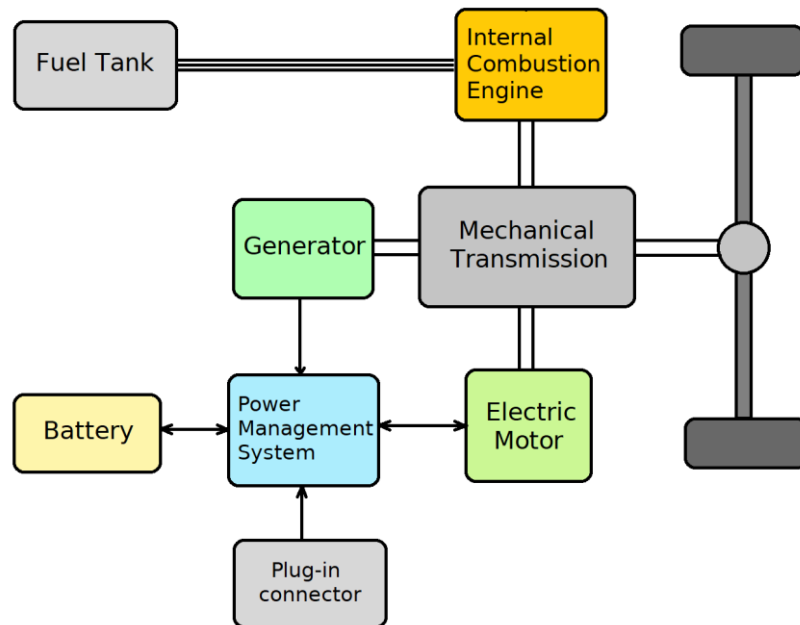


*Figure 19-Parallel/Series Hybrid schematic*

#### **2.1.4.1 Operating modes**

In the series-parallel hybrid system, it is possible to classify the different operation modes into two groups, engine-heavy and electric-heavy. The former indicates that the internal combustion engine works more than the electric motor during hybrid propulsion, while the electric-heavy indicates that the electric motor is more active. (K.T Chau, 2002).

- Engine-heavy series-parallel hybrid system: at startup, the battery solely provides the necessary power to propel the vehicle, while the engine is in the off mode. During full throttle acceleration, both the engine and electric motor proportionally share the required power to propel the vehicle. During normal driving, the engine solely provides the necessary power to propel the vehicle, while the electric motor remains in the off mode. During braking or deceleration, the electric motor acts as a generator to charge the battery via the power converter. For battery charging during driving, the engine not only drives the vehicle but also the generator to charge the battery via the power converter. When the vehicle is at a standstill, the engine can maintain driving the generator to charge the battery.

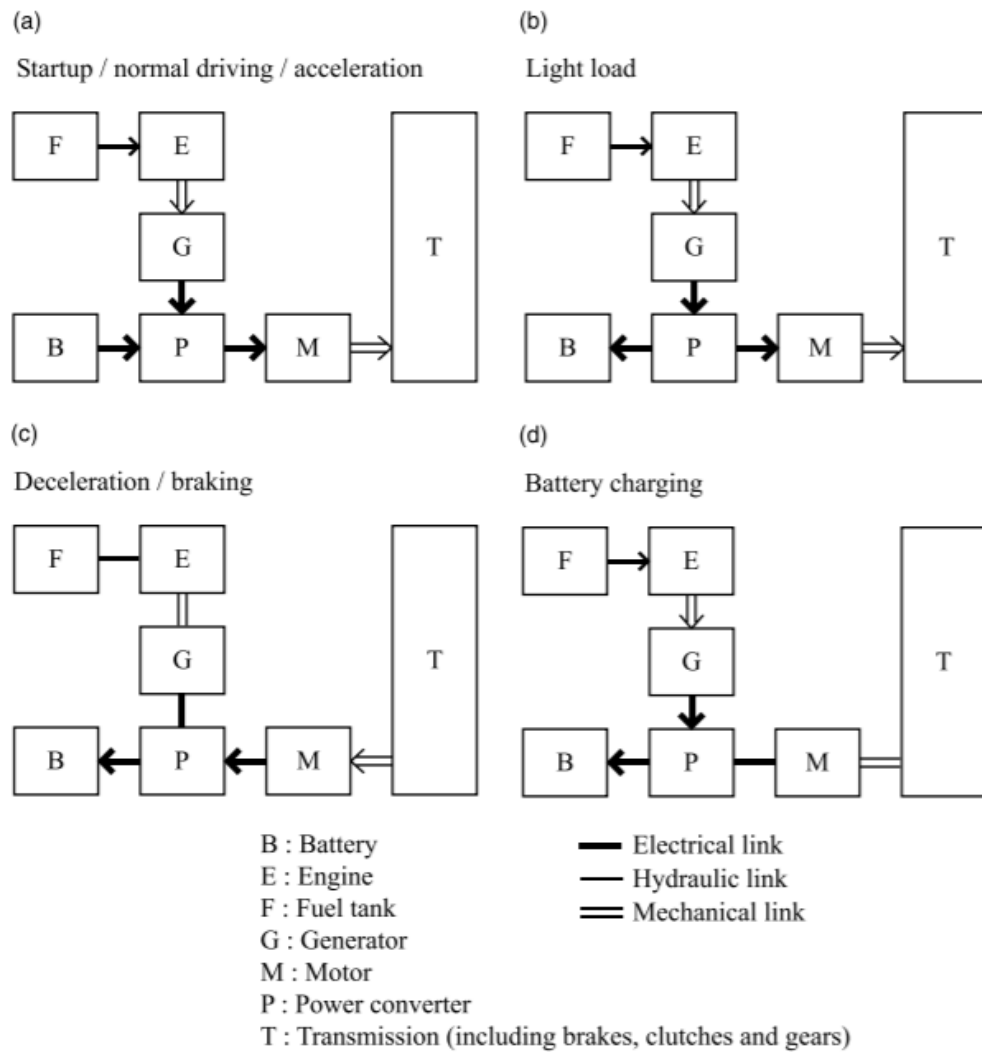


Figure 20-Engine-heavy series-parallel hybrid operating modes

- Electric-heavy series-parallel hybrid system: during startup and driving at light load, the battery solely feeds the electric motor to propel the vehicle, while the engine is in the off mode. For both full throttle acceleration and normal driving, both the engine and electric motor work together to propel the vehicle. The key difference is that the electrical energy used for full throttle acceleration comes from both the generator and battery, whereas that for normal driving is solely from the generator driven by the engine. Notice that a planetary gear is usually employed to split the engine output, hence to propel the vehicle and to drive the generator. During braking or deceleration, the electric motor acts as a generator to charge the battery via the power converter.

Also, for battery charging during driving, the engine not only drives the vehicle, but also the generator to charge the battery. When the vehicle is at a standstill, the engine can maintain driving the generator to charge the battery.

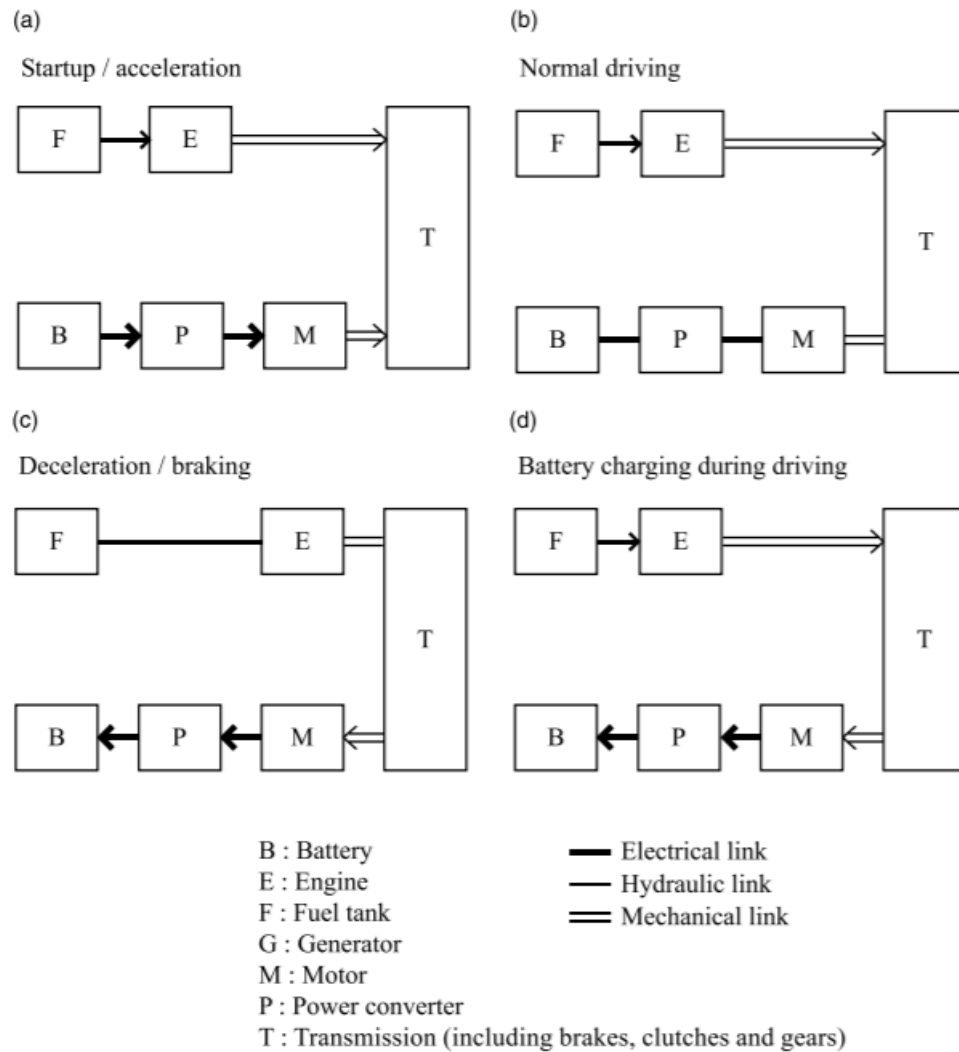


Figure 21-Electric-heavy series-parallel hybrid operating modes

## 2.2 Advanced Driver Assistance System (ADAS)

In recent years, continuous technological progress has led car manufacturers to equip their cars with electronic driver assistance systems developed to maximise driver and passenger safety. These electronic aids are referred to by the acronym ADAS or Advanced Driver Assistance Systems.

These assistance systems assist the user while driving and thus improve driving safety. They usually detect critical driving conditions and warn the driver with optical and acoustic signals, depending on the design.

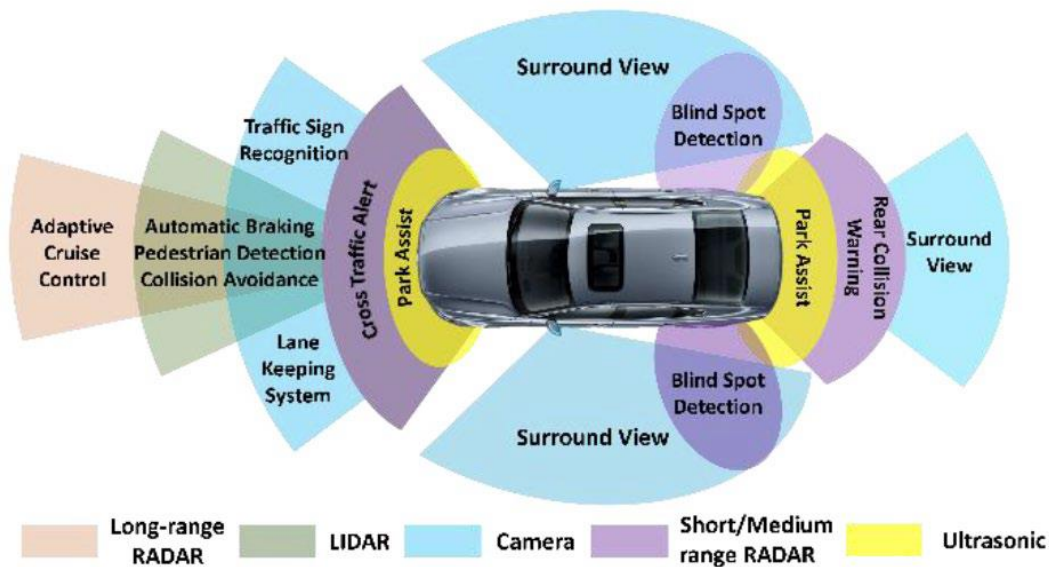


Figure 22-State-of-the-art ADAS and different sensors (Kukkala, Tunnell, Pasricha, & Bradley, 2018)

ADAS devices encompass various functionalities, and the following paragraphs will highlight some of the most innovative and secure technologies (Smirnov & Lashkov, 2015).

- **Adaptive Cruise Control (ACC)**

These systems use a radar sensor to maintain speed, a camera on the windscreen and directions from the navigation system. The cruise control maintains the driver's speed and adjusts it according to the speed of the previous car, accelerating or slowing down when and if necessary. This advanced driver assistance technology is perfectly applicable to motorways, where drivers need to monitor their cruise control systems for safety reasons constantly. Most of these systems automatically switch off below a certain speed threshold. It can also interact with Traffic Sign Recognition to adjust your pace to changing speed limits.

- **Autonomous Emergency Braking**

These range from simple systems, such as a camera, to more complex systems using radar. All, however, react at speeds of up to 30 km/h and, in this case, are referred to as City Brake Systems. Recognition of pedestrians or even cyclists are features of the more advanced systems, in the same way as operation at higher speeds requires radar. Some systems can act on the steering wheel to avoid collisions.

- **Adaptive Light Control**

Systems ranging from automatic activation of dipped headlights (with twilight sensor) to automatic high beam management. In the most advanced systems, "full LED matrix" headlights can modify the light beam by switching off areas corresponding to the vehicle in front or those coming in the opposite lane.

- **Automatic Parking System**

These systems can recognise parking spaces, indicate them to the driver and carry out manoeuvres by acting on the steering wheel, leaving the driver only the task of accelerating and braking. The most advanced systems need only 80 cm of space beyond the car's length to park longitudinally, can brake automatically in an emergency and use a series of ultrasonic sensors placed around the perimeter of the car.

- **Blind Spot Monitor**

Monitors the blind spot, the area where a passing vehicle does not yet enter the mirror's field of vision and is also hidden by the car's rear pillar. Other car detection systems use rear-mounted radar to monitor the area behind and beside the car. The system warns the driver of potential danger by activating an LED sensor in the rear-view mirror on the corresponding side. If the driver activates the indicator despite the warning, the LED starts flashing with increased intensity to draw the driver's attention to the potential danger. Some advanced systems can also act on the steering wheel.

- **Camera Monitor System**

These range from the simplest systems that use only the rear camera for manoeuvring, to those with four cameras on each side of the car and, thanks to software, to reconstruct an aerial view of the area and project it onto the interior monitor.

- **Cross-Traffic Alert**

Using cameras and sensors, it activates when approaching intersections, alerting the driver if any vehicles are approaching dangerously.



- **Driving Attention Assist**

Systems that monitor the driver's level of attention to help prevent nodding off. Some check driving style, others monitor gaze or head position and in the event of danger produce an audible alarm, often accompanied by a coffee cup symbol and an invitation to stop for a break.

- **Emergency Driver Assist**

This works by combining four driver assistance systems. If sensors detect that the driver is unconscious (has not used the brakes, accelerator or steering for a given time), the system initiates coordinated countermeasures. First, the driver is subjected to stimuli using acoustic, visual and physical warnings (hitting the brakes). If he does not react, the emergency stop procedure is activated: the four emergency lights are activated, and ACC facilitates automatic braking and helps to prevent the car from hitting the vehicle in front. Even on roads with several lanes, the system steers in a controlled manner to the rightmost lane until the car comes to a stop while calling for help

- **Hill Descent Control**

Mainly used on SUVs, it takes control of the car on steep gradients by coordinating brake action through ESC and maintaining a pre-determined speed (below 5 km/h).

- **Lane Change Assist**

Usually found in conjunction with the more advanced ACC system. It is capable of autonomously changing lanes to overtake. The driver is only required to operate the indicator.

- **Lane Keeping Assist**

Helps the driver maintain his or her own lane

- **Night View Assist**

Uses infrared sensors and/or a thermal camera to determine vehicles, humans and animals when driving at night.

- **Traffic Jam Assist**

This is an advanced ACC function that requires an automatic transmission, as it can stop and restart the car in a queue when stop-and-go traffic situations occur.

- **Traffic Sign Recognition**

Using information from the front camera, it can display the speed limit in force on that stretch of road on the dashboard.

## 2.3 Connected and automated vehicle

Autonomous driving and connected vehicles are solutions to cope with the increasing number of vehicles on the road.

So-called connected and autonomous vehicle technology (CAV) can provide a wide range of safety applications for safer, greener and more efficient intelligent transportation systems (ITS) (Wei, 2018). The previously described ADAS systems use the host vehicle's computing and sensing resources, so communication with other vehicles is not required. On the other hand, connected vehicle technology is a passive road safety technology, which relies on exchanging messages with vehicles to obtain information about the driving context. The advancement of research has made it possible to combine the two technologies into a single CAV (connected and autonomous vehicle) technology. SAE International, a standard-setting body in the automotive industry, established in 2014, through the Taxonomy and Definitions for Terms Related to On-Road Motor Vehicle Automated Driving Systems, six different levels of autonomous driving (International, 2016):

- **Level 0:** no automation, the driver must take full responsibility for driving the vehicle; steering and accelerator are completely dependent on the driver, even considering any hazard warning systems. Control of the surrounding environment is always the responsibility of the driver.
- **Level 1:** assisted driving, the user still has complete responsibility for driving the vehicle; however, the system informs the user of possible dangers or adverse situations through various visual and/or acoustic warnings. There are two main implementations of a level 1 vehicle compared to a level 0 vehicle: adaptive cruise control, which not only maintains a constant speed along the desired route but is also able to automatically slow the car down if it detects that it is too close to a vehicle in front; and Lane Keeping Assistance (LKA) and Emergency Lane Keeping (ELK) systems, which enable the car to make small steering corrections to avoid unintended lane

departure. Even for this level of automation, the user must be in complete control of their surroundings.

- **Level 2:** partial automation, with this level of automation, the vehicle becomes, in certain situations, potentially able to drive autonomously; the electronic system, particularly in predefined scenarios such as motorway journeys, can take control of the steering and accelerator, making use of assisted braking and emergency braking in some cases. The SAE specified that the substantial difference between a level 2 vehicle and a level 1 vehicle is that the user may not interact with the car by taking his hands off the steering wheel and his foot off the pedals at the same time. However, the driver still has full responsibility for the vehicle, and must be ready to intervene whenever the situation requires it; in this regard, the user must still take care of personally monitoring the vehicle's surroundings.
- **Level 3:** Conditional automation, cars reaching this level of automation begin to see themselves equipped with instruments capable of fully monitoring their surroundings. Even though the user is still required to intervene in certain situations, the substantial difference with a level 2 vehicle is that this would be limited to cases of danger; this allows the user, especially in more controlled situations such as driving at low speeds (we are talking about speeds below 60 km/h), paying minimal attention to the surrounding environment, leaving room for the possibility of engaging in other activities while driving. The discussion of user attention is the main argument that defines level 3 vehicles' borderline from level 2 vehicles.
- **Level 4,** high automation: with the achievement of level 4, the vehicle has almost total autonomy; in addition to including all the tools of the previous levels, it guarantees total automatic control over the vehicle in certain situations, such as busy areas or driving on country roads. Level 4 is the first level on the automation scale to allow the user to be completely unaware of the external environment, as the vehicle will always take action even if a dangerous manoeuvre is required. This level of autonomous driving is currently restricted, as already mentioned, not only to specific situations but also to specific geographical locations, so that the driver still has the possibility to take manual control of the vehicle.
- **Level 5:** total automation, is ideally the maximum degree of automation a vehicle could achieve. A vehicle with an automated driving system of this calibre would perform any

driving-related function, eliminating the driver's figure and making every user on board a simple passenger. This degree would be high enough to make components such as the steering wheel and pedals superfluous, as there would be no need for user intervention. The vehicle would be completely autonomous in identifying the route to follow, choosing the right direction and accelerating or slowing down according to external conditions, such as traffic or sudden situations

Considering the levels of automation described above, ADAS technologies can only meet levels 1 and 2. To increase the level of automation, connected vehicle technology is necessary.

CAV can support a wide range of applications, which can be divided into two categories: driving safety applications; transportation efficiency applications; and entertainment and comfort applications (Wei, 2018). Driving safety applications are mainly aimed at reducing traffic accidents and improving driving safety. These can be applied either with autonomous driving or separately connected vehicles or with both technologies. Besides, environmental measurements can be used to deliver messages to raise awareness of eco-friendly driving. By implementing algorithms for data analysis and engine control, vehicles have detected an obstacle to making decisions to remedy problems. Examples include emergency braking and lane departure warning. Transport efficiency applications are implemented for mobility management reducing fuel consumption and transport time. Through connected vehicle technology such as vehicle to infrastructure (V2I) and vehicle to networks (V2N), it is possible to receive information on current traffic, road works and the driving environment.

# 3 Modelling Approach

As explained in the literature review, electrification of vehicles, i.e. hybrid and electric vehicles, will represent the automotive world's future. The complexity of hybrid propulsion models forces many tests to calibrate the powertrain in different driving scenarios.

The study of the power management of a hybrid vehicle can be conducted using different analysis methods. Each of these approaches the problem from a different perspective, but all aim to evaluate the energy flows (and consequently estimate fuel consumption rather than determine the state of charge of the battery) of the various devices in the vehicle's various operating conditions. A first fundamental distinction that can be introduced is based on the "direction" of the calculation method adopted: from this point of view, a distinction is made between backward and forward methods.

## 3.1 Forward Approach Model

A forward approach is a method by which the analysis is conducted in the direction from the engine to the wheels through the various devices characterising the drive train: i.e. a reference driving cycle is assumed a priori, the behaviour of a hypothetical driver who acts on the accelerator/clutch/brake controls so that the vehicle follows the cycle considered is defined, the difference between the instantaneous speed of the vehicle and that of the cycle generates an error signal which, when retroactively activated, corrects the actions of the driver; in this case, the characteristic quantities of the various organs are determined according to the fundamental relations which describe their behaviour, but the input variables are equivalent to those which in the backward method will represent the output variables

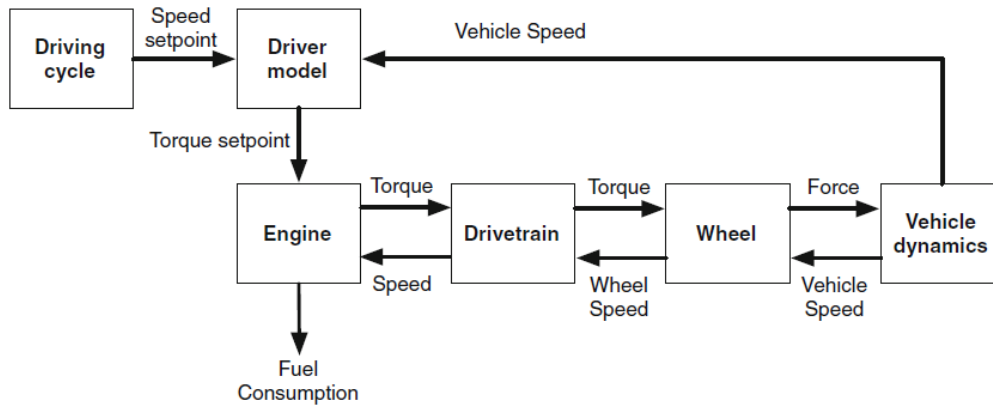


Figure 23- Information flow in a forward simulator (Simona, Lorenzo, & Giorgio, 2016)

### 3.1.1 Dynamic method

The dynamic method is a forward method based on a precise mathematical formulation of the relationships describing the devices' behaviour constituting the drive train under consideration. The description through this method allows us to consider many dynamic effects: some of these effects assume greater relevance in estimating fuel consumption (such as the engine temperature dynamics). In contrast, others (such as the effect of the vehicle's variation during the motion) lend themselves more to mechanical evaluations. Being a forward method, in the dynamic method, the inputs are represented by the same quantities that constitute the input of the real system, i.e. the driving controls operated by the driver. Although this method provides much flexibility, it requires a high computational capacity. The implementation can be done through MatLab/Simulink, which does not guarantee good flexibility of use since the eventual modification of the system's topology requires the re-definition of the mathematical model.

### 3.2 Backward Approach Model

A backward method is a method in which the analysis is carried out going back to the propeller through the study of the behaviour of the various parts of the drive train: i.e. considering a hypothetical temporal evolution of the vehicle's speeds, the characteristic quantities of the various parts are determined according to the fundamental relations which describe their

behaviour, proceeding from the wheels towards the engine responsible for propelling the vehicle.

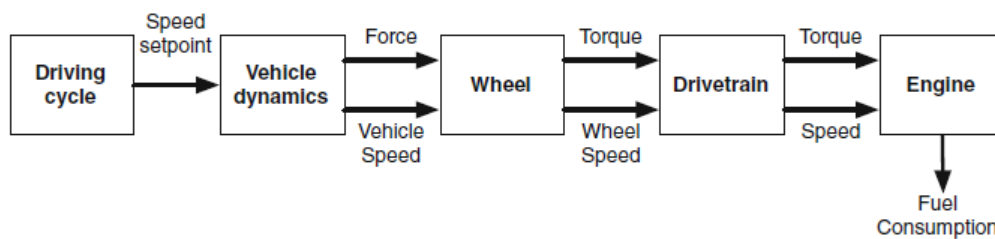


Figure 24- Information flow in a backward simulator (Simona, Lorenzo, & Giorgio, 2016)

### 3.2.1 Quasi-Static method

The quasi-static method is the backward method, which allows estimating a vehicle's energy consumption by assuming that its motion develops through a finite succession of static states, characterised by constant speeds and powers. This method's starting point is the driving cycle (assumed a priori) against which the vehicle behaviour is evaluated. As it is a backward method, the estimation of energy consumption and the state of charge of the batteries is approached from the wheels to the drive train's various elements, extracting only a few points from the driving cycle. In this method, the cycle is considered in its entirety and is divided into short intervals during which it is assumed that the system operates under static conditions. Consider the following speed profile:

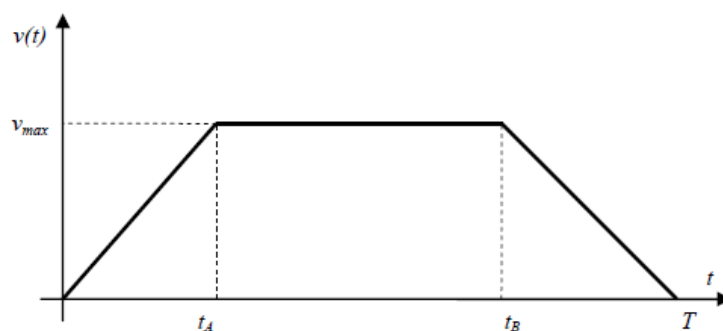
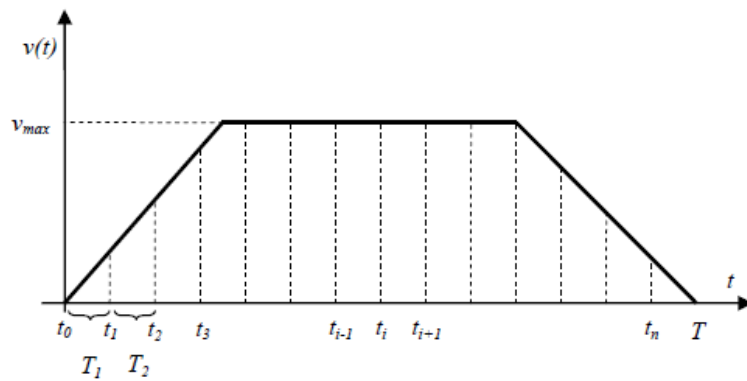


Figure 25- Generic speed profile

The represented profile can be described analytically as a function of time, but such a formulation cannot be treated numerically in the computer. Therefore, by operating a discretization of the time axis,  $T$  is the cycle's duration, and a step  $h$ , the intervals  $T/h$  and the instants  $t_i$  separating them are identified. Therefore, it is possible to extrapolate from the velocity profile the values that the velocity assumes in correspondence of the instants considered.



*Figure 26- Time axis discretisation*

The midpoint method is applied to each of the previous intervals to obtain a new velocity profile.

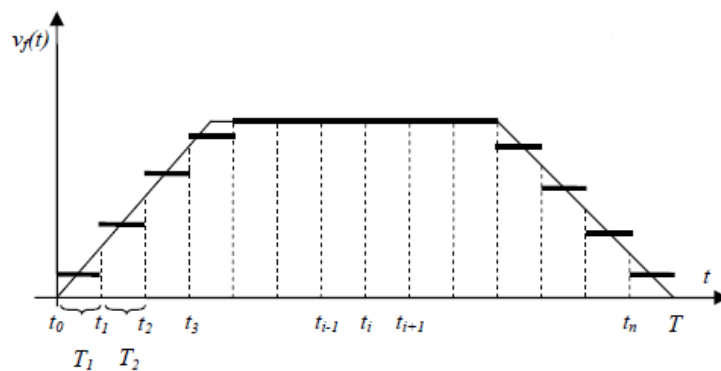


*Figure 27-Discrete and analytical speed profile*



The new speed profile represents an approximation of the actual speed of the vehicle. However, it allows an important simplification: the integral/differential equations describing the vehicle motion are reduced to finite difference equations, which can be easily treated in numerical form in the computer. Therefore, it is possible to trace the time profiles of the characteristic quantities of the devices that make up the drive train in question and consequently estimate the vehicle's energy consumption. The quasi-static method, therefore, lends itself to tackling energy minimisation problems of complex drive trains as it is possible to identify general rules for energy management whose effectiveness can then be verified by applying the method to different speed profiles. The main disadvantage of the method is that it requires precise knowledge of the entire driving cycle and therefore precludes the possibility of assessing, for example, the effects of randomness on a real route.

### **3.3 Conclusion**

The most evident difference between the two methods is that, while an analysis through a forward method requires the definition and the use of a model that emulates the behaviour of the driver (who can act freely or in such a way as to follow a predefined driving cycle), a backward method requires, as the only input, a hypothetical speed profile of the vehicle. Therefore, the choice of the calculation method is the first step to take to face the energy analysis of any vehicle. In this respect, it is necessary to bear in mind that each method is characterised by its own mathematical complexity and can offer a different precision of the results that cannot be ignored. The analysis methods introduced are independent of the vehicle's drive train configuration (hybrid, electric and conventional). In the present work, particular attention has been paid to the quasistatic method, which is the most widely used method and can offer good accuracy of results while keeping computational complexity low.

## 4 Model Overview

The model is implemented in the Simulink-Matlab environment. Matlab software collects input data such as vehicle mass, engine map, and code strings to identify the optimal operating line, which is fundamental for implementing the control strategy. The approach chosen for this work was that of the Backward Model, which is best suited to the objectives set, namely reducing consumption, and improving energy management. The Simulink environment's vehicle is subdivided into functional blocks; the following paragraphs will describe each of them and how they have been calibrated to obtain the desired results.

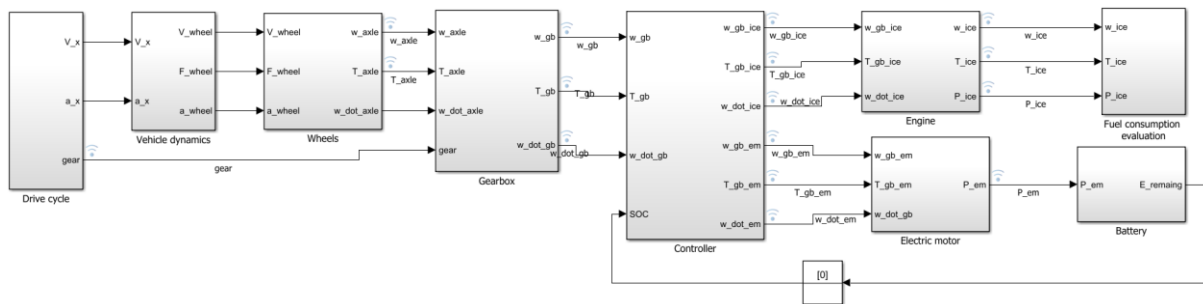


Figure 28- Backward Simulator of HEV P2

### 4.1 Drive Cycle

Before being sold, vehicles have to undergo a series of tests based on specific driving cycles to ensure that they comply with regulations. Driving cycles are speed profiles based on statistical data and implemented on chassis dynamometers to assess emissions and consumption. In the European context, the homologation cycles are the NEDC (New European Driving Cycle) and the WLTC (Worldwide Harmonised Light Vehicles Test Cycle). The Drive Cycle block allows the reference drive cycle to be implemented within the simulator.

#### 4.1.1 NEDC

The NEDC (New European Driving Cycle) was the driving cycle used within the European Union until August 2017.

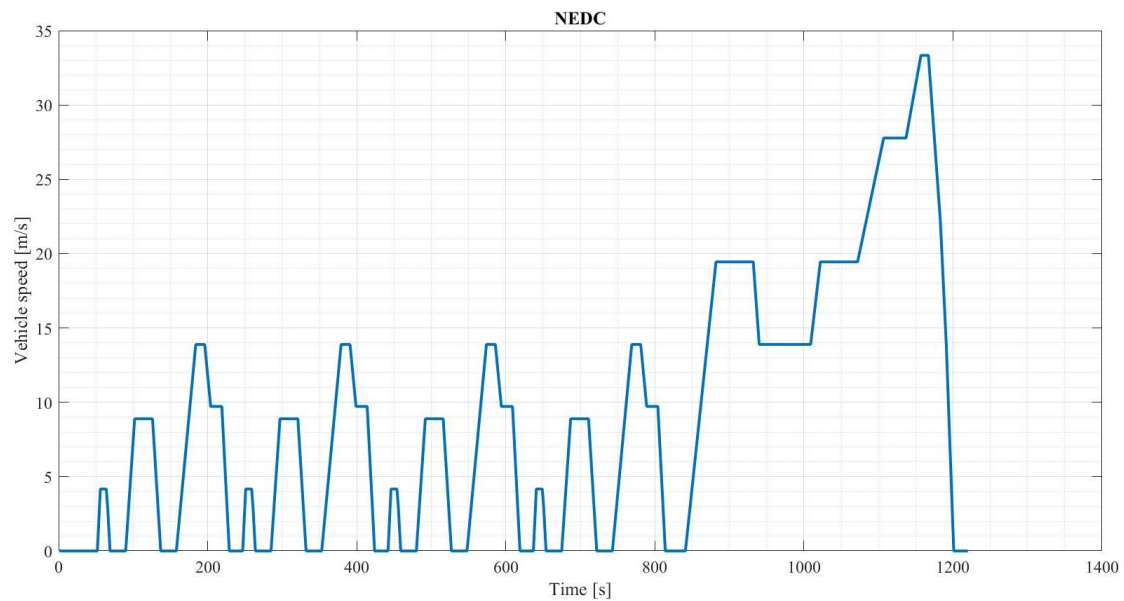
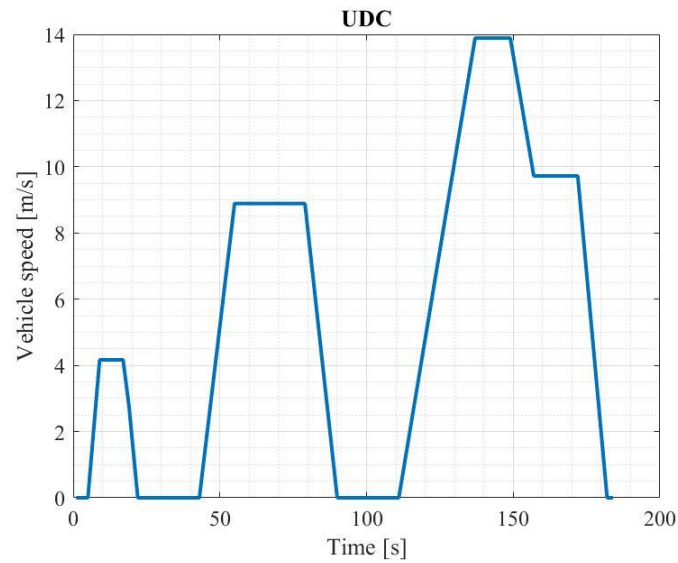


Figure 29 - New European Driving Cycle

It is a combination of two elementary modules: the UDC (Urban Driving Cycle) or ECE15, which is indicative of an urban cycle with a maximum speed of 50 km/h, and the EUDC (Extra Urban Driving Cycle), which is indicative of an extra-urban cycle with a top speed of 120 km/h. The overall driving cycle comprises four repetitions of the urban cycle and one repetition of the extra-urban cycle, performed without interruption. The average consumption is given by the combination of urban and extra-urban values. The **Table** shows the characteristic data for the cycle under consideration.

Characteristics	Unit	ECE 15	EUDC	NEDC†
Distance	km	0.9941	6.9549	10.9314
Total time	s	195	400	1180
Idle (standing) time	s	57	39	267
Average speed (incl. stops)	km/h	18.35	62.59	33.35
Average driving speed (excl. stops)	km/h	25.93	69.36	43.10
Maximum speed	km/h	50	120	120
Average acceleration <sup>1</sup>	m/s <sup>2</sup>	0.599	0.354	0.506
Maximum acceleration <sup>1</sup>	m/s <sup>2</sup>	1.042	0.833	1.042
† Four repetitions of ECE 15 followed by one EUDC				
<sup>1</sup> Calculated using central difference method				

Figure 30 - NEDC summary parameters (DieselNet, s.d.)



*Figure 31 - Urban Driving Cycle*

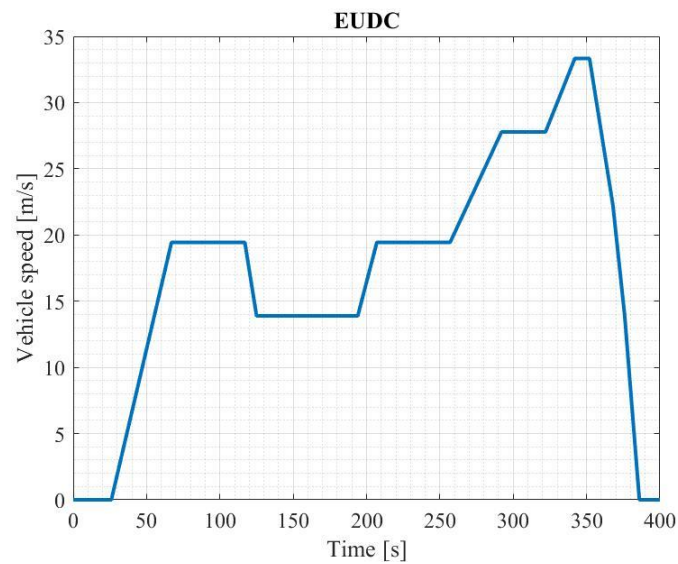


*Figure 32 - Extra Urban Driving Cycle*

#### 4.1.2 WLTP

Since September 2017, a new reference cycle, the World Harmonised Light Vehicle Test Procedure (WLTP) has been introduced. The WLTP uses new driving cycles (WLTC - Worldwide Harmonised Light-duty Vehicles Test Cycles) to measure the fuel consumption, CO<sub>2</sub> emissions and pollutant emissions of passenger cars and light commercial vehicles.

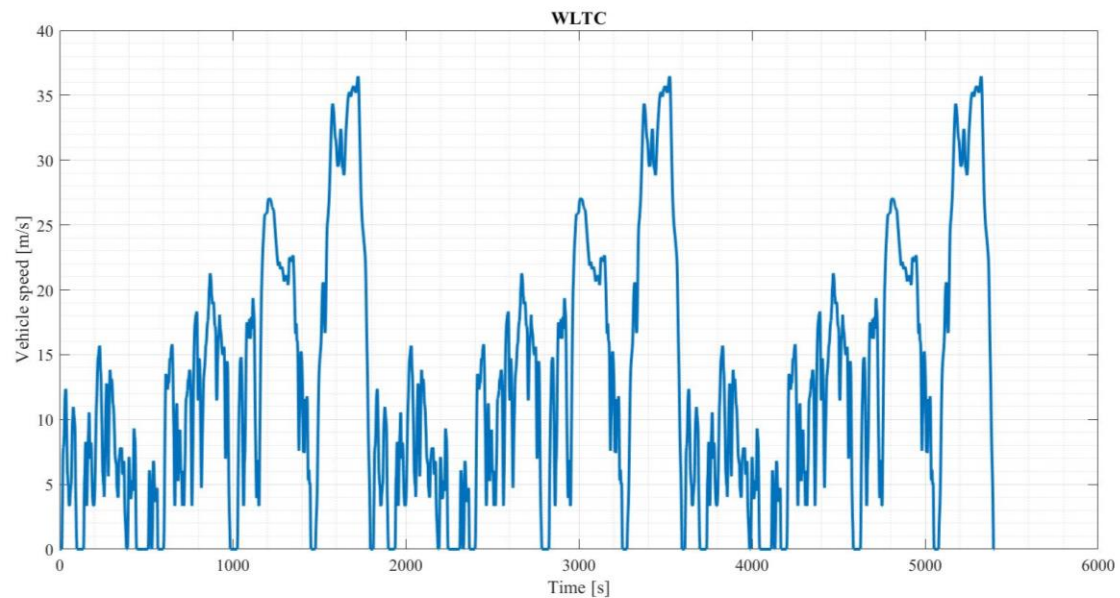
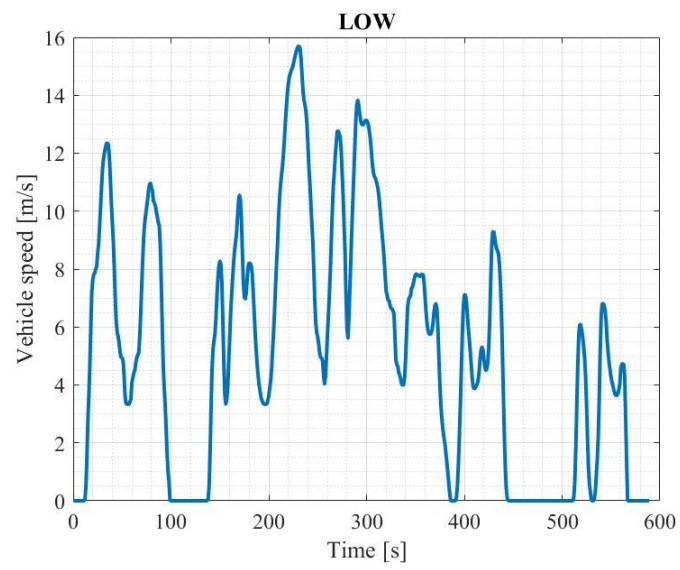


Figure 33 - Worldwide Harmonised Light-duty Vehicles Test Cycles

The WLTC is divided into four phases: Low speed (up to 56,5 km/h), Middle speed (up to 76,6 km/h), High speed (up to 97,4 km/h), Ex-High speed (up to 131,3 km/h). These parts of the cycle simulate urban and suburban driving and drive on country roads and highways. The cycle has been repeated three times. The procedure also considers all optional contents that influence aerodynamics, rolling resistance and vehicle mass, resulting in a CO<sub>2</sub> value that reflects the characteristics of the individual vehicle.

Phase	Duration	Stop Duration	Distance	p_stop	v_max	v_ave w/o stops	v_ave w/ stops	a_min	a_max
	s	s	m		km/h	km/h	km/h	m/s <sup>2</sup>	m/s <sup>2</sup>
Class 3b (v_max ≥ 120 km/h)									
Low 3	589	156	3095	26.5%	56.5	25.7	18.9	-1.47	1.47
Medium 3-2	433	48	4756	11.1%	76.6	44.5	39.5	-1.49	1.57
High 3-2	455	31	7162	6.8%	97.4	60.8	56.7	-1.49	1.58
Extra-High 3	323	7	8254	2.2%	131.3	94.0	92.0	-1.21	1.03
Total	1800	242	23266						

Figure 34 - WLTC summary parameters (DieselNet, s.d.)



*Figure 35 - WLTC LOW part*

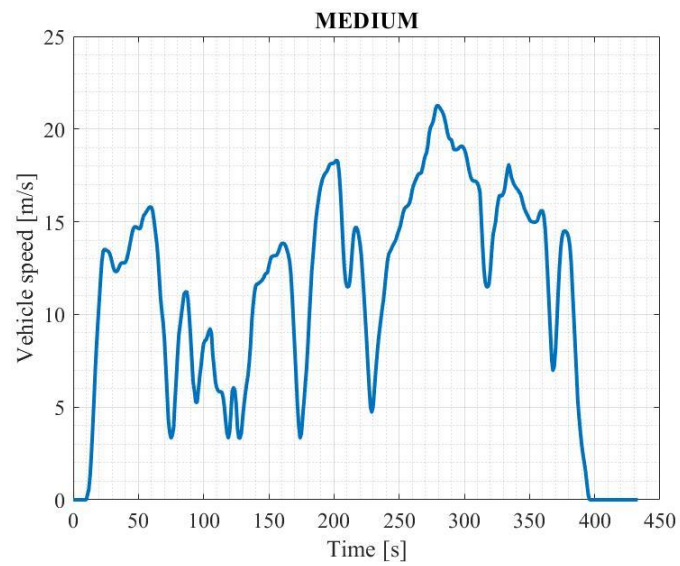


*Figure 36 - WLTC MEDIUM part*

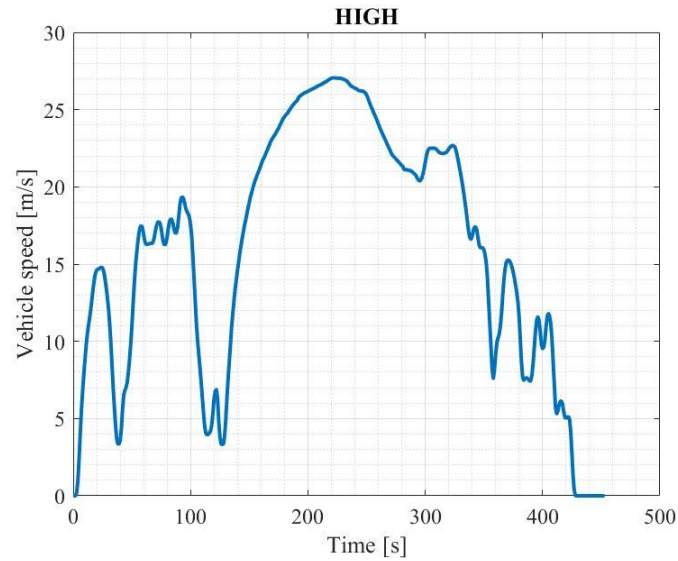


*Figure 37 - WLTC HIGH part*

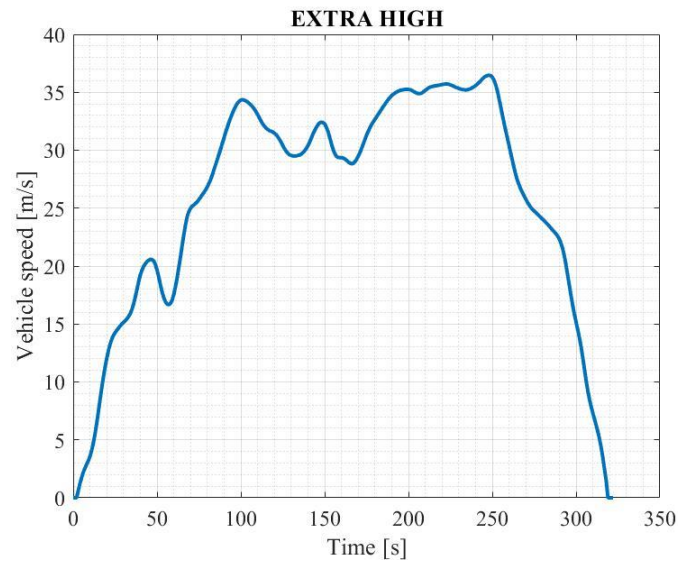


*Figure 38 - WLTC EXTRA HIGH part*

The need to introduce a new test procedure arise from the previous one's poor reliability in terms of scenario and driving style representation. The engine operating points are distributed over a much wider area than in NEDC, thus achieving maximum BMEP values. It considers a dynamic driving style; the vehicle mass is the sum of the curb mass, optional equipment, and laden mass. Also, for vehicles equipped with a manual transmission, the test provides for the definition of the gear shift profile depending on the vehicle's characteristics rather than a fixed profile. The graphs in Figure 39 and Figure 40 show the differences between the two cycles.

Parameter	NEDC	WLTC	Delta
Total time (s)	1180	1800	620
Distance (km)	11,0	23,3	12
Max speed (km/hr)	120	131	11
Average Speed (km/hr)	34	47	13
Max acceleration (m/s <sup>2</sup> )	1,1	1,7	0,6
Max deceleration (m/s <sup>2</sup> )	-1,4	-1,5	-0,1
Constant driving time (s)	475 (40%)	66 (3.5%)	-37%
Acceleration time (s)	247 (21%)	789 (44%)	23%
Deceleration time (s)	178 (15%)	719 (40%)	25%
Stop time (s)	280 (24%)	226 (12.5%)	-12%

Figure 39 - Comparison of NEDC and WLTC parameters

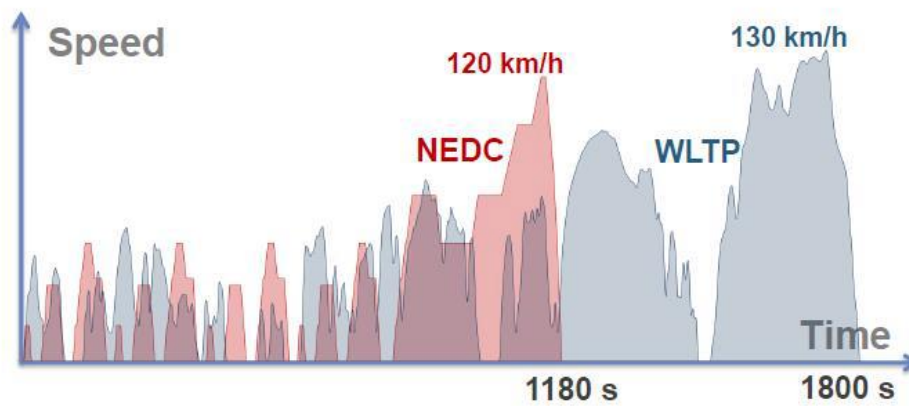


Figure 40 - Comparison of speed profiles between NEDC and WLTP cycles

#### 4.1.3 Drive Cycle block

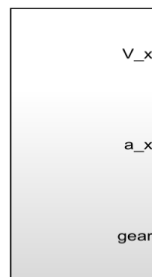


Figure 41- Drive Cycle Block

Inside the block, the vehicle's speed profile was loaded from which acceleration and longitudinal speed of the vehicle were evaluated. The third output is the gear of the vehicle.



The strategy adopted to calculate the gear is divided into shifting logic and downshifting logic. Both use speed-based shifting; there is a kind of hysteresis loop. In the first logic, if a certain speed is reached, the gear is changed, while in the downshifting logic, as soon as a certain lower speed is reached, the gear is downshifted.

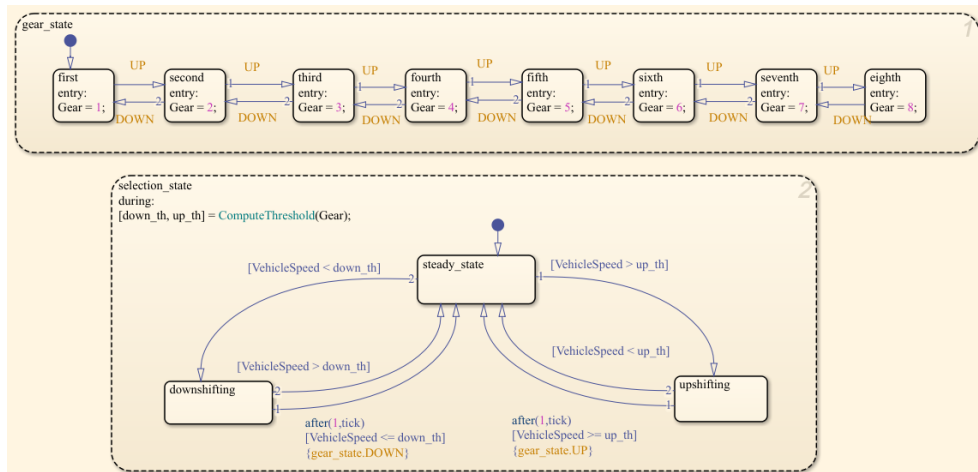


Figure 42- Gear shift strategy

## 4.2 Vehicle Dynamics

The vehicle dynamics blocks' inputs are speed and longitudinal acceleration, the outputs are speed, acceleration, and calculated wheel force.

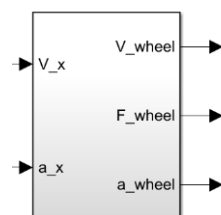


Figure 43- Vehicle Dynamics Block

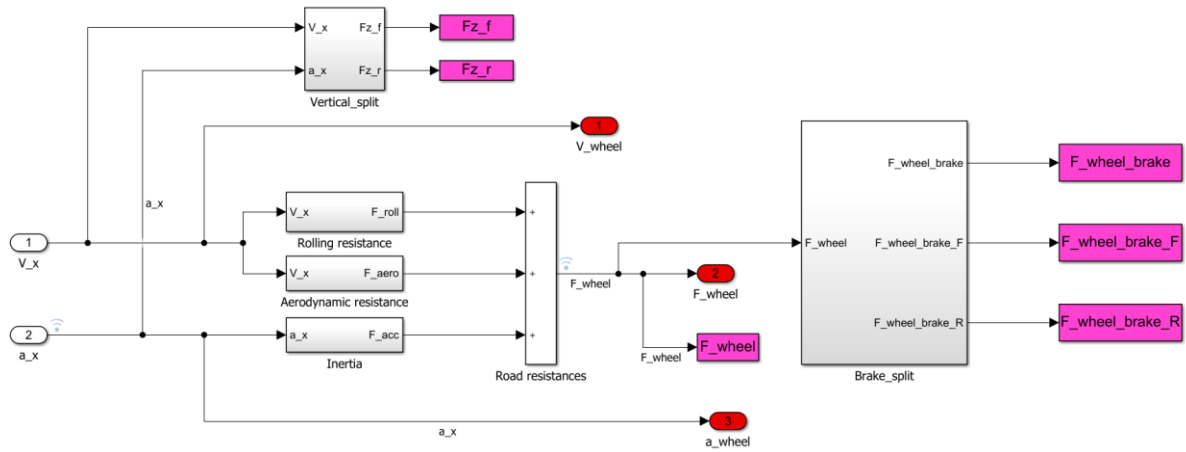


Figure 44- Vehicle Dynamics block from inside

Generally, the study of dynamics is carried out by representing the vehicle using an accurate model in such a way as to describe all the dynamic phenomena during motion. Since overly complex models become unmanageable both from the point of view of mathematical formulation and management of results, a relatively simple model with a few degrees of freedom has been implemented in such a way as to describe the salient aspects of motion. The simplifying assumptions are:

- No wheel slippage concerning the road surface.
- Constant vehicle mass during motion: the mass variation due to fuel consumption is negligible.

#### 4.2.1 Longitudinal force

The longitudinal force acting on all four wheels was taken into account in the calculation:

- Aerodynamic Resistance:

$$F_a = \frac{1}{2} \cdot \rho_a \cdot A_f \cdot C_d \cdot v_x^2 \quad Eq. 4$$

Where is  $\rho_a$  air density,  $A_f$  frontal air of the vehicle in the direction of motion,  $C_d$  drag coefficient in the direction of motion,  $v$  longitudinal velocity calculated in the previous block.

- Rolling Resistance:

$$F_r = m_v \cdot g \cdot f_r \quad \text{Eq. 5}$$

Where  $m_v$  vehicle mass,  $g$  gravitational acceleration,  $f_r$  rolling coefficient. Generally,  $f_r$  is a function of vehicle speed, tyre pressure and road surface condition. In many applications, particularly when the vehicle speed remains moderate, the rolling coefficient can be assumed as a constant value.

- Inertia:

$$F_a = m_v \cdot a_x \quad \text{Eq. 6}$$

Where  $m_v$  is vehicle mass, and  $a_x$  longitudinal acceleration.

### 4.2.2 Ideal Braking

This block aims to analyse the braking system of a vehicle in ideal condition. I analysed braking forces on the two axles using the four wheels' force to understand by entering in the ideal braking plot what should be the braking forces on the two axles to get an ideal braking condition. Then the curve was plotted on the Matlab environment.

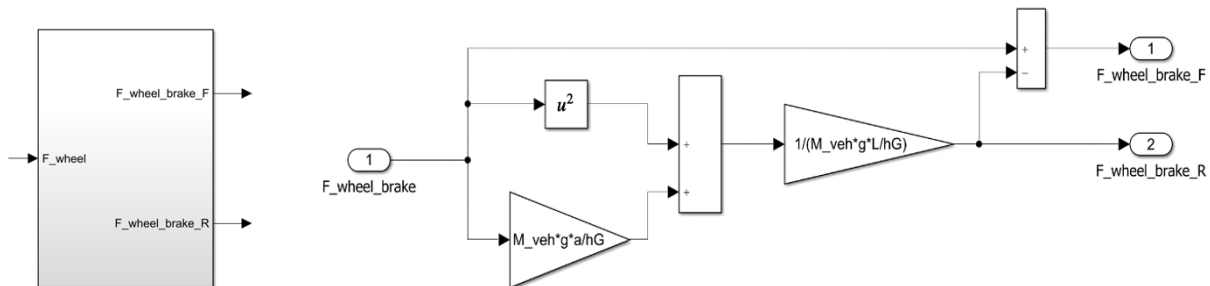


Figure 45- Brake split block (Ideal Braking Subsystem)

From dynamic equilibrium, the total braking force acting on a vehicle is:

$$F_x = \sum_i \mu_{xi} F_{zi} \quad \text{Eq. 7}$$

$F_{zi}$  is the vertical force acting on each tire and  $\mu_{xi}$  is the friction coefficient at wheel-ground contact of each braking wheel. It has been assumed that rolling resistance and aerodynamic forces are negligible, and friction coefficient  $\mu_{xi}$  equal for each wheel; the equation of motion in the longitudinal direction becomes:

$$m \frac{dV}{dt} = \mu_x m g \cos(\alpha) - m g \sin(\alpha) \quad Eq. 8$$

By simplifying the mass and considering the road grade ( $\alpha$ ) is equal to zero:

$$\frac{dV}{dt} = \mu_x g \quad Eq. 9$$

From the (Eq.7) it is possible to understand that for the evaluation of longitudinal forces is necessary to compute vertical forces acting on the front and rear axle. If I keep neglecting rolling resistance and aerodynamics, vertical forces become:

$$F_{z1} = \frac{m}{l} \left[ g b \cos(\alpha) - g h_G \sin(\alpha) - h_G \frac{dV}{dt} \right] \quad Eq. 10$$

$$F_{z2} = \frac{m}{l} \left[ g a \cos(\alpha) + g h_G \sin(\alpha) + h_G \frac{dV}{dt} \right] \quad Eq. 11$$

By substituting  $F_{x1} = \mu_x F_{z1}$  and  $F_{x2} = \mu_x F_{z2}$ , I found the following equation:

$$(F_{x1} + F_{x2})^2 + m g \cos^2(\alpha) \left( F_{x1} \frac{a}{h_G} - F_{x2} \frac{b}{h_G} \right) = 0 \quad Eq. 12$$

This expression relates the front braking force  $F_{x1}$  with the rear braking force  $F_{x2}$ : it is easy to notice that this equation represents a parabola with symmetry axis corresponding with the bisector of the second and fourth quadrant. The line I obtained is the best situation for a braking condition, since It has been imposed  $\mu_{x1} = \mu_{x2}$ .

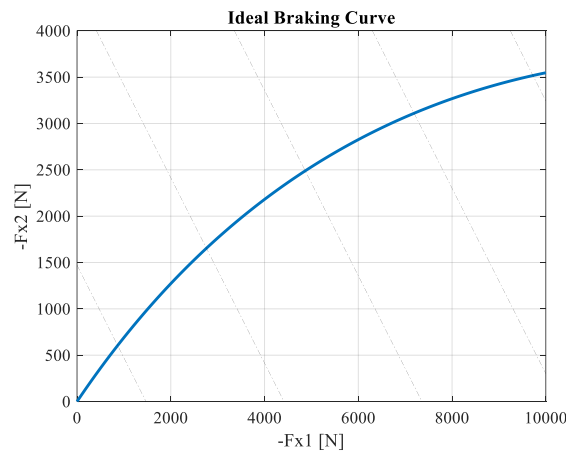


Figure 46- Ideal braking curve

The most important part of the graph in the first quadrant region is close to the origin because it represents braking forces' real values. All the points on the continuous curve correspond to the intersections between two straight lines corresponding to an equal value of  $\mu x_1$  and  $\mu x_2$ . I could expect this because continuous curves represent the ideal situation (in which  $\mu x_1 = \mu x_2$ ).

### 4.3 Wheels

This block calculates, based on the forces applied to the wheels, what the torque is on both axes taking into account the wheels' inertia.

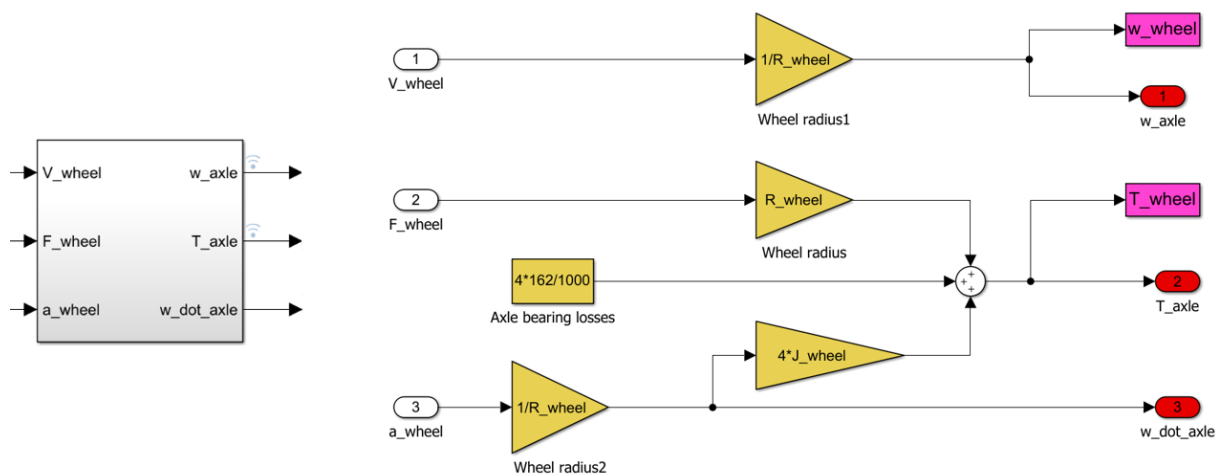


Figure 47- Wheels Block

### 4.4 Gearbox

The gearbox is a mechanical device used to increase the output torque or change the motor's speed (RPM).

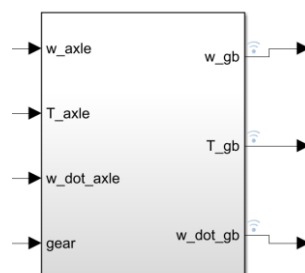


Figure 48- Gearbox block

The motor's shaft is connected to one end of the gearbox and through the internal configuration of gears of a gearbox, provides a given output torque and speed determined by the gear ratio.

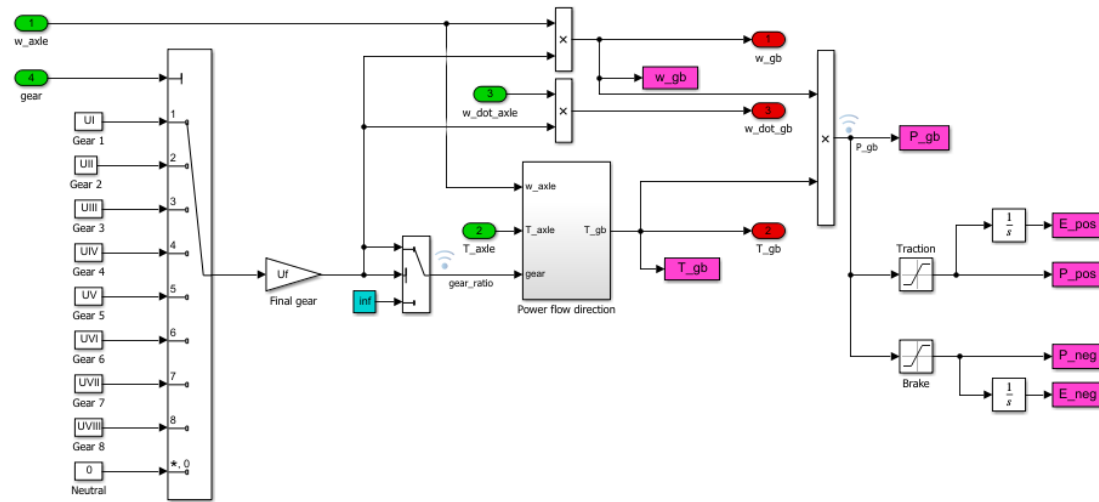


Figure 49- Gearbox block from inside

The gearbox's efficiency and the final drive were taken into account within the block, and a Power Flow Direction sub-system was created through which it is possible to identify whether the torque coming from the axle is a traction braking torque. This information has enabled the control strategy to be managed optimally so that the next block does not need to be checked for torque sign.

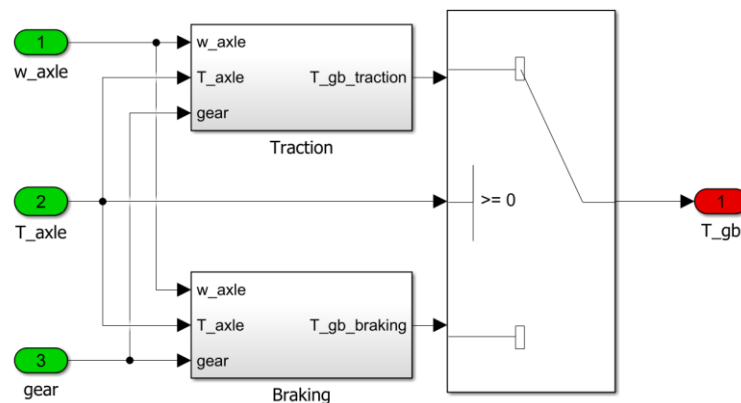


Figure 50- Power Flow Direction Subsystem

## 4.5 Controller

A new controller block has been created. It is responsible for performing the power management optimisation of the hybrid vehicle. Speed, acceleration, and torque are sent from the gearbox block, while SOC comes from the battery model as feedback. The block can distribute the torque and speed for the ICE and the electric motor according to the control strategy's modes of operation.

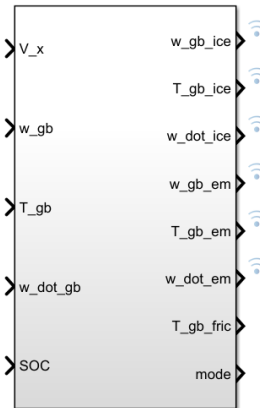


Figure 51- Controller block

A Stateflow approach was used. It is a Matlab toolbox that allows the simulation of state machines and flows diagrams through a graphical representation of states, transitions, and data.

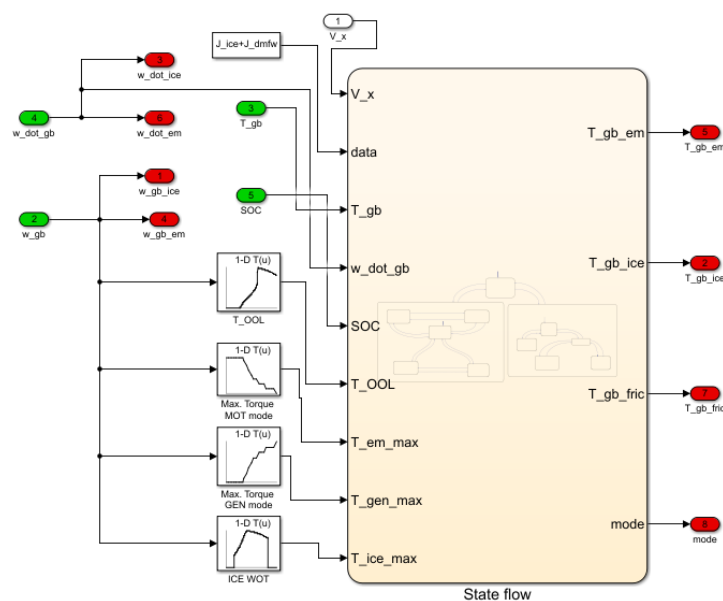


Figure 52-Controller block from inside

Interfacing with Simulink is done in two different ways: input and output ports to the chart and Data Store blocks. The torque value required by the driving cycle and the battery state is given through a port. The limit torque values of the internal combustion engine and the optimal operating line torque are implemented through a 1-D look-up table, which has as input the current engine rpm. The optimal operating line is obtained, as described in paragraph 5.2.4.

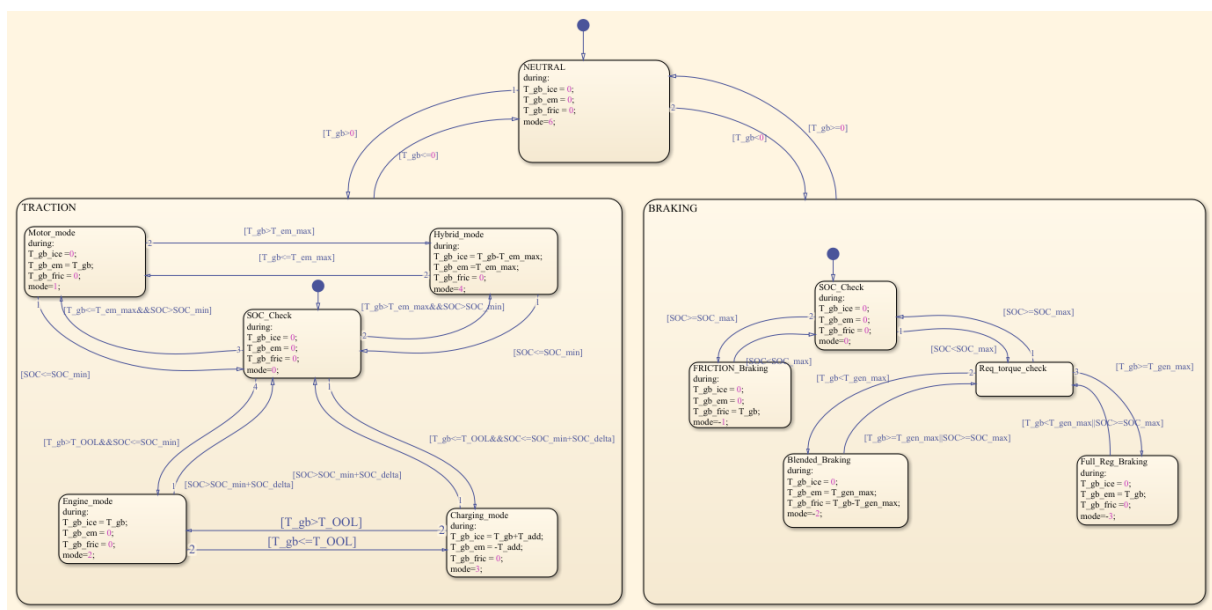


Figure 53-Stateflow chart

The Stateflow chart shows how the control strategy is executed. Depending on the torque value required by the drive cycle, the control enters the "TRACTION" or "BRAKING" block. At this point, the torque limit values set by the electric motor and internal combustion engine are taken into account, and depending on the state of charge of the battery, the command will be executed within one of these blocks until the conditions required to enter the functional block are no longer valid and then move into a new operating mode.



## 4.6 Engine

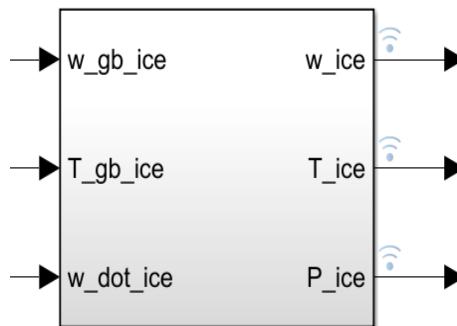


Figure 54- Engine block

The engine block, which is shown in figure 54, has as input speed and acceleration at the gearbox output and as output speed, power and torque required by the internal combustion engine. To calculate the power required by the internal combustion engine, the torque coming from the gearbox and the torque due to the engine's inertia are added together. Once the product of torque and angular velocity, given as input, has been made, it has been possible to evaluate the power required from the engine in which the auxiliaries (e.g. air conditioning system) are also taken into account.

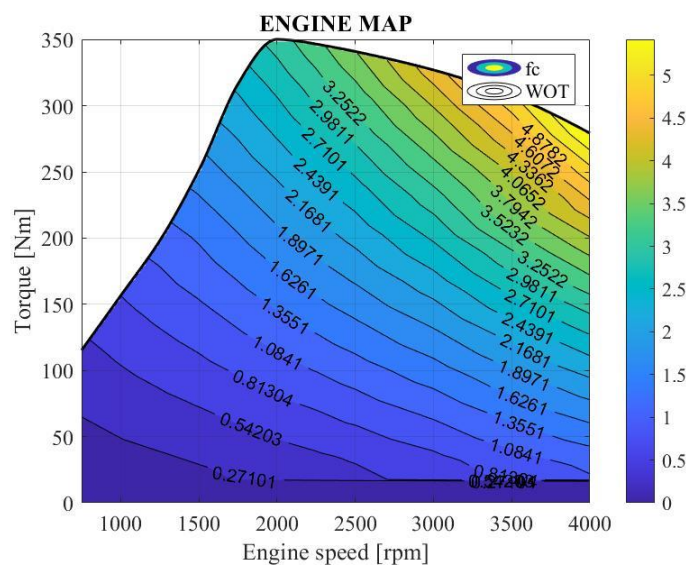


Figure 55- Engine map

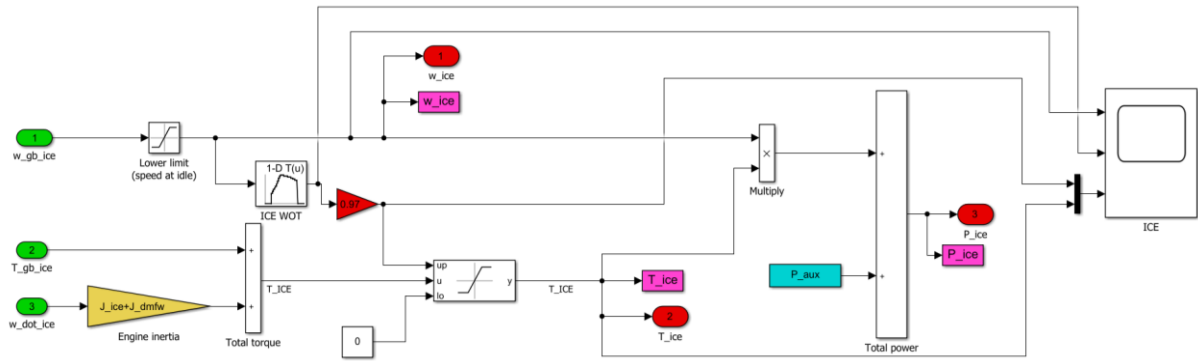


Figure 56- Engine block from inside

## 4.7 Fuel Consumption and CO<sub>2</sub> emission evaluation

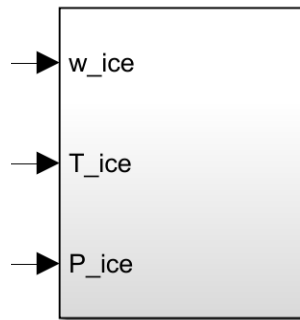


Figure 57- Fuel Consumption and CO<sub>2</sub> emission block

The fuel consumption, evaluated in the subsystem highlighted in yellow, was calculated in kg. Since it is usual to report the fuel consumed in [l/km], the previously calculated amount was divided by the fuel density and then calculated in litres. The amount of CO<sub>2</sub> emitted by the engine per km is correlated to the quantity of the fuel injected and burned along the cycle, and therefore to the fuel economy (V).

$$m_{CO_2} = \frac{\rho_f}{0.0315} \cdot V \quad \left[ \frac{g}{km} \right] \quad Eq. 13$$

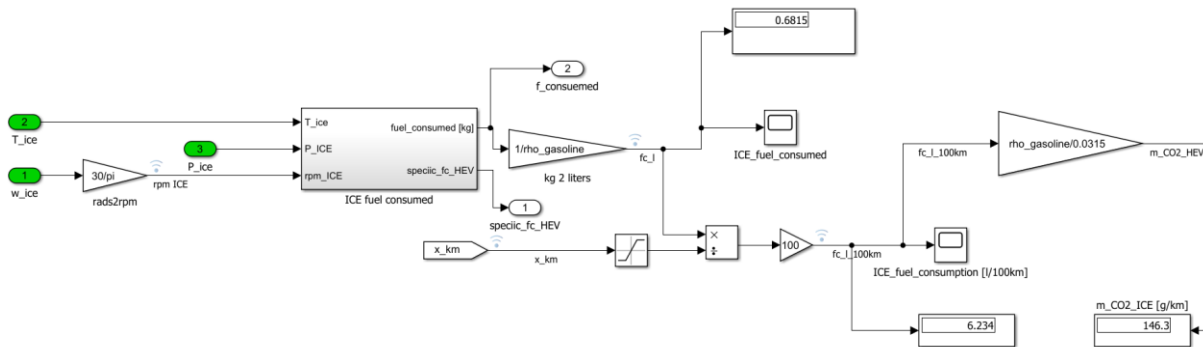


Figure 58-Fuel Consumption block from inside

In the subsystem, the amount of fuel consumed was calculated using the fuel rate map and imported into the simulator as a 2-D Lookup Table.

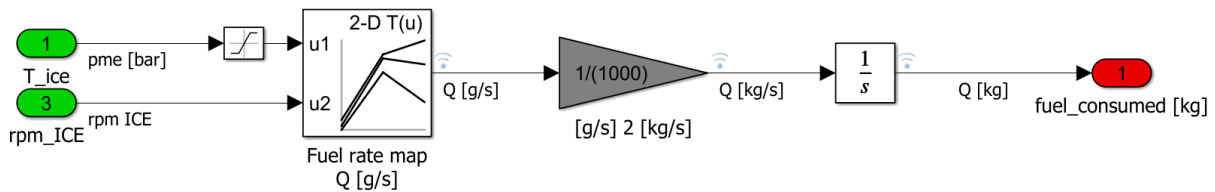


Figure 59- ICE fuel consumed subsystem.

## 4.8 Electric Motor

The Simulink block aims to calculate the power delivered or absorbed by the electric motor during its operation. The machine can work either as a motor or as a generator, depending on the driving situation. When the machine works in motor mode, it delivers positive power, and this happens when the vehicle is moving in pure electric mode or when it supports the engine during the hybrid mode. The machine works as a generator, and therefore delivers negative power, during regenerative braking or when the internal combustion engine is used to

recharge the battery, and therefore provides enough power to restore the battery's state of charge.

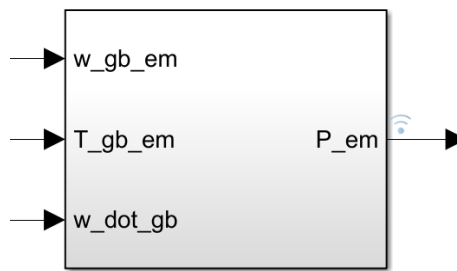


Figure 60- Electric Motor block

Going into detail for what concern the specific block, the first operation that can be highlighted is the determination of the electrical machine's current efficiency, using a 2-D look-up table, which takes as input the angular speed of the motor and the current torque of the motor including inertia. This was done by considering both possible operations of the machine, i.e. as an engine or as a generator. Two saturation blocks (one for motor mode and another for generator mode) were added to take into account the maximum torque value that the electric motor can handle.

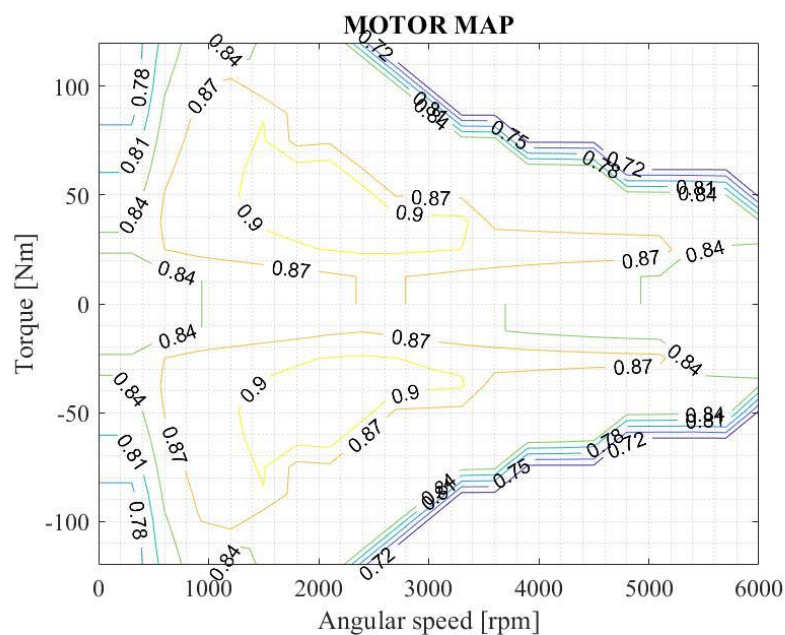


Figure 61- Electric motor map

Finally, the torque was multiplied with the angular speed and the respective efficiency to calculate the electric motor's current power.

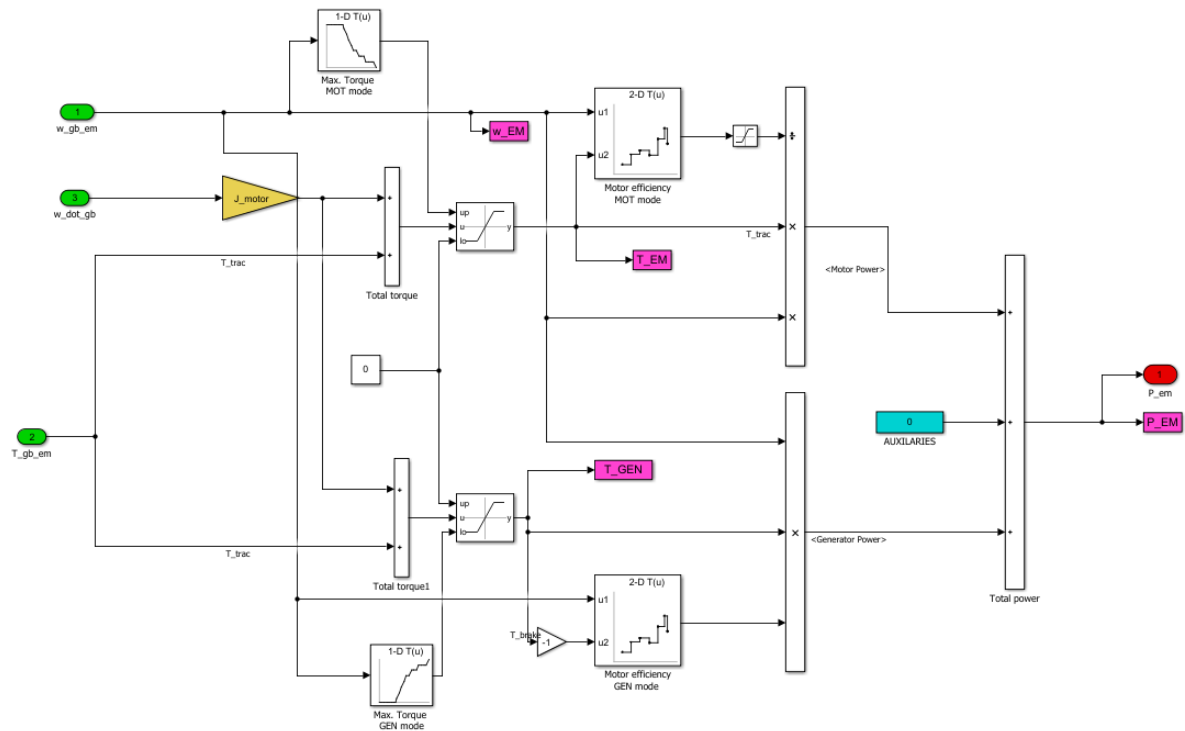


Figure 62- Electric Motor block from inside

## 4.9 Battery

The aim of this block is to represent the battery pack of the hybrid vehicle.

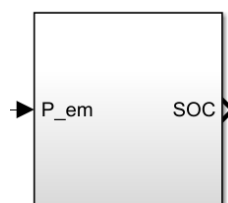
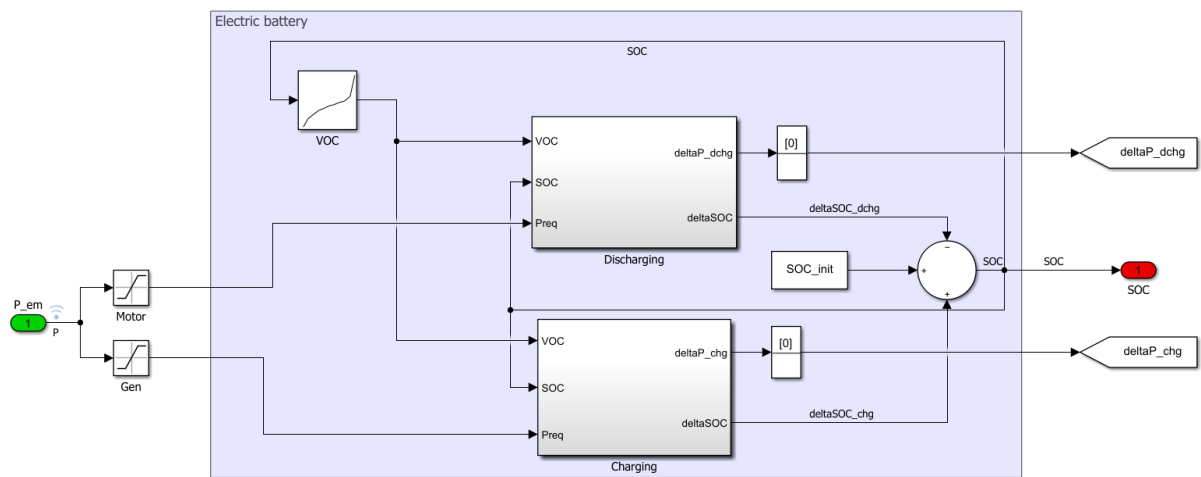


Figure 63 - Battery block

The only input of the block, according to its sign, is the power absorbed by the motor to ensure the motion of the vehicle or the power needed to charge the battery pack during regenerative braking and charging mode.

The output of the model is the state of charge of the battery. This is sent as feedback to the controller, which split the torque required to move the vehicle between the internal combustion engine and the electric motor. The parameters required for operation, such as battery pack weight, efficiency, charge and discharge resistance, capacity and peukert constant (section 4.9.1), are loaded into the Matlab program.



*Figure 64 - Battery block from inside*

The battery is a 48 V lithium-ion battery, 0.5 kWh. It has been dimensioned based on the electric motor's constraints and the type of strategy implemented. The electric motor requires

a maximum power of 23 kW. Figure 65 shows the charging and discharging power curve as a function of the SOC.

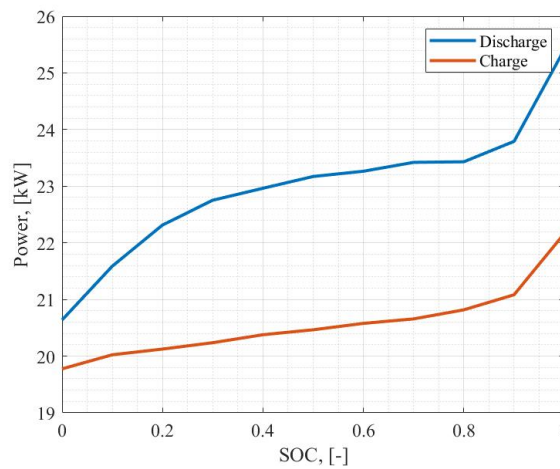


*Figure 65 - Discharge/Charge power vs SOC*

A further test was carried out with a larger capacity battery pack, 13.2 Ah. The results showed that the increase in capacity leads to a 2% increase in fuel consumption than the 8.8 Ah capacity battery pack. A higher current will lead to a higher power, and that means more electrical energy.

Since the strategy is a charge sustaining strategy, we will charge the battery through the internal combustion engine. This means that the electric motor will always use the battery's energy, but the internal combustion engine will charge the battery. So having a high capacity battery will lead to higher consumption.

The choice to have a capacity of 8.8 Ah can be considered as a limitation for the battery. However, it is also an advantage because it allows the privilege of using the traditional traction system instead of having a continuous charging and discharging of the battery during the charge-sustaining strategy. There are studies in the literature that show the disadvantage of oversizing lithium-ion batteries. The dimensioning should balance the energy recovery through regenerative braking and the use of the energy stored. The additional energy coming from the internal combustion engine considers the losses through the energy path flows from the internal combustion engine to the battery pack.

### 4.9.1 Peukert

The electrical charge that a battery can supply to a load is a vital parameter. In the international system, the charge is measured in Coulombs, but when talking about a battery, it is common to use the ampere per hour quantity, denoted Ah, to indicate the current in A supplied by the battery a given time in h. The battery is a highly non-linear element. A battery with a nominal capacity of 100 Ah can provide this capacity if, and only if, it is discharged with a constant current and in a certain time. This is called the nominal discharge time. If the battery is discharged in less time than the nominal time, then the charge delivered is definitely less than the nominal charge. It becomes essential to associate the time to which the capacity value refers to discharge time. Figure 66 shows how a battery's capacity varies greatly depending on whether it is discharged slowly or rapidly.

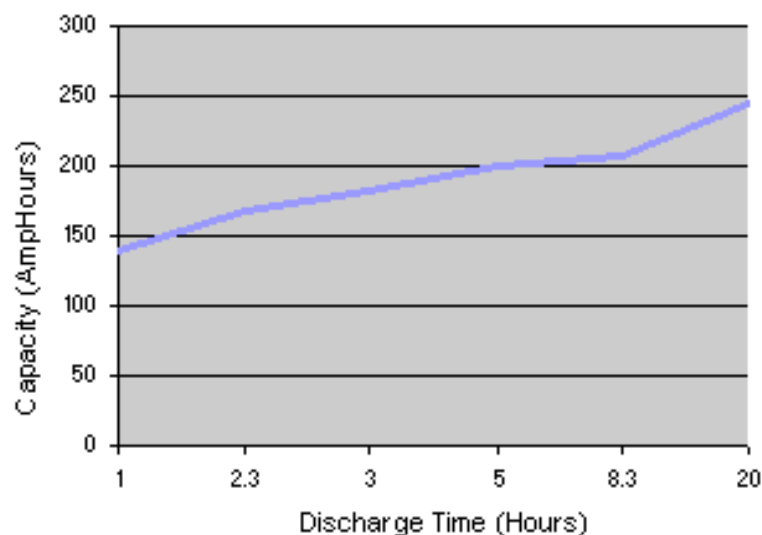


*Figure 66- Capacity vs Discharge Time (Battery and Energy Technologies, 2019)*

It is easy to see that as the discharge time decreases, there is a significant reduction in capacity. This phenomenon is more pronounced with high discharge currents and shorter discharge times (Cristian, 2010). Estimating the capacity trend as a function of the current supply is of fundamental importance in hybrid and electric vehicles. In these cases, the currents delivered are very high, and the battery's energy can be considerably lower than the nominal energy. Peukert's model provides a tool for analysing battery behaviour (Bossche, Coosemans, & Mlerto, 2013). Pekuert was the first to point out that discharging a battery with



very high currents drastically reduces the battery's capacity. The starting point of this model is that, for every battery, there is a capacity, called Peukert capacity, which is given by the following relationship:

$$C_p = I^k \cdot T \quad [Ah] \quad \text{Eq. 13}$$

where k is a constant, called Peukert's coefficient, k varies from battery to battery and is calculated through experiments.

#### **4.9.1.1 Experimental**

In the literature, the various experiments differ only in whether or not the temperature of the battery pack's environment is taken into account. In this project, it was assumed that the temperature was neglected when calculating the Peukert coefficient. It is then reported how the constant has been evaluated in the literature.

The battery is subject to charge and discharge cycles. The experiment is based on testing the available capacity at different current rates. The capacity test at different current rates must set different charges and discharge rates according to the battery's power characteristics. In the test, the battery was first fully charged using a constant current and constant voltage strategy. Once current was applied to the battery, the capacity was monitored and recorded. In (Gong, Li, & Liao, 2020) they fitted the Peukert constant for the lithium-ion battery using the training sets of discharge data experimentally measured. Secondly, they used the Peukert constant obtained earlier to predict the test set data's discharge time and calculated the relative error. Finally, they demonstrated the effect of different Peukert constants on prediction results.

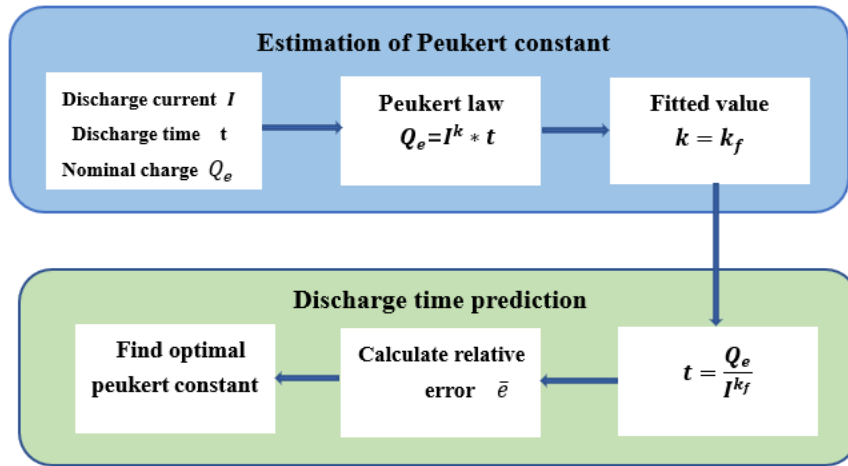


Figure 67- The block diagram of the method based on Peukert's law proposed in (Gong, Li, & Liao, 2020)

Using the values of the coefficient  $k$  calculated previously, it was possible to evaluate the average error as a constant function. Figure 68 shows that the average error decreases until it reaches the minimum value of 1.072 and then increases to 1.136. For this work, it was decided to take  $k=1.072$  into account in the battery model.

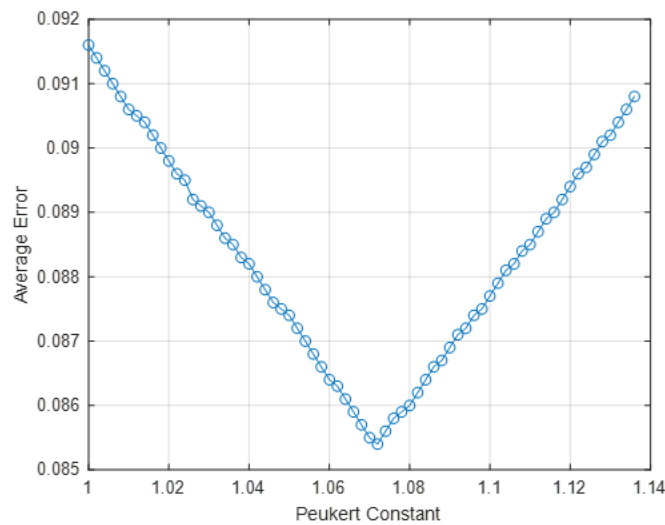
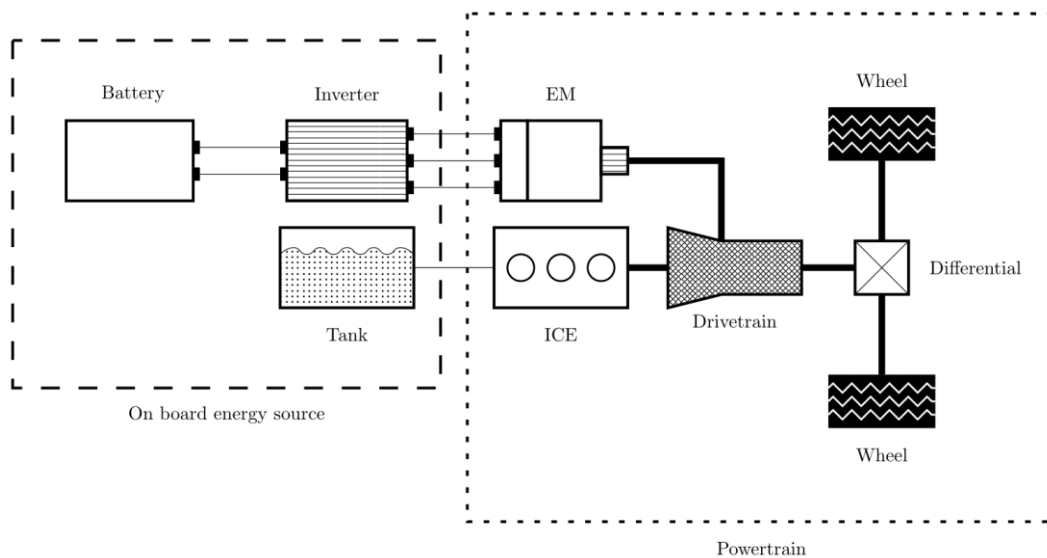


Figure 68- The average error varies with Peukert's constant (Gong, Li, & Liao, 2020)

# 5 Case studies

## 5.1 Test Case

The case study is a P2 Diesel Mild Hybrid Electric Vehicle already available on the market. The ICE is a conventional 2.3 litres Diesel engine 350 Nm and 146 horse power, the e-motor is a 25 kW/440 Nm in the P2 position. The hybrid powertrain is coupled with an 8-speed transmission gearbox and a torque converter that transfers torque to the rear axle according to rear wheel configuration.



*Figure 69 - vehicle architecture*

As already highlighted during the literature review, parallel hybrids can perform multiple propulsion since both the internal combustion engine and the electric motor can be directly connected to the transmission and can therefore provide the mechanical power to drive the wheels. The power from the two onboard energy sources (chemical and electrical) is added together mechanically. Since the engine is connected directly to the wheels, this architecture eliminates the inefficiency of converting mechanical power into electrical power and vice versa, making these hybrids quite efficient on the motorway.

## **5.2 Power management strategy**

The main objective of all control strategies is to minimise consumption compared to conventional vehicles, without lowering performance. Another aspect that characterises the strategies is the knowledge of the future driving situation.

In the current car market, strategies based on deterministic rules are mainly used to optimise consumption using empirical approaches. An attempt has been made to make optimum use of the battery charge by distributing the power required between the two engines according to consumption sensations such as speed or the state of charge of the batteries. It is not easy to exploit the characteristics of a hybrid car: on the one hand, we have to use the batteries to the maximum, making them work to keep the internal combustion engine away from low-efficiency regimes; on the other, having too large batteries mounted on a car, particularly a small one, penalises the car's weight too much. A small electric car is convenient in terms of weight but penalises the car greatly in terms of performance and energy recovery. In this work, a type of rule-based strategy has been adopted.

### **5.2.1 Rule-Based Control**

Rule-based control strategies are structured based on simple relationships and are particularly effective in real-time vehicle management as they do not require any prior knowledge of driving profile data. The basic idea for this type of strategy is based on the concept of load-levelling: a load-levelling strategy aims to move the operating point of the internal combustion engine as close as possible to the optimum efficiency point. Generally, the operating point is shifted to lower torque and speed values than the optimum point, resulting in reduced fuel consumption due solely to energy recovered during braking. In parallel, the state of charge of the battery was taken into account. A charge sustaining strategy was adopted to control the battery, where the SOC level is maintained within a certain range and does not reach the minimum state of charge. The difference between the power required by the driver and the power developed by the internal combustion engine is then compensated for by the electric motor, which can also act as a generator to keep the battery charge above the minimum chosen threshold. In the following paragraph, the strategy and procedure followed to obtain the optimal points at which the internal combustion engine will work is explained. The block responsible for implementing this strategy is the Controller mentioned in paragraph 4.5.

### 5.2.2 Description

To make the most of the characteristics of a parallel topology, the ICE is located at each instant in operating points that minimise consumption; thus, it has been ensured that the combination of the two pairs, thermal and electrical, satisfy the requirements for vehicle propulsion. The strategy is then based on optimising the instantaneous thermodynamic efficiency of the ICE, taking it to work in the points enclosed in the optimal operating line, using the accumulators as an energy 'reservoir', capable of storing if the torque is in excess, or supplying energy if the power is in deficit. The control strategy is executed within the simulator through a "State Flow" decision logic.

Depending on the state mode decided by the supervisory controller, the power split among the two machines is determined differently, according to the engine and motor-generator torque, which are the variable control input (see section 5.4).

- **NEUTRAL (mode 6):** when the vehicle is stopped or idling.
- **EM (mode 1):** only the motor torque affects the vehicle. This occurs when the required torque is within the speed-torque map of the electric motor ensuring a battery state of charge above its limit.
- **ENGINE (mode 2):** only the internal combustion engine affects the vehicle. This occurs when the battery charge is below the minimum threshold and the torque required for propulsion is greater than the torque the engine would have when operating on the optimal operating line.
- **CHARGING (mode 3):** If the battery state of charge is below the minimum value, the ICE operates in the region around the optimal operating line and the excess torque is sent to the electric motor, which acts as a generator to increase the SOC. In this way, the internal combustion engine operates in the high-efficiency region and the battery state of charge is restored.
- **HYBRID (mode 4):** the electric motor assists the internal combustion engine, which works on the points outlined by the optimal operating line, supplying the torque necessary to move the vehicle, always guaranteeing a battery charge status above the minimum value.
- **FRICTION BRAKING (mode -1):** braking will be handled entirely by the conventional braking system.

- **BLENDED BRAKING (mode -2):** if the required torque exceeds the allowable torque of the generator, the latter will work at maximum capacity while the other part will supply by the conventional braking system.
- **FULL REGENERATIVE BRAKING (mode – 3):** the electric motor works as a generator to recover kinetic energy if the braking torque is within the speed-torque map of the electric motor and if the SOC is below the threshold value.

The figure shows the simulator in which the model of the hybrid vehicle implies the control strategy, and in parallel, there is the vehicle model equipped only with an internal combustion engine. The results obtained are described in the following paragraphs.

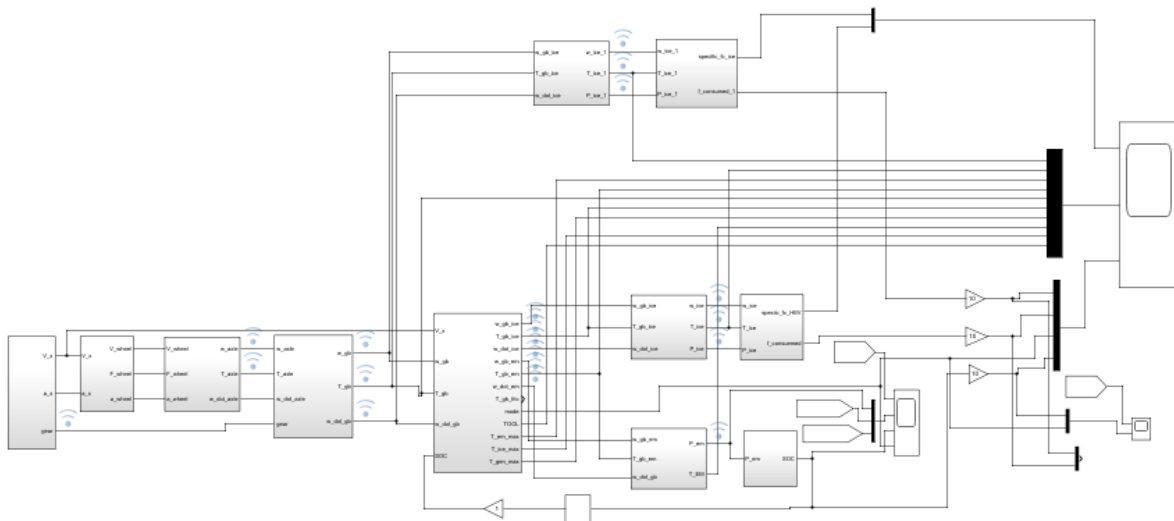


*Figure 70- Simulator "Power Management" strategy*

## 5.2.3 Control Summary

### TRACTION

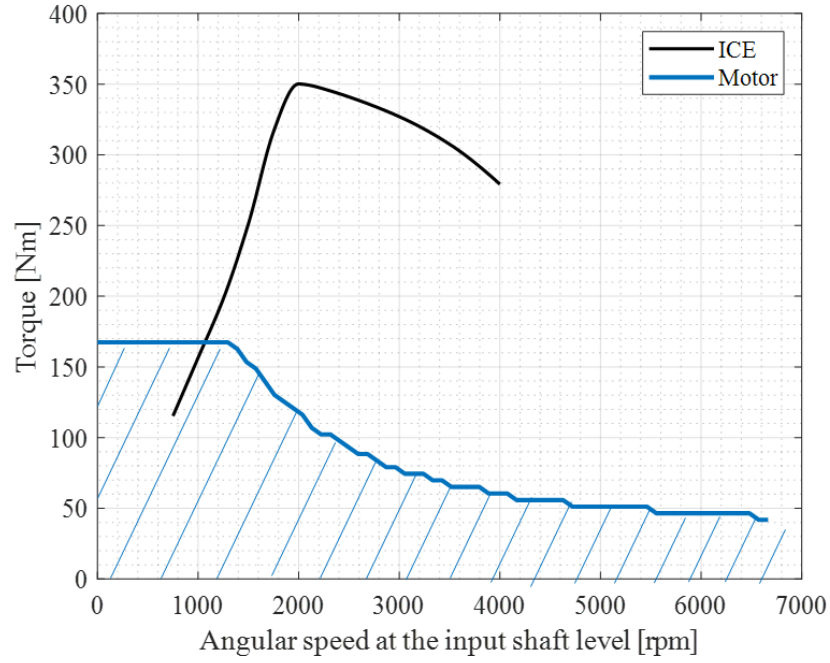


Figure 71-Torque-Speed map: Traction

- $T_{req.trac} \leq T_{em,max} \ \&\& \ SOC > SOC_{min}$

**EM mode**

$$T_{em} = T_{req.trac}$$

$$T_{ICE} = 0$$

- $T_{req.trac} > T_{em,max} \ \&\& \ SOC > SOC_{min}$

**Hybrid mode**

$$T_{em} = T_{em,MAX}$$

$$T_{ICE} = T_{req.trac} - T_{em,MAX}$$

- $T_{req.trac} > T_{OOL} \ \&\& \ SOC \leq SOC_{min}$

**Engine mode**

$$T_{em} = 0$$

$$T_{ICE} = T_{req.trac}$$

- $T_{req.trac} \leq T_{OOL} \ \&\& \ SOC \leq SOC_{min}$

**Charging mode**

$$T_{em} = -T_{add}$$

$$T_{ICE} = T_{req.trac} - T_{add}$$

## BRAKING

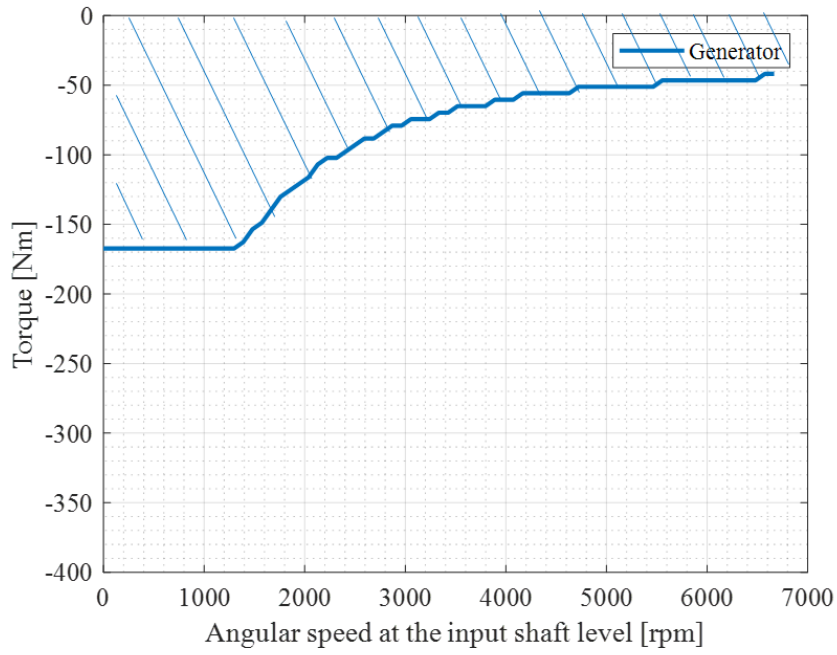


Figure 72-Torque-Speed map: Braking

- $T_{req.brake} \leq T_{gen.max} \ \&\& \ SOC < SOC_{max}$

**Full Regenerative Braking mode**

$$T_{req} = T_{gen}$$

- $T_{req.brake} > T_{gen.max} \ \&\& \ SOC < SOC_{max}$

**Blended Braking mode**

$$T_{gen} = T_{gen.max}$$

$$T_{req} = T_{gen.max} + T_{friction.brake}$$

- $T_{req.brake} \leq T_{gen.max} \ \&\& \ SOC < SOC_{max}$

**Conventional Braking mode**



$$T_{friction.brake} = T_{req.brake}$$

## 5.2.4 Optimal Operating Line (OOL)

This section shows the procedure implemented to evaluate the optimal operating line, having chosen in the control strategy to operate the internal combustion engine at the points of maximum efficiency. Optimal operating line is the place of all the points that power by power it has the max engine efficiency for that power.

### 5.2.4.1 Procedure

The first step was to calculate the brake specific fuel consumption of the internal combustion engine having available the fuel consumption rate, the torque and the angular speed. The brake power is described by Eq.13.:

$$P_{b_{map}} = T_{ICE} \cdot \omega_{ICE} \quad [kW] \quad Eq. 13$$

The most efficient points are those where the brake specific fuel consumption is the lowest, for this purpose it has been calculated.

$$BSFC_{map} = \frac{\dot{m}_{fuel}}{P_b} \quad \left[ \frac{g}{kWh} \right] \quad Eq. 14$$

Figure 73 shows an example of a BSFC map, along the vertical axis are values of fuel consumption at a constant speed, along with the horizontal axis values of fuel consumption at constant power. Since the  $\dot{m}_{fuel}$  contains non-numerical values (Not a Number), these

have been replaced with numerical values chosen in such a way as not to influence the search for the minimum.

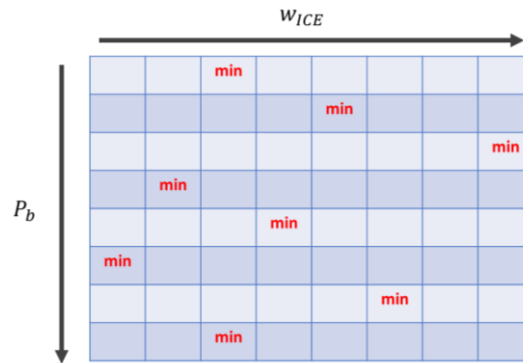


Figure 73-BSFC map

A for loop was implemented in the Matlab environment , then the torque and speed values corresponding to the optimal operating line were plotted.

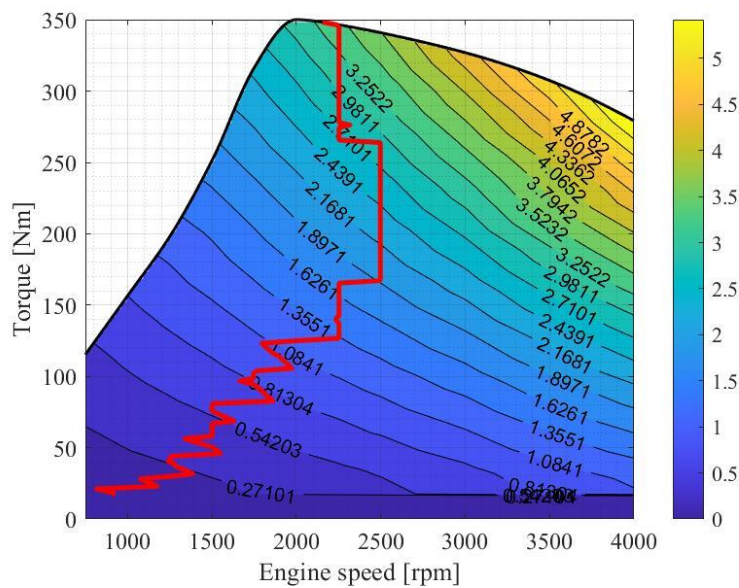


Figure 74-Optimal Operating Line

The speed and torque values of the OOL are entered into the simulator using a Look-up Table. The Look-up Table working method dictates that the data entered into it is unique for each input. Based on this, the optimal operating line was approximated by considering those points that allow to implement the curve within the simulator and extending the working points to speeds above 2500 rpm along the wide-open throttle

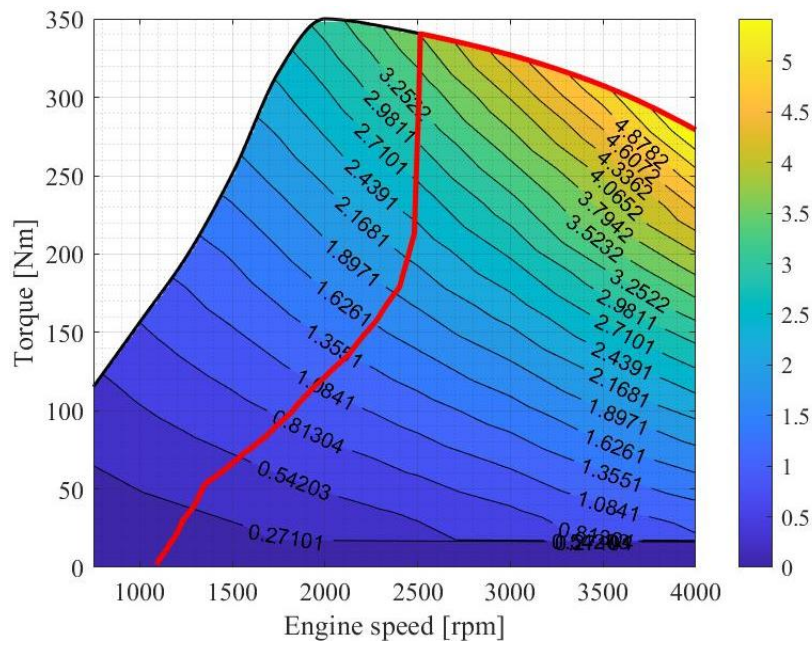


Figure 75- Optimal Operating Line def.

## 5.2 Look-ahead - predictive operation strategy

Once the control strategy has been validated, a scenario in which the ego vehicle travels through the NEDC driving cycle and during its driving will receive information about the amount of charge it will recover during the future regenerative braking has been simulated.

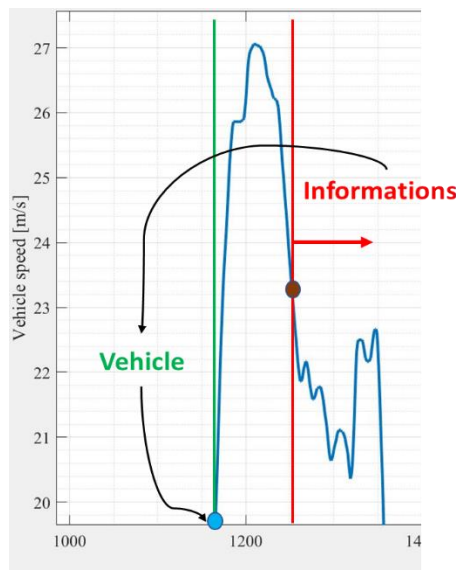


Figure 76 - Look-ahead scenario

The ego vehicle moves following the blue point, and during its motion it will receive information from the brown point which in turn moves following the same driving cycle. The shift between the vehicle and future information was parameterised as a function of space, considering the operating ranges of ADAS systems such as short-range cameras.

## 5.2.1 Future information

With the backward model, there is no possibility of modulating the data after the simulation has started. The primary input data are driving cycle values. With the backward model, there is no possibility of modulating the data after the simulation has started. The primary input data are driving cycle values. To know how much the vehicle will gain in braking, a model that only processes braking data is needed. The "information model represents this model".

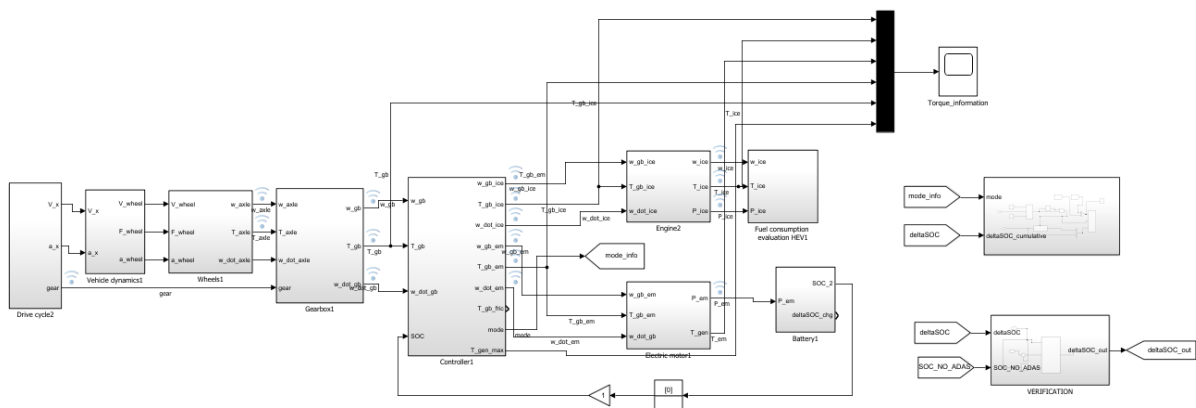
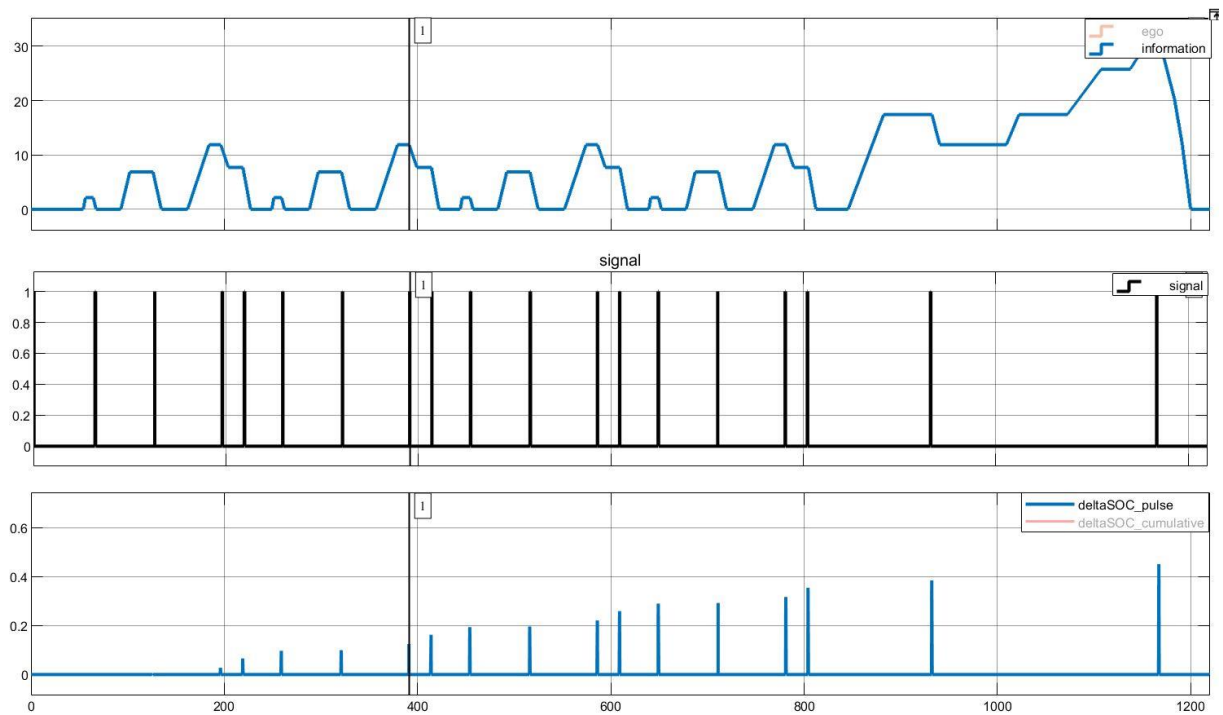


Figure 77- Information model

This backward model has NEDC data as input, and it can detect only braking phases and calculate how much the vehicle will recover in terms of SOC. A verification block has been created to prevent the battery from discharging below its limit value because the battery model considers the recovery of the future state of charge as a prediction and not as the actual amount available. From the Figure 78, it is possible to understand how the amount of SOC gained in braking is estimated.



*Figure 78- Future information procedure*

In the first plot, there is a speed profile that the information model follows. As soon as the model detects braking, a signal (second plot) is emitted, identifying the start of the braking phase a time  $T$ , and then, it will give as output (third plot) the amount of delta SOC. This data have been sent to the vehicle, represented by another backward model working in parallel.

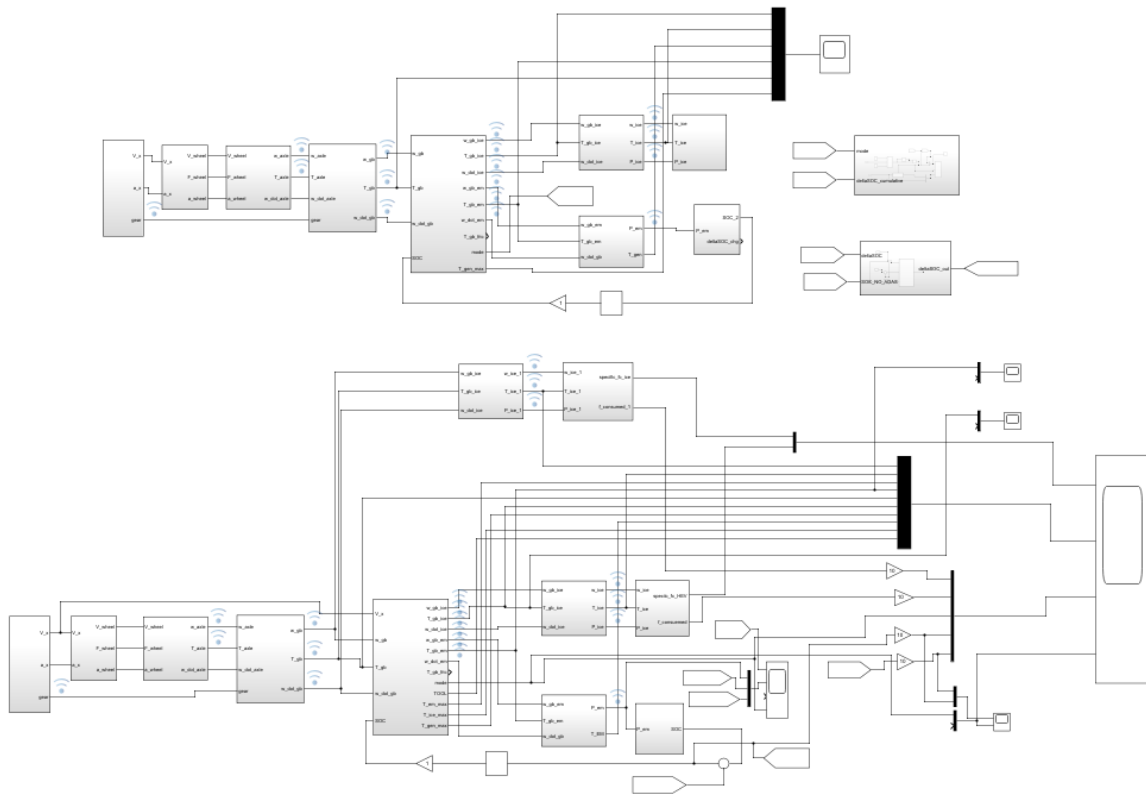


Figure 79-Information model (top) vehicle model (bottom)

The backward model requires that the two models to work in parallel, they must have equal size as input data vectors. To have a prediction, a vector of equal size with the same data as NEDC has been created but shifted so that the ego vehicle receiving the information (brown) will start later and see the information received as a prediction.

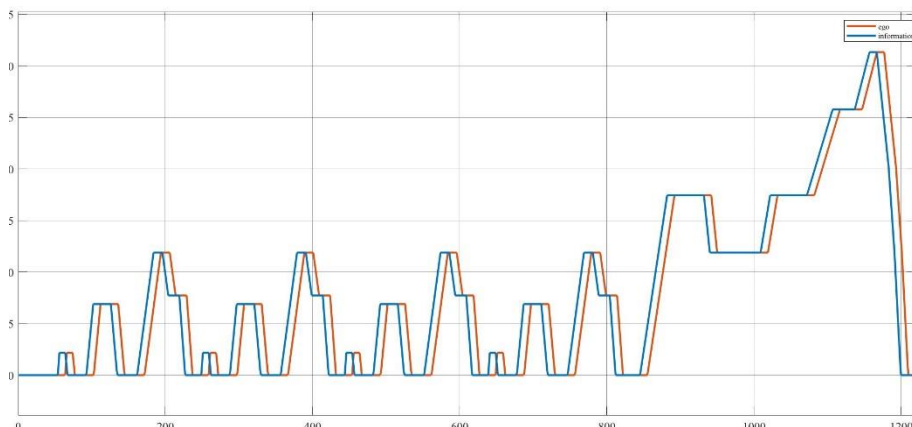
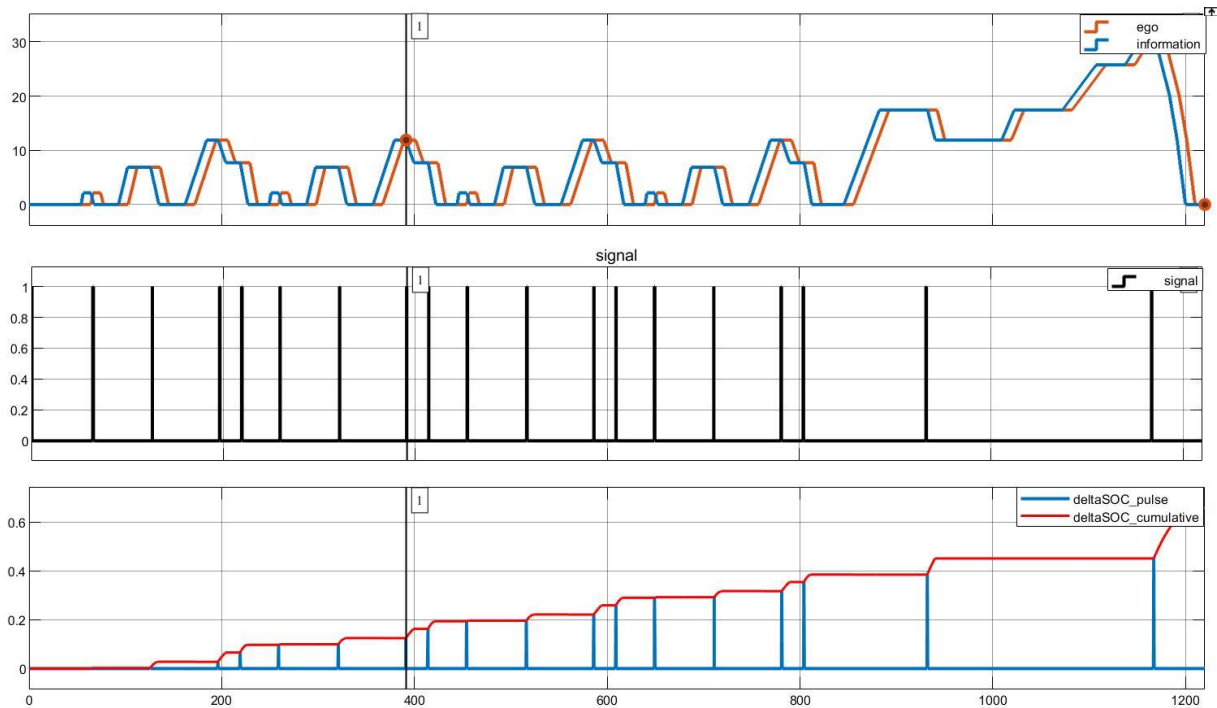


Figure 80- Speed profile information model and vehicle model

The quantity of SOC that the vehicle will gain has been given according to the model's constraints, i.e. in a cumulative way. This implementation has been seen like the situation in which the vehicle knows in advance that it will recover a certain amount of charge during braking in the whole driving cycle.



*Figure 81- deltaSOC information*

The simulator will present three models running in parallel. The first from the top is the model that generates future information sent to the central model. The latter will process the data obtained from NEDC and the future state of charge recovery information and then calculate fuel consumption and CO<sub>2</sub> emissions. The bottom model represents the hybrid vehicle model operating without the ability to have this information to compare the benefits of this predictive strategy.





# 6 Simulations results

This chapter will show the results obtained from the implementation of the control strategy (section 6.1 and section 6.2) and those obtained from the use of information from ADAS systems (section 6.3). Once the model had been validated, it was possible to run the simulation acquire the data and compare them.

## 6.1. Control Strategy results: NEDC

The first ran test was the NEDC described in section 4.1.1.

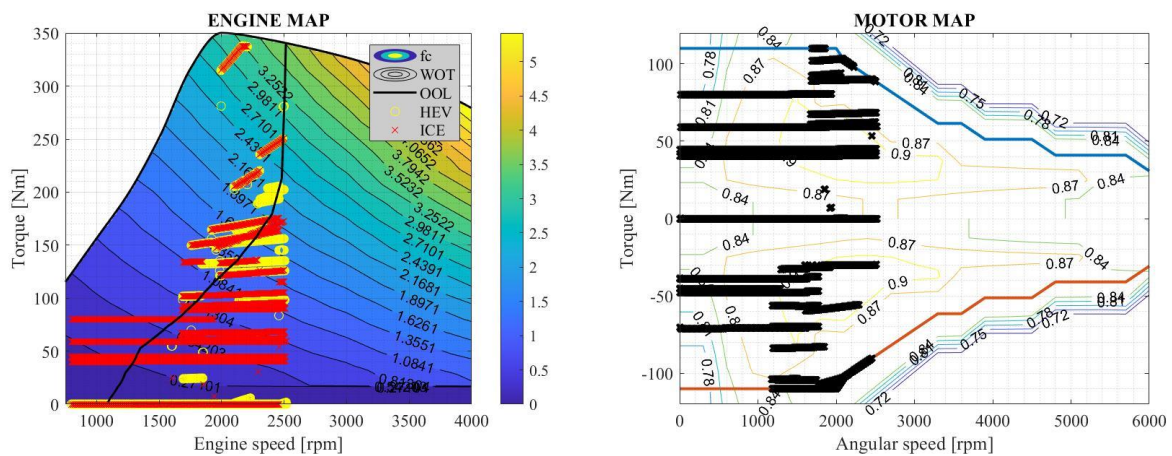
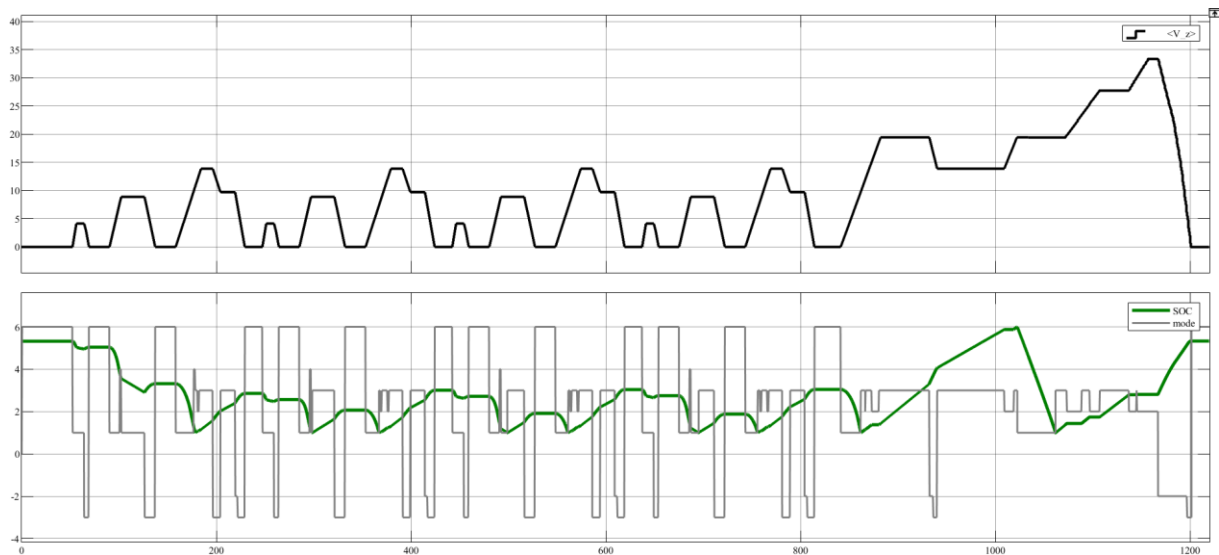


Figure 83 – Engine & Motor Map (NEDC)

Figure 83 shows in the left plot the working points of the internal combustion engine for the model equipped only with ICE (red) and the HEV model (yellow), while in the right plot the working points of the electric motor. The reduction of the working points due to the electric motor's presence can be seen in the engine map. Another advantage of the control strategy is reducing the working points at low load and low rpm, i.e. at high fuel consumption and low efficiency, by making the ICE of the hybrid model work in a region close to the optimal operating line. This operation method takes place during charging mode, where the surplus power provided by the internal combustion engine is used to increase the state of charge of the battery when the value is below the limit.

In the figure 84 we have the speed profile of the driving cycles under consideration and the SOC with the various operating modes



*Figure 84 - Speed profile, SOC & Operating modes (NEDC)*

Mild hybrid vehicles usually use the support of the electric motor at low speeds and during start-up. In this simulation was used a driving cycle in which a speeds of up to 120 km/h in the extra-urban part has been reached. Nevertheless, some advantages can also be seen in this part of the cycle: recovery of kinetic energy, and for some acceleration spots, there is the possibility of driving in electric mode, which justifies a drastic reduction in the state of charge towards the end of the cycle while still maintaining a final state of charge close to the initial one. A reduction of 5.3% in terms of fuel consumption has been achieved. About CO<sub>2</sub> emissions, a reasonable reduction has been achieved. The legislation states that from 2020, a new commercial vehicle with the exact dimensions as the vehicle under consideration cannot emit more than 149 g/km of CO<sub>2</sub>. The engine in question is an old one, but thanks to the implementation of the control strategy and the electric motor's support, it would still comply with European regulations if it were considered a new vehicle.

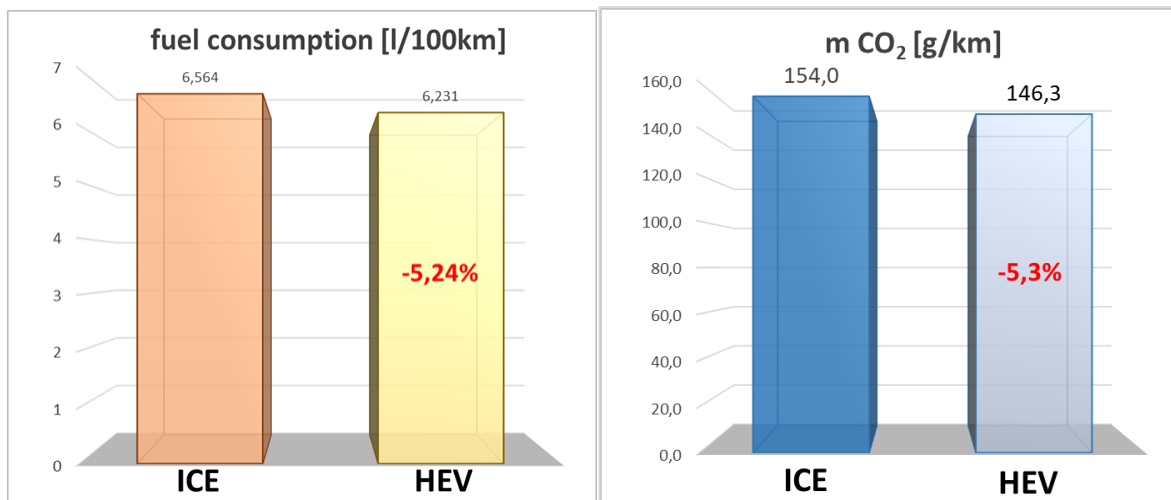


Figure 85 - Fuel consumption & CO<sub>2</sub> emission (NEDC)

Next, I highlighted the contributions from the various cycles that make up the NEDC, showing in Figure 86 and 87 the fuel consumption and CO<sub>2</sub> emissions for both ECE15 and EUDC.



Figure 86 - ECE15 & EUDC fuel consumptions

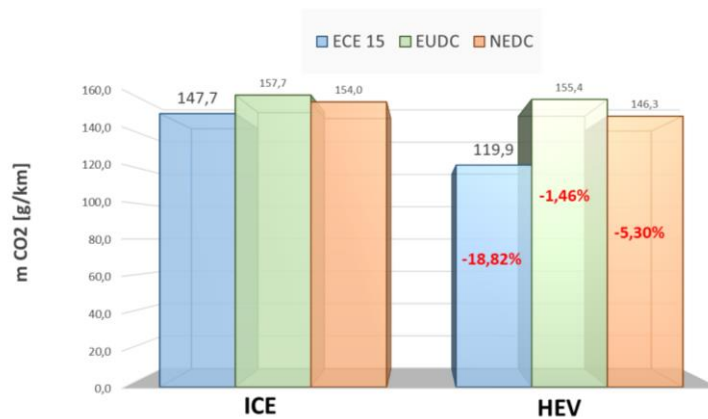


Figure 87 - ECE15 & EUDC CO<sub>2</sub> emissions

The most significant benefit comes from the urban cycle, with a fuel consumption reduction of around 19 %. This result is obtained because mild hybrid vehicles exploit their advantages more in an urban environment than an extra-urban one. The control strategy still allows the electric motor to be exploited, providing a reduction of just 2 %.

## 6.2 Control Strategy results: WLTC

In questa sezione sono riportati i grafici e risultati della simulazione con il WLTC.

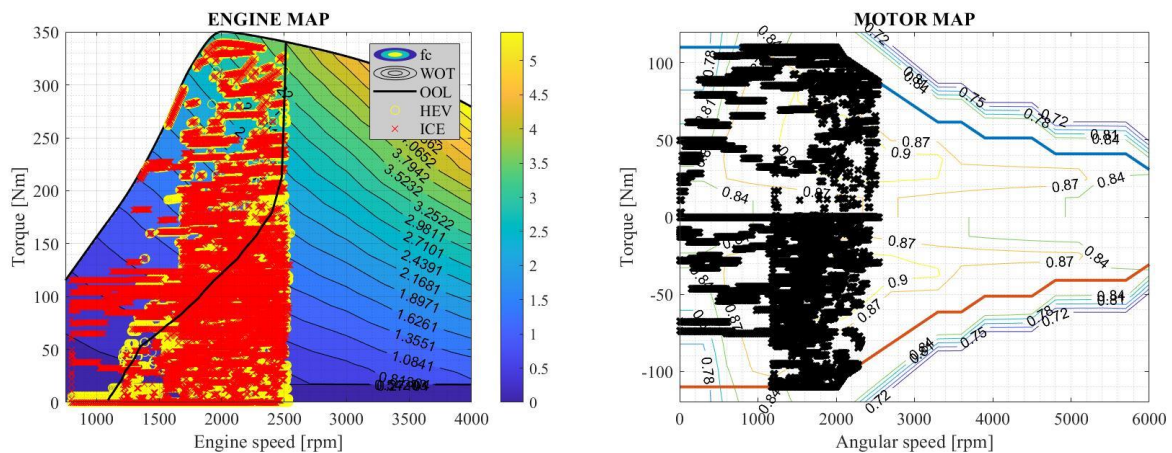


Figure 88 - Engine & Motor Map (WLTC)

It is possible to see from the engine map the advantages that were highlighted in section 6.1.1. Namely, reducing the working points using the hybrid configuration and the greater possibility for the hybrid model's ICE to work in high-efficiency zones. Figure 89 shows the speed profile of the WLTC repeated three times, the change of charge state during the whole procedure and the different operation methods.

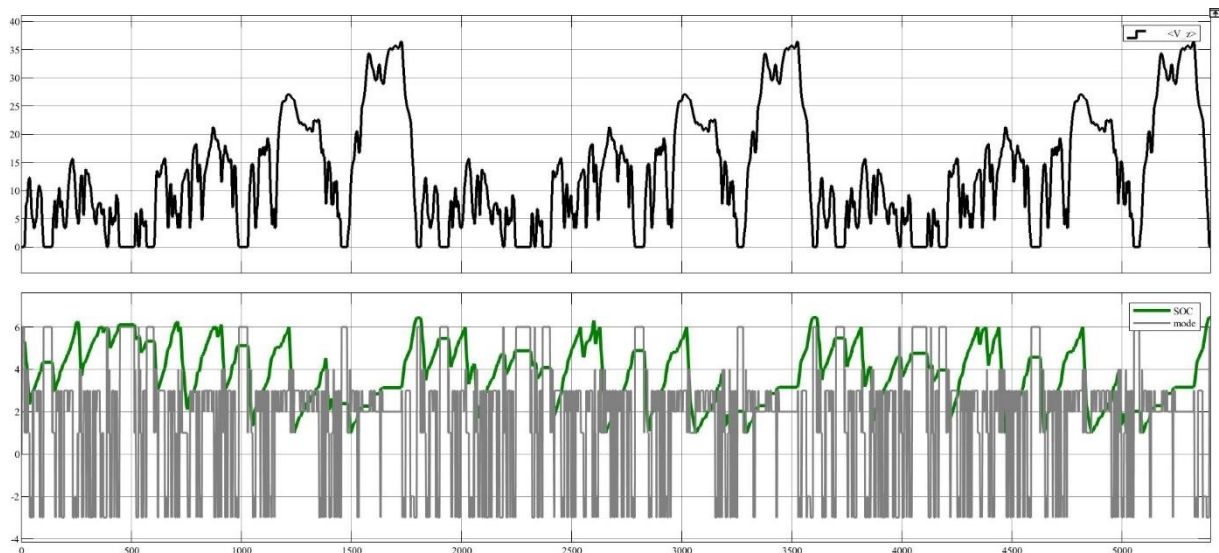


Figure 89 - Speed profile, SOC & Operating modes (WLTC)

A lower reduction compared to NEDC is justified by the difference in driving cycles. WLTC is more aggressive than NEDC, covering a broad region of duty points. There is an average speed increase of 28% with a maximum speed of about 130 km/h, a constant driving reduction of 80% and an acceleration increase of 67% (section 4.1.2).

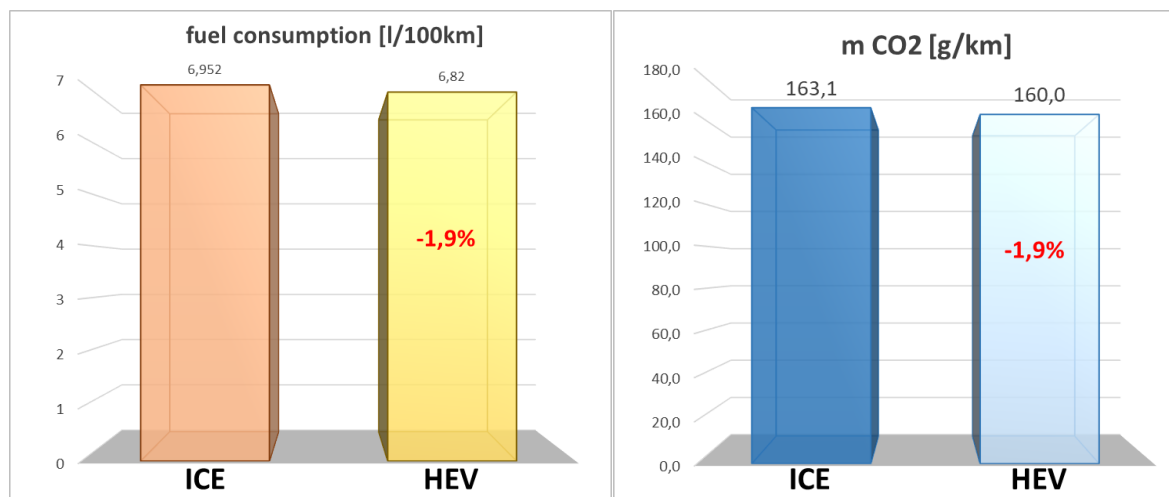


Figure 90 - Fuel consumption & CO2 emission (WLTC)

In figures 91 and 92, I have highlighted each part of the cycle's contributions, low, medium, high and extra-high part. As we could see in the NEDC, for the WLTC, the low part also allows

obtaining the most significant reduction, just because the cycle's conformity is much more similar to an urban environment than the extra-high part. Indeed, moving towards the more aggressive parts of the cycle, there is a reduction in benefits, albeit in small amounts.

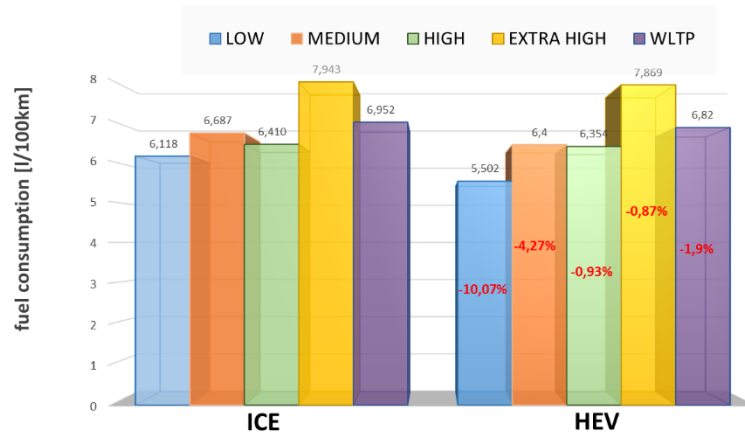


Figure 91 - LOW, MEDIUM, HIGH, EXTRA HIGH fuel consumptions

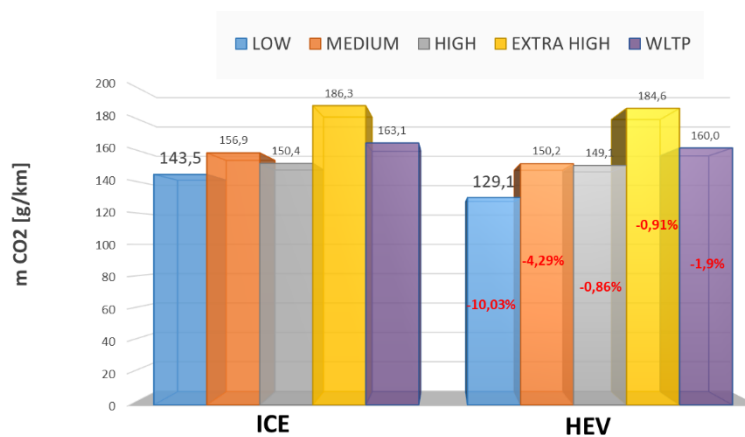
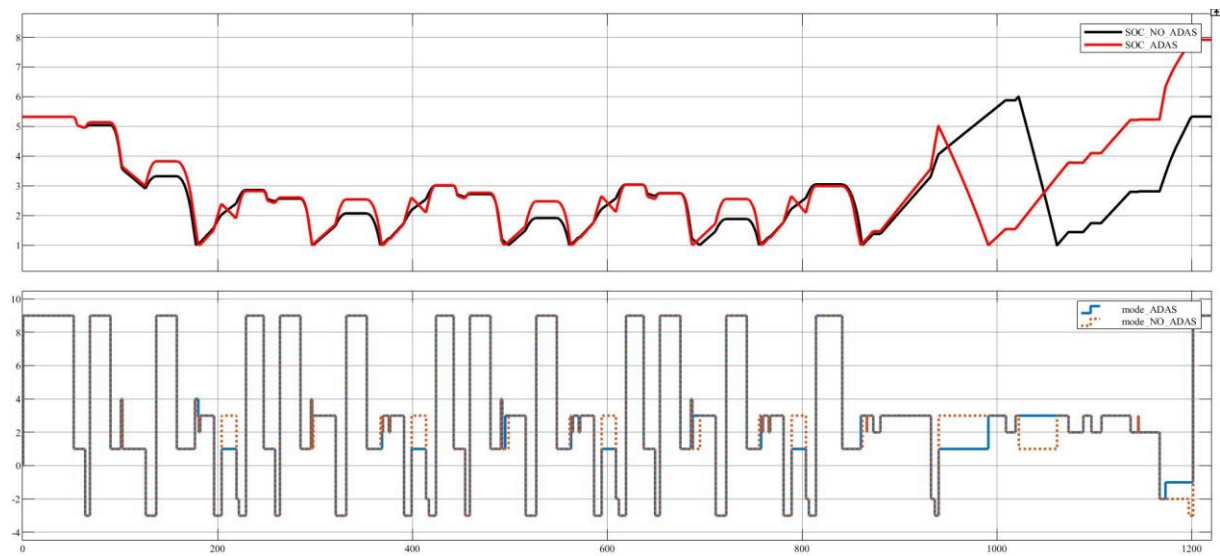


Figure 92 - LOW, MEDIUM, HIGH, EXTRA HIGH CO<sub>2</sub> emissions

### 6.3 Look-ahead strategy results

This implementation's results were obtained by parameterizing the time shift as a function of space, thus obtaining a sort of window with dimensions dictated by the range of operation of the ADAS systems as a Short-Range Radar. Figure 93 shows the ADAS model's charge state

profile compared to the model where future information is not available (NO\_ADAS) and the respective operating modes.



*Figure 93 - SOC profile & operating modes*

Looking at the second plot, the differences between the two operating modes can be seen. The knowledge of future information allows us to better manage the state of charge of the battery by increasing the range of electric mode by about 22%, highlighted by a decrease in charge, especially in the cycle's extra-urban area. Figure 94 and 95 shows the reduction in the torque required by the internal combustion engine, which is instead provided by the electric motor, while still preserving the battery's health thanks to the verification block implemented in the simulator.



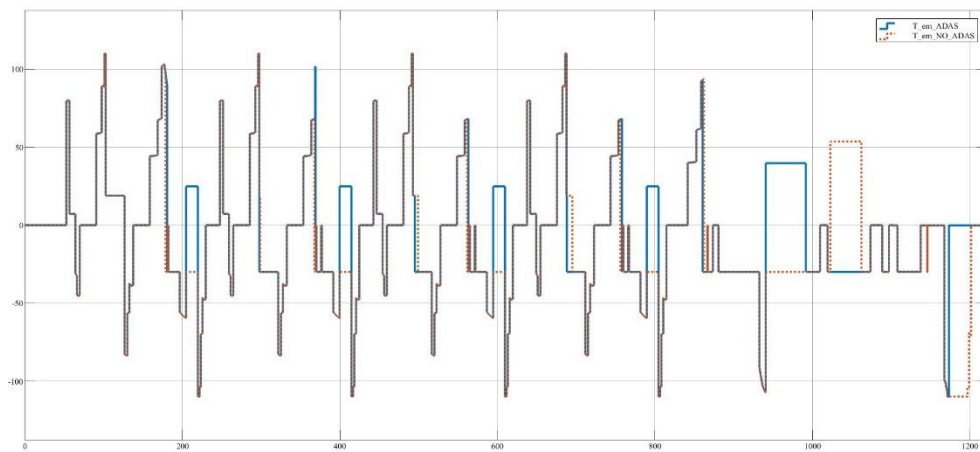


Figure 94 - E-motor torques

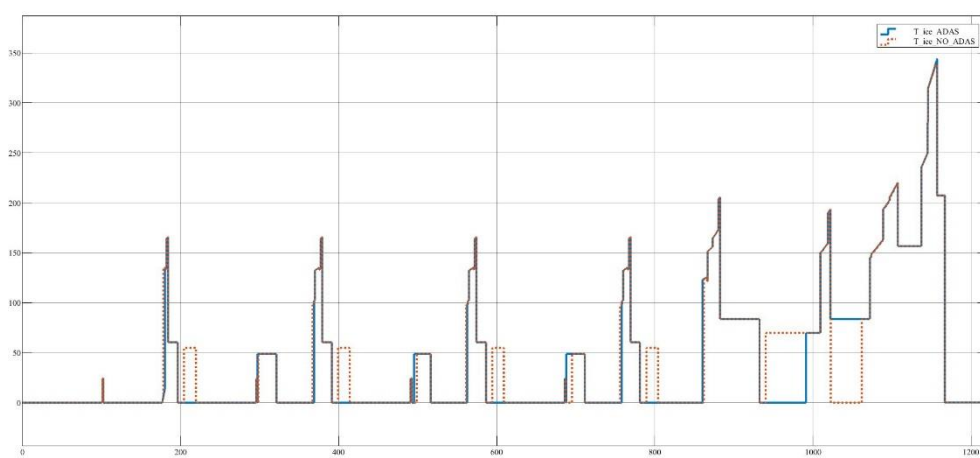
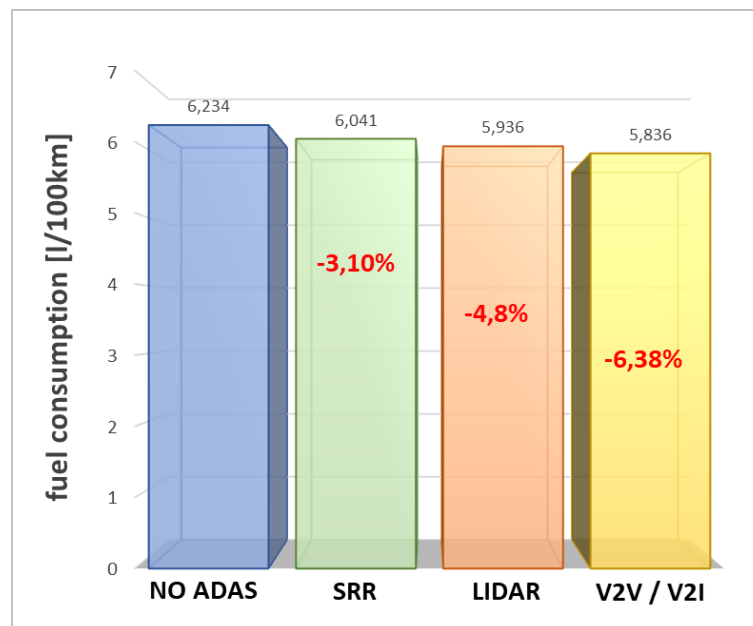


Figure 95 - ICE torques

Using the proposed system, a reduction of about 3% is obtained compared to the hybrid vehicle without the Short-Range Radar. Given the results obtained, the model was tested by increasing the window up to 100 metres, the operating range of a LIDAR (Laser Imaging Detection and Ranging) system, and up to 175 metres. In case of long distances, it would be



necessary to resort to CAV technologies, i.e. Vehicle to Vehicle and Vehicle to Infrastructure connections, to reduce fuel consumption by about 7%.



*Figure 96 - Fuel consumption Look-Ahead*

# Conclusions

At present, the costs of electric vehicles and charging infrastructure make the radical switch to electric technology not yet complete. The temporary solution seems to be that of hybrid technology.

In this thesis, the advantages and disadvantages of the various hybrid configurations are highlighted, focusing on mild-hybrid technology. This technology has the advantage of being inexpensive compared to conventional cars. It uses a small electric motor that acts as an alternator/starter, motor-generator, and support for the internal combustion engine during acceleration. During braking, the electric motor acts as a generator, recharging the small battery pack.

The thesis work gives a software tool capable of simulating a mild-hybrid vehicle's longitudinal dynamic behaviour with a backward approach.

Strategies based on deterministic rules can be designed for control, consisting of control rules from simulated results or experimental outcomes: these are the most popular on the market.

The implemented control strategy is a charge sustaining strategy supported by an optimum operating point strategy. The observation made was that the internal combustion engine's consumption is not proportional to the power delivered, but rather the efficiency of the engine takes on different values depending on the torque and angular speed required. Therefore, engine consumption depends on the operating point required at that moment. By combining this observation with the potential of hybrid technology to store excess power in the battery, a new control scheme was developed. It provides that the operating point required of a vehicle's internal combustion engine is now shifted to a high-efficiency point within a suitable tolerance range. This idea allows the engine's optimum use while minimising both CO<sub>2</sub> emissions and fuel consumption concerning the power delivered.

Once the control strategy was validated, the possibility of having a prediction of the subsequent energy recovery during regenerative braking was evaluated by exploiting ADAS technologies. The evaluation of recovered energy was possible thanks to a priori knowledge of the driving cycle and made it possible to optimise the energy stored in the battery pack.

The backward model working on fixed data does not allow to implement of a realistic scenario. Possible future developments may concern the use of a model through a forward approach. Therefore, implementing a car following scenario or introducing traffic conditions through a vehicle to vehicle and vehicle to infrastructure connection to understand how the control strategy behaves and what will be the margins of improvement in the recovery of kinetic energy.

# Appendix: Matlab code

```
set(0,'defaultAxesFontName', 'Times New Roman',...
    'defaultTextFontName', 'Times New Roman',...
    'defaultAxesFontSize', 12,...
    'defaultTextFontSize', 12,...
    'defaultLineLineWidth',2,...
    'DefaultAxesXGrid','on',...
    'DefaultAxesYGrid','on',...
    'DefaultTextInterpreter','Tex')
close all
h = 0.01;

load('NEDC')
plot(T_z,V_z)
xlabel('Time [s]'), ylabel('Vehicle speed [m/s]')
grid minor

g = 9.81;          % Gravitation constant
rho = 1.21; % Mass density of the air, [kg/m3]
Time = max(T_z); %Simulation time 1h, [s]

%%% VEHICLE
M_veh = 3000; % Vehicle mass, [kg]
Cx = 0.316; % Aerodynamic drag coefficient
Cz = 0.03; % Aerodynamic lift coefficient
CM_y = 0; % Pitching moment coefficient

L = 3.3; %Wheelbase, [m]
a=925/2155*L; %Horizontal distance from CG to front axle, [m]
b=1230/2155*L; %Horizontal distance from CG to rear axle, [m]
hG=1.2; %Height of vehicle CG above the ground, [m]

A_f =1.996*2.7*0.85; % Frontal area of the vehcile, [m2] 0.607

%%% WHEEL
%225/65R16

R_wheel = (16*25.4/2+0.65*225)/1000; % wheel radius [m]
J_wheel = 0.32; %Moment of inertia [kgm2]
f_r = 0.01; %Rolling resistance coefficient

%%% INTERNAL COMBUSTION ENGINE 2.3l Diesel engine

load('Engine_map.mat');

Q_ice_map = Q_ice_map/(1.2511*1.35); %/1.251 1.65
J_ice = 0.05; % Engine moment of inertia [kgm2]
J_dmf_w = 0.323; % Dual mass flywheel moment of inertia [kgm2]
w_CE_idle = min(w_ice_map)*pi/30+5 % [rad/s] idling speed
P_aux = 0; % Enigne auxilary power requirement

H_gasoline = 4.4e7; %[J/kg] Low heating power of the gasoline
Vol = 2300/1e6; %[cm3] Volume
```

```

i = 2; %[-]      4 stroke engine
T2pme = i*2*pi/(Vol)/1e5; %[bar/Nm]      Torque 2 pme multiply factor
rho_gasoline = 0.739; %[kg/dm3] Gasoline density
CV2W = 735.49875; %[CV/W] Conversion between CV and W
pme2T = (Vol*1e5)/(i*2*pi); %[bar/Nm]      Torque 2 pme multiply factor

%%% Idling hyp.
for i=1:10
    for j=1:200
        Q_ice_map(i,j)=0;
    end
end

%% TRANSMISSION

eff_gb = 0.94; % Efficiency of the gearbox
eff_pulley = 0.90; % Efficiency of the pulley belt transmission
0.9:0.02:0.98

UI = 4.71; % First gear ratio
UII = 3.14; % Second gear ratio
UIII = 2.11; % Third gear ratio
UIV = 1.67; % Fourth gear ratio
UV = 1.28; % Fifth gear ratio
UVI = 1; % Sixth gear ratio
UVII= 0.84; % Seventh gear ratio
UVIII = 0.67; % Eighth gear ratio
Uf=3.615; % Final gear ratio
Upulley = 2.7;
% Gear shift strategy
Pmax = max( pi/30*w_ice_map.*T_ice_max/T2pme/1e3); % [kW] Max power of the
engine

n_max_acc_1 = 2500;
n_min_acc = 1200;

V1_2 = n_max_acc_1/UI/Uf*pi/30*R_wheel; % Gearshift from 1->2
V2_3 = n_max_acc_1/UII/Uf*pi/30*R_wheel; % Gearshift from 2->3
V3_4 = n_max_acc_1/UIII/Uf*pi/30*R_wheel; % Gearshift from 3->4
V4_5 = n_max_acc_1/UIV/Uf*pi/30*R_wheel; % Gearshift from 4->5
V5_6 = n_max_acc_1/UV/Uf*pi/30*R_wheel; % Gearshift from 5->6
V6_7 = n_max_acc_1/UVI/Uf*pi/30*R_wheel; % Gearshift from 6->7
V7_8 = n_max_acc_1/UVII/Uf*pi/30*R_wheel; % Gearshift from 7->8

V2_1 = n_min_acc/UII/Uf*pi/30*R_wheel; % Gearshift from 1->2
V3_2 = n_min_acc/UIII/Uf*pi/30*R_wheel; % Gearshift from 2->3
V4_3 = n_min_acc/UIV/Uf*pi/30*R_wheel; % Gearshift from 3->4
V5_4 = n_min_acc/UV/Uf*pi/30*R_wheel; % Gearshift from 4->5
V6_5 = n_min_acc/UVI/Uf*pi/30*R_wheel; % Gearshift from 5->6
V7_6 = n_min_acc/UVII/Uf*pi/30*R_wheel; % Gearshift from 6->7
V8_7 = n_min_acc/UVIII/Uf*pi/30*R_wheel; % Gearshift from 7->8

G_up = [1 2 3 4 5 6 7 8];
V_g_up = 3.6*[V1_2 V2_3 V3_4 V4_5 V5_6 V6_7 V7_8 190/3.6];
G_down = [2 3 4 5 6 7 8];
V_g_down = 3.6*[V2_1 V3_2 V4_3 V5_4 V6_5 V7_6 V8_7];
plot(V_g_up, G_up, 'ro', V_g_down, G_down, 'bd')

```

```

legend 'Upshift' 'Downshift'
grid on
grid minor

%% ELECTRIC MOTOR
load('Motor_map.mat');

J_motor = 0.008; % Motor shaft inertia [kgm2]

%% ELECTRIC BATTERY
%           Nominal Cell Voltage: 3.6V
%           Total Cells: 14s2p (14 cells series 2 parallel)
%           Nominal Voltage: 48 V
%           Published Capacity: 8.8 Ah
eb_soc=[0 0.1 0.2 0.3 0.4 0.5 0.6 0.7 0.8 0.9 1]; % (--)
eb_coulombic_eff= .905;
eb_num_module=7.5; %num of series cells
eb_r_dis=[ 0.0377 0.0338 0.0300 0.0280 0.0275 0.0268 0.0269 0.0273
0.0283 0.0298 0.0312];
eb_r_chg=[ 0.0235 0.0220 0.0205 0.0198 0.0198 0.0196 0.0198 0.0197
0.0203 0.0204 0.0204];
eb_voc=[7.2370 7.4047 7.5106 7.5873 7.6459 7.6909 7.7294 7.7666
7.8078 7.9143 8.3645]*eb_num_module;
eb_cap_max=8.8*3600; % (A*sec), max. capacity at 6.5 A
eb_crnt_max=8.8; % current at eb_cap_max
eb_cap_chg=8.8*3600; % (A*sec), charging capacity
I_max_dchg=60*eb_crnt_max; % max. discharging current Amperes
I_max_chg = 40*eb_crnt_max; % max. charging current Amperes
eb_cap_time=eb_cap_max/eb_crnt_max;
eb_module_mass=0.98; % (kg)
eb_k=1.07; % an exponent
eb_peukert_cap=(eb_crnt_max^eb_k)*eb_cap_time;
SOC_max=1; % (--), highest limit of soc
SOC_min=0.1; % (--), lowest limit of soc

P_max_dchg = I_max_dchg.*eb_voc-eb_r_chg.*I_max_dchg^2;
P_max_chg = I_max_chg.*eb_voc+eb_r_chg.*I_max_chg^2;
figure(9)
plot(eb_soc,P_max_dchg/1000, eb_soc, P_max_chg/1000)
legend 'Discharge' 'Charge'
xlabel('SOC, [-]')
ylabel('Power, [kW]')
grid minor

%% BSFC map
w_ice_map_rads=w_ice_map*2*pi/60; %[rad/s]
bmep=(T_ice_map.*2)/Vd; %[N/m2]
bmep_bar=bmep*10^-5; %[bar]
Pb=T_ice_map.*w_ice_map_rads/1000; %[kW]
[W_ice_map,T_b_ice_map]=meshgrid(w_ice_map,T_ice_map);
W_ice_map=W_ice_map.*(2*pi/60); %[rad/s]
P_B=T_b_ice_map.*W_ice_map; %[W]
fc_map=Q_ice_map.*3600; %[g/h]
BSFC=fc_map./P_B*1000; %[g/kWh] %%% modify it

BSFC=round(BSFC,5); %rounds to N digits;

%% find min value
BSFC(isnan(BSFC))=0; %Replace Nan with 0
for i=1:200
    for j=1:200
        if BSFC(i,j)==0

```

```

        BSFC(i,j)=100000; %place instead of 0 high values so they don't
affect my minimum value
        continue;
    end
end
end
min_value=ones(200,1); %vector 200 rows 1 column
index=ones(200,1); %vector 200 rows 1 column
for i=1:200
    min_value(i,1)=BSFC(i,1); %store the first value of each row
                                %as a temporary minimum value to be used as
                                %a comparison in the next for loop

    for j=1:200
        if BSFC(i,j) < min_value(i,1)
            min_value(i,1)= BSFC(i,j);
            index(i,1)=j; %store the index of the column in which it is
located
        end
        continue;
    end
end

%% Optimal Operating Line
for i=1:199
    w_OOL(i)= w_ice_map(index(i));
end
w_OOL(200)=w_OOL(199);
BSFC=fc_map./P_B*1000; %[g/kWh] Restore BSFC map

for i=1:200
    T_OOL(i)=fc_map(i,index(i))/(BSFC(i,index(i))*(w_OOL(i)*pi/30))*1000;
    %[Nm]
end

w_OOL=smoothdata(w_OOL)
for i=2:200
    new_OOL(1)=w_OOL(1)
    if w_OOL(i)> w_OOL(i-1)
        new_OOL(i)=w_OOL(i)
        new_T_OOL(i)=T_OOL(i)
    else
        new_OOL(i)=new_OOL(i-1)+0.5
        new_T_OOL(i)=T_OOL(i)

        if new_T_OOL(i)> T_ice_max(i)

            new_OOL(i)=w_ice_map(i)

            new_T_OOL(i)= T_ice_max(i)

            continue
        end
    end
end

%% VAR
load('matlab_TOOL_wOOL.mat');
SOC_init = 0.532;
SOC_delta = 0.5;
T_add = 30;

%% Look-ahead
rel_dist=0; %m

```

```

for i=1:length(V_z)
    V_z_3(i)=V_z(i)-rel_dist;
    if V_z_3(i)<0
        V_z_3(i)=0;
    end
end
V_z_3=V_z_3';

shift=10; %shift in seconds
T_z_2=T_z+shift; %time ego vehicle

%%
open('IVECO_Daily_Conv_OOL.slx')
sim('IVECO_Daily_Conv_OOL.slx')
% open('IVECO_Daily_P2_SIM_OOL_ADAS.slx')
% sim('IVECO_Daily_P2_SIM_OOL_ADAS.slx')

%% Post processing
figure(1)
T_OOL(1)=T_OOL(2);
w_OOL(1)=w_OOL(2);
contourf(w_ice_map, T_ice_map, Q_ice_map,20,'linestyle','none')
colorbar
hold all
contour(w_ice_map, T_ice_map, Q_ice_map,20, 'k', 'ShowText','on');
plot(w_ice_map, T_ice_max,'k','linewidth',1.5)
plot(w_ice*30/pi, T_ice,'oy','linewidth',0.5) % ADAS
plot(w_ice_1*30/pi, T_ice_1,'xr','linewidth',0.5) %only ICE
% plot(w_ice_3*30/pi, T_ice_3,'oy','linewidth',0.5) % NO ADAS
plot(w_OOL,T_OOL,'k','linewidth',1.5)
xlabel('Engine speed [rpm]')
ylabel('Torque [Nm]')
legend('BSF','WOT','OOL','HEV ADAS','ICE')
% title('NEDC')
grid on
grid minor

figure(2),
plot(w_ice_map, T_ice_max,'k','linewidth',1.5)
hold all
plot(w_EM_max/Upulley, T_EM_max,'Color',[0,0.45,0.74])
plot(w_EM_max/Upulley, T_GEN_max,'Color',[0,0.45,0.74])
plot(w_OOL,T_OOL,'k','linewidth',1.5)
legend 'ICE' 'Motor'
xlabel('Angular speed at the input shaft level [rpm]'), ylabel('Torque [Nm]')
grid minor

figure(3),
contour(w_em_motor, T_em_motor, eff_motor, [0:0.03:1],'ShowText','on')
hold all
contour(w_em_gen, T_em_gen, eff_gen, [0:0.03:1],'ShowText','on')
plot(w_EM_max, T_EM_max)
plot(w_GEN_max, T_GEN_max)
plot(w_EM*30/pi, T_EM,'xk')
plot(w_EM*30/pi, T_GEN,'xk')
xlabel('Angular speed [rpm]'), ylabel('Torque [Nm]')
grid minor
ylim([-120 120])

```



```
figure(4),  
plot(w_GEN_max, pi/30000*w_EM_max.*T_GEN_max)  
hold on, plot(w_GEN_max, pi/30000*w_EM_max.*T_EM_max)
```

# Bibliography

Affairs, N. P. (2011). *Connected vehicles- v2v communications for safety*.

*Battery and Energy Technologies*. (2019, October). Retrieved from Electropaedia .

Bossche, P. V., Coosemans, T., & Mlerto, J. V. (2013). *Peukert Revisited, Critical Appraisal and Need for Modification for Lithium-Ion Batteries*. Brussel: Energies.

Cristian, M. (2010). *Sistema di accumulo misto, batteria e super condensatore, per la propulsione elettrica*.

DieselNet. (n.d.). *Standarsd Cycle*. Retrieved from DieselNet: <https://dieselnet.com/standards.php>

EuropeanCommision. (2020, Gennaio 29). *Environment*. Retrieved from Europa.eu.

Fifueiredo, L., Jesus, I., Ferreira, J. R., & Carvalho, M. d. (2001). Towards the development of intelligent transportation systems. *IEEE*.

Gong, Y., Li, H., & Liao, H. (2020). Estimation of Peukert Constant of Lithium-ion Batteries and its Application in Battery Discharging Time Prediction. *2020 IEEE Energy Conversion Congress and Exposition (ECCE)*, 905-910.

Group, W. (2018, Dicembre 13). *IPCC*. Retrieved from IPCC.

Guzzella, L., & Sciarretta, A. (2013). *Vehicle propulsion Systems introduction to modelling and optimization*. London: Springer.

International, S. (2016). Taxonomy and Definitions for Terms Related to Driving Automation Systems for On-Road Motor Vehicles. *SAE J3016\_201806*.

K.T Chau, Y. W. (2002). Overview of pomer management in hybrid electric vehicles, energy conversion and management. *Issue 15*, 1953-1968.

Khajepou, A., Fallah, S., & Goodarzi, A. (2014). Hybdrid and Electric Vehicles Technologies, Modelling and Control: A Mechatronic Approach. *Wiley*.

Kukkala, V., Tunnell, J., Pasricha, S., & Bradley, T. (2018). Advanced Driver Assistance Systems: A path toward Autonomous Vehicles. *IEEE Consumer Electronics Magazine*, 18-25.

- L.Rolando. (2012). An innovative methodology for the development of HEV energy management. *Science Direct*, 563-571.
- Munich, T. U., & Audi. (2018, June). *Travolution*. Retrieved from Stast Inglostadt.
- Rind, S. &. (2017). COnfiguration and control of traction motors for electric vehicles. *Chinese Journal of Electrical Engineering*, 1-17.
- S, L., & A, E. (2004). Effects of drivetrain hybridisation on fuel economy and dynamic performance of parallel hybrid electric vehicles. *IEE Transaction on Vehicular Technology*, 385-389.
- Simona, O., Lorenzo, S., & Giorgio, R. (2016). *Hybrid Electric Vehicles, Energy Management Strategies*. London: Springer-Verlag London.
- Smirnov, A., & Lashkov, I. (2015). State of the art analysis of available advanced driver assistance systems. *17th COnf. Opene Innov. Assoc. Fruct. Yarosl. RUss.*, 345-349.
- Wei, J. J. (2018). *Hybrid mobile computing for connected autonomous vehicles*.
- Xue, Q., Zhang, X., Teng, T., Zhang, J., & Feng, Z. (2020). A Comprehensive Review on Classification, Energy Management Strategy, and Control Algorithm for Hybrid Electric Vehicles. *Energies*.